

1
2
3
4
5
6
7
8
9
10
11
12
13
14
15
16

Spatial mapping of key plant functional traits in terrestrial ecosystems across China

Nannan An^{1,2,3}, Nan Lu^{2,3}, Weiliang Chen², Yongzhe Chen^{2,4}, Hao Shi^{2,3}, Fuzhong Wu¹, Bojie Fu^{2,3}

¹Key Laboratory for Humid Subtropical Eco-Geographical Processes of the Ministry of Education, School of Geographical Sciences, Fujian Normal University, Fuzhou 350117, PR China

²State Key Laboratory of Urban and Regional Ecology, Research Center for Eco-Environmental Sciences, Chinese Academy of Sciences (CAS), Beijing 100085, PR China

³University of Chinese Academy of Sciences, Beijing 101408, PR China

⁴State Key Laboratory of Hydrosience and Engineering, Department of Hydraulic Engineering, Tsinghua University, Beijing 100084, PR China

Correspondence to: Nan Lu (nanlv@rcees.ac.cn)

17 **Abstract**

18 Trait-based approaches are of increasing concern in predicting vegetation changes and linking
19 ecosystem structures to functions at large scales. However, a critical challenge for such approaches
20 is acquiring spatially continuous plant functional trait ~~distribution~~maps. Here, ~~eight-six~~ key plant
21 functional traits were selected ~~to as they can reflect plant resource acquisition strategies and~~
22 ~~ecosystem functions~~represent two dimensional spectrum of plant form and function, including
23 specific leaf area (SLA)~~leaf area (LA)~~, leaf dry matter content (LDMC), leaf N concentration (LNC),
24 leaf P concentration (LPC), ~~plant height, seed mass (SM), leaf area (LA) specific leaf area (SLA)~~
25 and wood density (WD). A total of ~~52477-34589 in-situ~~ trait measurements of ~~4291-3447~~ seed plant
26 species were collected from ~~1541-1430~~ sampling sites in China and were used to generate ~~a~~-spatial
27 plant functional trait ~~plant functional trait dataset~~maps (~1 km), together with environmental
28 variables and vegetation indices based on two machine learning models (random forest and boosted
29 regression trees). The two models showed a good accuracy in estimating WD, LPC and SLA, with
30 average R² values ranging from 0.45 to 0.66. In contrast, both the two models had ~~a~~ weak
31 performance in estimating ~~SM and~~ LDMC, with average R² values below 0.25. Meanwhile, LA,
32 ~~SM and plant height~~ showed considerable differences between two models in some regions. To
33 obtain the optimal estimates, a weighted average algorithm was further applied to merge the
34 predictions of the two models to derive the final spatial plant functional trait ~~dataset~~maps. ~~The~~
35 ~~optimal estimates showed that e~~Climatic effects were more important than those of edaphic factors
36 in predicting the spatial distribution of plant functional traits. Estimates of plant functional traits in
37 northeast China and the Qinghai-Tibet Plateau had relatively high uncertainties due to sparse
38 samplings, implying a need of more observations in these regions in future. Our spatial trait ~~dataset~~
39 maps could provide critical support for trait-based vegetation models and allows exploration into
40 the relationships between vegetation characteristics and ecosystem functions at large scales. The
41 ~~eight-six~~ plant functional traits ~~datasets~~maps for China with 1 km spatial resolution are now
42 available at <https://figshare.com/s/c527c12d310cb8156ed2> (An et al., 2023).

43 **1 Introduction**

44 Climate change has been affecting vegetation distributions and biogeochemical cycling globally and
45 altering their feedbacks to the climate system (Kirilenko et al., 2000; Finzi et al., 2011; Jónsdóttir et
46 al., 2022). Dynamic global vegetation models (DGVMs) are powerful tools for predicting changes
47 in vegetation and ecosystem-atmosphere exchanges (e.g., water, carbon, and nutrient cycling) in a
48 changing climate (Foley et al., 1996; Peng, 2000). However, conventional DGVMs are still
49 insufficient realistic, largely due to their dependence on the plant functional types (PFTs) assumption
50 (Sitch et al., 2008; Yurova and Volodin, 2011; Scheiter et al., 2013). PFTs in conventional DGVMs
51 commonly have fixed attributes (mostly trait values) (Van Bodegom et al., 2012; Wullschlegel et
52 al., 2014) that do not reflect plant adaptation to environments, limiting the quantification of carbon-
53 water-nutrient feedback between terrestrial ecosystems and the atmosphere (Zaehle and Friend,
54 2010; Liu and Yin, 2013). Trait-based approaches can provide robust theoretical basis for developing
55 the next generation of DGVMs (Van Bodegom et al., 2012; Sakschewski et al., 2015; Matheny et
56 al., 2017). Plant functional traits, which are closely associated with ecosystem functions (Diaz et al.,
57 2004; Yan et al., 2023), can effectively reflect response and adaptation of plants to environmental
58 conditions (Myers-Smith et al., 2019; Qiao et al., 2023).

59 Attempts to predict spatially continuous trait data-maps have been conducted at regional to
60 global scales (Madani et al., 2018; Moreno-Martínez et al., 2018; Boonman et al., 2020; Loozen et
61 al., 2020; [Dong et al., 2023](#)). Webb et al. (2010) proposed that the environment creates a filtered
62 trait distribution along an environmental gradient, and such trait-environment relationships offer
63 fundamental supports to predict the spatial distribution of plant functional traits through
64 extrapolating local trait measurements. Boonman et al. (2020) mapped the global patterns of specific
65 leaf area (SLA), leaf N concentration (LNC) and, wood density (WD) and plant height-based on a
66 set of climate and soil variables. As the number of available global trait databases increases ([Kattge
67 et al., 2011](#); Wang et al., 2018; [Kattge et al., 2020](#)), trait-environment relationships are becoming
68 increasingly quantitative and accurate (Bruehlheide et al., 2018; Myers-Smith et al., 2019).
69 Alternatively, remote sensing approaches, such as empirical methods and physical radiative transfer
70 models (e.g., partial least squares regression, PROSPECT model), have been developed to estimate
71 plant physiological, morphological, and chemical traits (e.g., leaf chlorophyll content, SLA, LNC
72 and leaf dry matter content (LDMC)) (Darvishzadeh et al., 2008; Romero et al., 2012; Ali et al.,
73 2016). Vegetation indices, such as the normalized difference vegetation index (NDVI) and the
74 enhanced vegetation index (EVI), have been successful in estimating plant functional traits of crops,
75 grasslands and forests (Clevers and Gitelson, 2013; Li et al., 2018; Loozen et al., 2018). Loozen et
76 al. (2020) demonstrated that EVI was the most important predictor for mapping the spatial pattern
77 of canopy nitrogen in European forests. Admittedly, recent studies have suggested that combining
78 environmental variables and vegetation indices can improve the predictive accuracy of canopy
79 nitrogen compared to those based on vegetation indices alone (Loozen et al., 2020).

80 Although there have been reports on plant functional trait distribution in China in some global
81 or regional research (Yang et al., 2016; Butler et al., 2017; Madani et al., 2018; Moreno-Martínez et
82 al., 2018; Boonman et al., 2020), they are still of large uncertainties in characterizing the spatial
83 distribution of plant functional traits in China. First, global studies generally have relatively few,
84 unevenly distributed sampling sites in China (Butler et al., 2017; Madani et al., 2018; Boonman et
85 al., 2020), impeding our understanding of the true spatial characteristics of trait variability. Second,
86 the spatial pattern of traits among these studies are usually inconsistent. For example, Moreno-
87 Martínez et al. (2018) and Madani et al. (2018) demonstrated that SLA values were low in the
88 southeast areas but high in the southwest areas of China, whereas Boonman et al. (2020) found the
89 opposite. Third, most studies mainly focused on leaf traits (Yang et al., 2016; Loozen et al., 2018;
90 Moreno-Martínez et al., 2018), whereas traits associated with the whole-plant ~~and reproductive~~
91 strategies, such as ~~WD and seed mass (SM)~~, were ignored. Therefore, mapping and verifying the
92 spatial patterns of key functional traits that reflect the whole plant economics spectrum in China is
93 a top priority.

94 In this study, our main objective was to generate ~~a spatial dataset maps~~ for several key plant
95 functional traits, through combining field measurements, environmental variables and vegetation
96 indices. ~~To achieve this goal, we used a processing routine to predict the spatial distribution of~~
97 ~~plant functional traits. selected six plant functional traits including SLA, LDMC, LNC, LPC, LA~~
98 ~~and WD. As key leaf economics traits, SLA, LDMC, LNC and LPC were selected because they are~~
99 ~~closely linked to plant growth rate, resource acquisition and ecosystem function (Wright et al., 2004;~~
100 ~~Diaz et al., 2016). LA is indicative of the trade-off between carbon assimilation and water-use~~
101 ~~efficiency (Wright et al., 2017), and WD reflects the trade-off between plant growth rate and support~~
102 ~~cost, with a higher WD linked to a lower growth rate, a higher survival rate and a higher biomass~~
103 ~~support cost (King et al., 2006). For each plant functional trait, we predicted spatial patterns at a 1~~
104 ~~km resolution using an ensemble modelling algorithm based on two machine learning methods (i.e.,~~
105 ~~random forest and boosted regression trees).~~

106 ~~First, eight plant functional traits (i.e., SLA, LDMC, LNC, LPC, LA, plant height, WD and~~
107 ~~SM) were selected because they reflect plant adaptation to environment constraints and trade-offs~~
108 ~~between plant form and function (Reich and Cornelissen, 2014; Diaz et al., 2016). Second, we used~~
109 ~~random forest and boosted regression trees to predict the spatial patterns of plant functional traits~~
110 ~~by training the relationships between plant functional traits and environmental variables and~~
111 ~~vegetation indices. To obtain the optimal estimates, an ensemble model (i.e., weighted average~~
112 ~~algorithm) was further applied to merge the predictions of the two models. Finally, plant species~~
113 ~~were aggregated to PFTs, and the spatial abundance of PFTs at 1 km resolution was calculated using~~
114 ~~land cover map (100 m). We derived the spatial trait datasets via calculating community weighted~~
115 ~~trait values within grid cells (1 km) based on these abundances of each PFT and predicted trait~~
116 ~~values.~~

2 Materials and Methods

2.1 Overview

The spatial maps of plant functional traits in China were generated based on machine learning algorithms trained by a large dataset of in-situ field measurements, environmental variables and vegetation indices in three steps (Fig. 1). First, in-situ field measurements of six plant functional traits were collected from TRY and China databases as well as published literature, and the PFTs of plant species were classified based on plant growth form, leaf type and leaf phenology. Multiple gridded predictors of climate, soil, topography and vegetation indices were used after avoiding the collinearity among them. Second, random forest and boosted regression trees were used to train the relationships between plant functional traits and predictors for each PFT individually. Third, the spatial abundance of each PFT within 1 km grid cell was calculated using land cover map (100 m). Community-weighted trait values within 1 km grid cell were calculated based on these abundances of each PFT and their predicted trait values in Step 2. To reduce the variability of different single-models, we derived the final spatial maps of plant functional traits using ensemble model to merge the predictions of random forest and boosted regression trees according to their cross-validated R^2 values.

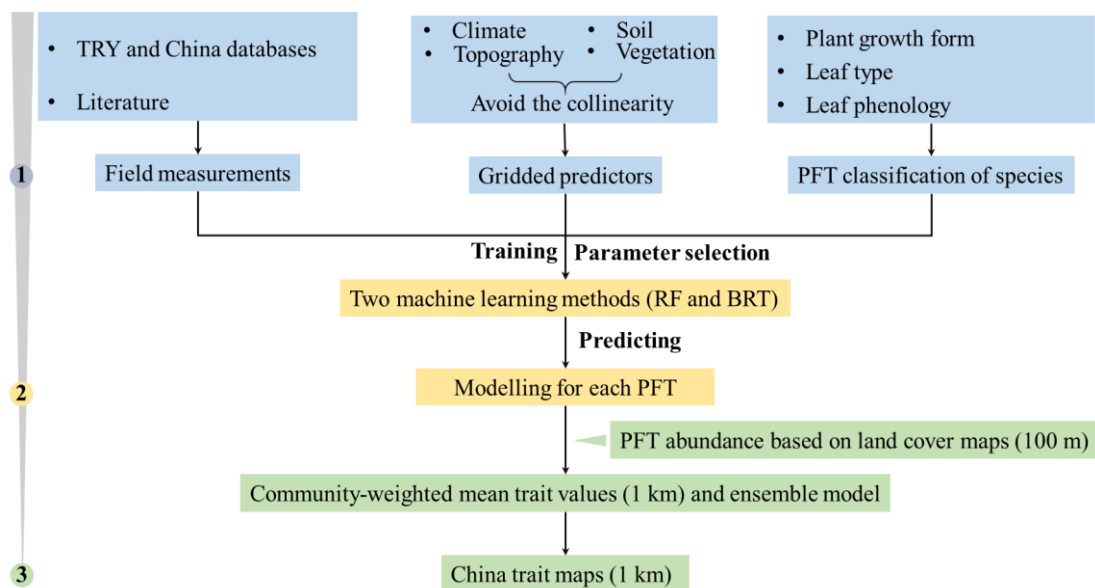


Figure 1. Methodological workflow for spatial mapping of plant functional traits. Trait mapping is performed in three steps. Step 1: in-situ field measurement of plant functional traits, PFT classification of plant species and gridded predictors were collected. Step 2: two machine learning methods were used to predict trait values by training the field measurements and predictors for each PFT. Step 3: spatialization of trait maps by calculating the abundance of each PFT using 100 m land cover map and predicted trait values within 1 km grid cells. PFT, plant functional type; RF, random forest; BRT, boosted regression trees.

2.1.2 Plant functional trait collection and data processing

The information on the ~~eight~~ six plant functional traits and their ecological meanings are described in Table 1. Plant trait data was obtained and collected via two main sources. The first source was public trait databases, including the TRY database (Kattge et al., 2020) and the China Plant Trait Database (Wang et al., 2018). The second source was from literature (listed in Appendix A). To ensure data quality and comparability, we only included trait observations that met the following five criteria: 1) Measurements must be obtained from natural terrestrial fields in order to minimize the influences of management disturbance, and observations from cropland, aquatic habitat, control experiments or gardens were excluded; 2) According to the mass ratio hypothesis, the effect of plant species on ecosystem functioning is determined to an overwhelming extent by the traits and functional diversity of the dominant species and is relatively insensitive to the richness of subordinate species (Grime, 1998). Thus, we only included studies that measured plant trait observations from all species or dominant species within a community; 3) In order to consider the intraspecific trait variation, when the same species occurred in the same sampling site from different studies, we included all original observed data from different studies rather than averaging the values at the species level ~~In order to account for the trait variation within and between communities, we only considered real measurements of traits from individual plants, and not species-level averages~~ (Jung et al., 2010; Siefert et al., 2015); 4) Plant trait observations must be made on mature and healthy plant individuals, so some specific growth stages (e.g., seedling) and size classes (e.g., sapling) were excluded to reduce the confounding effect of ontogeny and seasonality (Thomas, 2010); 5) We only included studies with clear geographical coordinates to ensure alignment with predictor variables. The sampling location and sampling sample-time information ~~from the original studies~~ were also included in the dataset. The sampling time mostly focused on the growing season of a year (i.e., May-October), which ensures the relative consistency of sampling time to minimize the effects of seasonality.

Plant functional traits must be sampled and measured according to standardized measurement procedures (Perez-Harguindeguy et al., 2013) to reduce the variation and uncertainty among different data sources. In this study, we included SLA measurements on ~~both sun-leaves and shade-leaves,~~ and WD measurements on both heartwood and sapwood of tree species, ~~SM measurements on both seeds and fruits, and plant height measurements on both vegetative and generative organs,~~

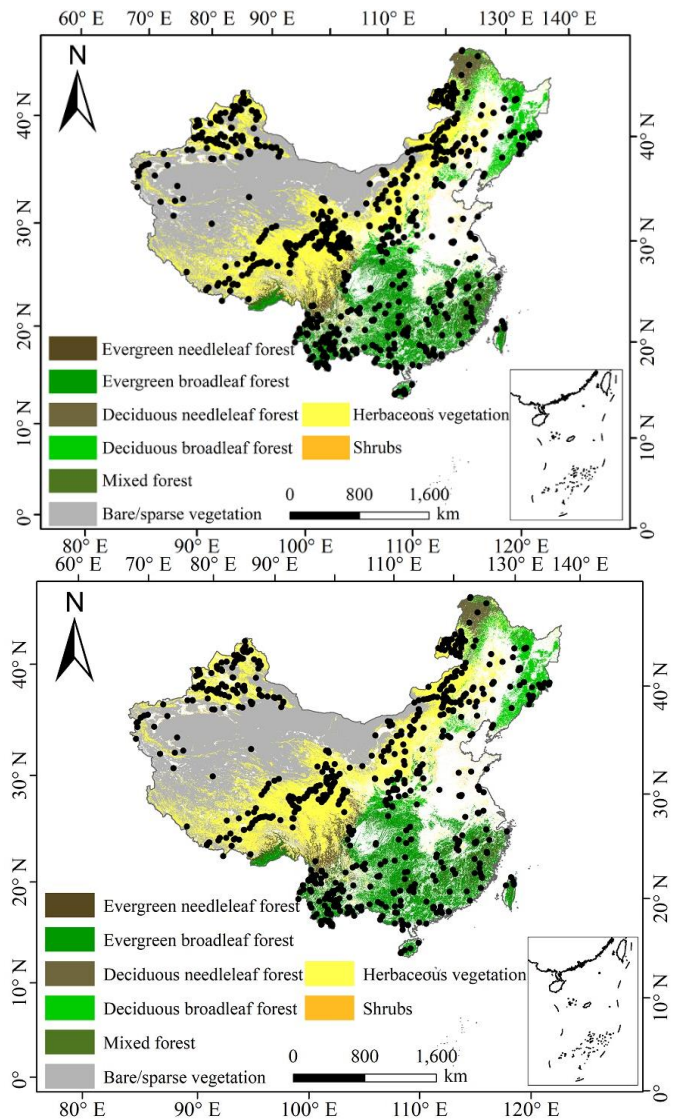
171 **Table 1** Description of plant functional traits selected in this study and their relevant ecosystem
 172 functions.

Trait	Abbreviation	Description	Relevant ecosystem functions
Specific leaf area	SLA	As a core leaf economics trait (Wright et al., 2004), it is related to trade-off between leaf lifespan and C acquisition as well as light competition (Reich et al., 1991)	Productivity, litter decomposition, competitive ability (Bakker et al., 2011; Smart et al., 2017)
Leaf dry matter content	LDMC	Strongly related to resource availability and potential growth rate (Hodgson et al., 2011)	Productivity, litter decomposition, herbivore resistance, and drought tolerance (Bakker et al., 2011; Smart et al., 2017; Blumenthal et al., 2020)
Leaf N concentration	LNC	As a core leaf economics trait, it is strongly related to photosynthetic capacity (Wright et al., 2004)	Productivity, nutrient cycling, litter decomposition (LeBauer and Treseder, 2008; Bakker et al., 2011)
Leaf P concentration	LPC	As a core leaf economics trait, it is strongly related to photosynthetic capacity (Wright et al., 2004)	Productivity, nutrient cycling, litter decomposition (LeBauer and Treseder, 2008; Bakker et al., 2011)
Leaf area	LA	Trade-off between C assimilation and water use efficiency, it is related to energy balance (Wright et al., 2017)	Productivity (Li et al., 2020)
Plant height	/	A major determinant of a plant's ability to compete for light (Moles et al., 2009)	C storage, animal diversity (Conti et al., 2013; Roll et al., 2015)
Wood density	WD	A measure of carbon investment, representing the trade-off between growth and mechanical support (Martínez-Vilalta et al., 2010)	Drought tolerance, productivity (Hoeber et al., 2014; Liang et al., 2021)
Seed mass	SM	Closely related to seed dispersal and seed predation, as well as seedling establishment, growth, and survival (Leishman et al., 2000)	Competitive ability (Zepeda and Martorell, 2019)

173 The plant trait data was checked for possible errors and corrected ~~as per~~in three steps as follows.
 174 First, species name and taxonomic nomenclature were corrected and standardized according to the
 175 Plant List (<http://www.theplantlist.org/>) using the “plantlist” package. Second, illogical values,
 176 repeated values and outliers were removed, which were defined by observations exceeding 1.5
 177 standard deviations of the mean trait value for a given species (Kattge et al., 2011). Third, we
 178 appended information on plant growth form (~~tree, shrub, and herb~~), leaf type (~~broadleaved and~~
 179 ~~needle-leaved~~) and leaf phenology (~~evergreen and deciduous~~) from the TRY categorical traits
 180 database (<https://www.try-db.org/TryWeb/Data.php#3>) and *Flora Reipublicae Popularis Sinicae*
 181 (<http://www.iplant.cn/frps>), ~~which were used~~. ~~Furthermore, in order~~ to match species names to
 182 PFTs, ~~we~~We associated each species (~~i.e., plant growth form, leaf type and leaf phenology~~) with
 183 a corresponding PFT based on plant growth form (tree, shrub and grass), leaf type (broadleaf and
 184 needleleaf) and leaf phenology (evergreen and deciduous). For example, the information on *Salix*
 185 *matsudana* is: tree, deciduous and broadleaf, thus, we were able to associate the PFT of deciduous

186 broadleaf forest (DBF) to this species. The species that did not correspond to any PFT were
 187 discarded. After these treatments, we collected a total of ~~3458952477~~ trait measurements from ~~1541~~
 188 ~~1430~~ sampling sites for our database, representing ~~4291-3447~~ species from ~~212-195~~ families and
 189 ~~1230-1066~~ genera (Fig. ~~12~~ and Fig. B1 in Appendix B). Information on the statistics for the ~~eight~~
 190 ~~six~~ plant functional traits collected in this study is shown in Table B1 in Appendix B.

191



192

193 **Figure 12.** Location distribution and land cover map in China.

194

194 **2.2.3 Preparing predictor variables** ~~Environmental data~~

195

195 **2.2.3.1 Climate data**

196

196 Twenty-one climate variables were used in this study, including 19 bioclimate variables, solar
 197 radiation (RAD), and aridity index (AI) (Table B2 in Appendix B). The 19 bioclimate variables and
 198 RAD were obtained from the WorldClim ~~dataset (version 2.11)~~ for the period from 1970 to 2000
 199 (<https://www.worldclim.org/data/worldclim21.html>). The AI data was extracted from the CGIAR
 200 Consortium of Spatial Information (CGIAR-CSI) website for the period from ~~1950-1970~~ to 2000
 201 (<http://www.csi.cgiar.org>) (Trabucco and Zomer, 2018). The spatial resolution of climate data ~~was~~

202 is 1 km.

203 **2.23.2 Soil data**

204 Twelve soil variables were included in this study, representing the different aspects of soil properties,
205 i.e. soil texture, bulk density (BD), pH, and soil nutrients (Table B2 in Appendix B). All soil
206 variables were extracted from the Soil Database of China for Land Surface Modeling
207 (<http://globalchange.bnu.edu.cn/research/soil2>) (Shangguan et al., 2013). Given the importance of
208 topsoil properties on community composition (Bohner, 2005), we averaged the first four layers to
209 the soil data was averaged to represent the top soil-30 cm of soil properties (~ 30 cm) in our study.
210 The spatial resolution was-is 1 km.

211 **2.23.3 Topography**

212 The topographic variable was elevation. Elevation data was extracted from the STRM 90m dataset
213 in China, based on the SRTM V4.1 database (<https://www.resdc.cn/data.aspx?DATAID=123>). The
214 spatial resolution was-is 1 km.

215 Given the collinearity among climate and soil variables, we reduced the number of
216 environmental predictors based on Pearson's correlation coefficient (r) (Figs. B1-B2 and B2-B3 in
217 Appendix B). Among a set of highly correlated variables ($r > 0.75$), only one variable was retained
218 in subsequent analysis to ensure a combination of different environmental variables. The final
219 selection of environment predictors included nineteen variables: mean annual temperature (MAT),
220 mean diurnal range (MDR), min temperature of coldest quarter (Tmin), max temperature of coldest
221 warmest quarter (Tmax), temperature seasonality (TS), mean annual precipitation (MAP),
222 precipitation seasonality (PS), precipitation of wettest quarter (PEQ), precipitation of driest quarter
223 (PDQ), AI, RAD, elevation, soil sand content (SAND), pH, BD, soil total N (STN), soil total P
224 (STP), soil available P (SAP), soil alkali-hydrolysable N (SAN), and cation exchange capacity
225 (CEC).

226 **2.3-3.4 Vegetation indices**

227 Three categories of vegetation indices were included in this study (Table B2 in Appendix B). First,
228 EVI The first selected was EVI, which was extracted from the MOD13A3 V006 product
229 (<https://lpdaac.usgs.gov/products/mod13a3v006/>). This product is available as a monthly average
230 with spatial resolution of 1 km, ranging from January 2000 to December 2018. Second, MODIS
231 reflectance data was also extracted from the MOD13A3 V006 product. This, included-including
232 MIR reflectance, NIR reflectance, red reflectance, and blue reflectance. Third, the MERIS terrestrial
233 chlorophyll index (MTCI) was extracted from the Natural Environment Research Council Earth
234 Observation Data Centre (NERC-NEODC, 2005) (<https://data.ceda.ac.uk/>). MTCI data is available
235 globally as a monthly average at 4.63 km spatial resolution, and ranges from June 2002 to December
236 2011. It is noted that valid MTCI values should be greater than 1, so our study deleted any values
237 less than 1.

238 To avoid collinearity, we also reduced the number of vegetation indices based on Pearson's
239 correlation coefficient (r) (Figs. B3-B4 in Appendix B). Most selected variables were related to

growing seasons due that plant functional traits were measured during the growing season. Furthermore, based on the results of Pearson's correlation coefficient (r), MTCI, MIR, NIR, red and blue in January showed low correlations with those in growing season, thus they were included in subsequent analysis. Furthermore, given that most plant functional traits were measured during the growing season, the variables related to the growing season were determined to be important predictors. The final selection included 36 variables: annual EVI, EVI (May, June, July, August and September), MTCI, MIR, NIR, red and blue (all for January, June, July, August and September).

Both environmental variables and vegetation indices variables were resampled to a consistent spatial resolution of 1 km using the nearest neighborhood method.

PFT is also an important factor in influencing the variation of plant functional traits (Verheijen et al., 2016; Loozen et al., 2020), thus the trait predictions were performed for each PFT individually. PFT was included as a predictor in this analysis. We used the 2015 land cover map at a 100 m spatial resolution to calculate the relative abundance of each PFT within 1 km grid cells, which was extracted from the Copernicus Global Land Service (CGLS-LC100, Version 3) (<https://land.copernicus.eu/global/products/lc>) (Buchhorn et al., 2020). We focused on natural terrestrial vegetation, so all artificial or crop areas were thus eliminated in our dataset. Seven categories were included: evergreen needleleaf forest (ENF), evergreen broadleaf forest (EBF), deciduous needleleaf forest (DNF), deciduous broadleaf forest (DBF), shrubland (SHL), grassland (GRL) and bare/sparse vegetation. Furthermore, in order to match species names to PFTs, we associated each species (i.e., plant growth form, leaf type and leaf phenology) with a corresponding PFT. For example, the information on *Salix matsudana* is: tree, deciduous and broadleaf, thus, we were able to associate the PFT of deciduous broadleaf forest (DBF) to this species. The species that did not correspond to any PFT were discarded.

2.4.4 Model fitting and validation

To predict spatial patterns of plant functional traits, we used two machine learning models, i.e., random forest and boosted regression trees.

Random forest is an ensemble machine learning method based on classification and regression trees using collections of regression trees to classify observations according to a set of predictive variables (Breiman, 2001). This method repeatedly constructs a set of trees from random samples of training data, and the final prediction is produced by integrating the results of all individual trees, which makes it a robust method. The models are controlled by two main parameters: the number of sampled variables (mtry) and the number of trees (ntree). The parameter mtry was set to range from 1 to 57 (at an interval of 1), and the ntree was set as 500, 1000, 2000, 5000 and 10000 in subsequent runs. This analysis was performed using the 'randomForest' function in the 'randomForest' package (Liaw and Wiener, 2002).

Boosted regression trees is a machine learning methods based on generalized boosted regression models, and using a boosting algorithm to combine many sample tree models to optimize

277 predictive performance (Elith et al., 2006). There is no need for prior data transformation or the
 278 elimination of outliers, and this method can fit complex non-linear relationships while automatically
 279 handling interaction effects between predictors (Elith et al., 2008). The four parameters to optimize
 280 in these models are the number of trees, interaction depth, learning rate and bag fractions. We varied
 281 the parameter settings to find the optimal parameter combination that achieves minimum predictive
 282 error. The number of trees was set to 3000, the interaction depth varied from 1 to 7 (at an interval
 283 of 1), the learning rate was set to 0.001, 0.01, 0.05 and 0.1, and the bag fraction was set to 0.5, 0.6,
 284 0.7 and 0.75. PFT was used as a dummy variable in the boosted regression trees models. This
 285 analysis was conducted using the ‘gbm’ function in the ‘gbm’ package (Ridgeway, 2006).

286 ~~We built separate predictive model for each plant functional trait. We used a 10-fold cross~~
 287 ~~validation~~ To select the optimal parameter combination and to evaluate the final model performance
 288 for each trait, ~~we calibrated the models 10 times using randomly selected 80% of the data for training~~
 289 ~~the models and validating against the remaining 20% based on cross-validation (Table B3 in~~
 290 ~~Appendix B).~~ We split the data into two parts: 80% of the trait data was used to train the models,
 291 and the remaining 20% was used to assess model’s performance. The predictive performance was
 292 ~~evaluated by regressing the predicted and observed trait values from all repetitions of the cross-~~
 293 ~~validation.~~ The fitting performances of the random forest and boosted regression trees methods were
 294 evaluated using determinate coefficient (R^2), normalized root-mean-square error (NRMSE), and
 295 mean absolute error (MAE). These scores are calculated following Eq. (1), Eq. (2) and Eq. (3):

$$296 \quad R^2 = 1 - \frac{\sum_{i=1}^n (p_i - o_i)^2}{\sum_{i=1}^n (p_i - \hat{o}_i)^2} \quad (1)$$

$$297 \quad RMSE = \sqrt{\text{NRMSE}} = \frac{\sqrt{\frac{1}{n} \sum_{i=1}^n (p_i - o_i)^2}}{p_{max} - p_{min}} \quad (2)$$

$$298 \quad MAE = \frac{1}{n} \sum_{i=1}^n |o_i - p_i| \quad (3)$$

299 where p_i and o_i are the predictive values and observed values, respectively, \hat{o}_i is the mean of
 300 the observed values.

301 To quantify the relative importance of each predictor ~~consistently~~ across the two models
 302 consistently, we used the method proposed by Thuiller et al. (2009). This method applies correlation
 303 between the standard predictions fitted with the original data and predictions where the variable
 304 under investigation has been randomly permuted. If the correlation is high, which indicates little
 305 difference between the two predictions, the variable permuted is considered not important for the
 306 model. The correlations between fitted values and predictions were calculated using permuted
 307 values for the predictor of concern. This step was repeated ~~a user-defined number of~~ multiple times
 308 for each predictor, and the mean correlation coefficient over runs was recorded. Then the relative
 309 importance of each predictor was quantified as one minus the Spearman rank correlation coefficient
 310 (see Boonman et al., 2020). In addition, we used generalized additive models to fit the relationships
 311 between plant functional traits and the most important variables using the ‘gam’ function in the
 312 ‘mgcv’ package.

2.5.5 Generation of plant functional trait maps and model performance

The generation of spatial maps of plant functional was performed in three steps. First, we predicted trait values for each PFT within 1 km grid cell separately. Second, the abundance of individual PFT within 1 km grid cell was estimated using a land cover map with a spatial resolution of 100 m. Third, refer to the Eq. (4) that has been widely applied in a community (Garnier et al., 2004), the ~~The final community weighted mean trait values in a given 1 km grid cell were calculated according to as the sum of the predicted trait values and multiplying by corresponding abundance of each PFT.~~

$$CWM = \sum_{i=1}^n W_i X_i \quad (4)$$

where n is the total number of PFT in a given grid; W_i is the relative abundance of the i th PFT; and X_i is the predicted trait value of the i th PFT. ~~To calculate community weighted mean trait values, the abundance of individual PFT within 1 km grid cell was estimated using a land cover map with a spatial resolution of 100 m. The final community weighted mean trait values were calculated according to the predicted trait values and corresponding abundance of each PFT.~~

~~To reduce the variability of different single-models and to construct a more stable and accurate model, To obtain the optimal estimates,~~ the ensemble model was further applied to merge the predictions of random forest and boosted regression trees according to their cross-validated R^2 values. ~~The predictive value of ensemble model was calculated in a given grid cell as described by Eq. (5) (Marmion et al., 2009). The model accuracy was calculated by regressing the predictive values of ensemble model against the observed trait values. The accuracy of the ensemble model was calculated by regressing the 20% of cross validation data used for testing against the observed trait values.~~

$$Pred_EM_t = \frac{\sum_{m=1}^2 (pred_{m,t} \times r_{m,t}^2)}{\sum_{m=1}^2 r_{m,t}^2} \quad (5)$$

where $Pred_EM_t$ is the predictive values of t trait in the ensemble model; $pred_{m,t}$ is the predictive values of t trait in m model; $r_{m,t}^2$ is the cross-validated R^2 of t trait in m model.

To evaluate the model performance (i.e. the variability in the prediction across models), the coefficient of variation (CV) was calculated as the difference between the predictions of random forest and boosted regression trees methods and the ensemble prediction ~~weighted by the predictive performance of each of the models~~. CV is calculated as following Eq. (46):

$$CV_t = \frac{\sqrt{\sum_{m=1}^2 (pred_{m,t} - obs_t)^2 * r_{m,t}^2}}{\sum_{m=1}^2 r_{m,t}^2} \quad (46)$$

where $pred_{m,t}$ is the predictive values of t trait in m model; obs_t is the values of t trait in the ensemble model; $r_{m,t}^2$ is the cross-validated R^2 of t trait in m model.

2.6.6 Uncertainty assessments

Multivariate environmental similarity surface analysis (MESS) was used to identify the range of the extrapolated predictor values across the locations in the plant trait dataset (Elith et al., 2010). This

347 method is often used to evaluate the extent of extrapolation and the applicability domain. If the
 348 values are negative, this indicates that at a given grid cell, at least one predictor variable is outside
 349 the extent of referenced predictor layer. This analysis was conducted using the ‘mess’ function in
 350 the ‘dismo’ package.

351 All analyses were performed in R 4.0.2 (R Core Team, 2020).

352 3 Results

353 3.1 Performances of prediction models

354 Cross-validation showed that the performance of the predictive models differed greatly among the
 355 plant functional traits (Table 2, [Tables C1 and C2 in Appendix C](#)). WD had the best performance in
 356 all three models, with R² values of 0.64, 0.68 and 0.67 for random forest, boosted regression trees
 357 and ensemble model, respectively. ~~SLA, LPC, height~~ and ~~LPC, SLA~~ had R² values greater than 0.45,
 358 while ~~SM and~~ LDMC performed the worst, with R² values below 0.25. ~~In addition, the ensemble~~
 359 ~~model performed better than the random forest and boosted regression trees alone (Tables C1 and~~
 360 ~~C2 in Appendix C).~~

361 **Table 2** Results of plant functional traits for cross-validated R², ~~N~~R~~M~~SE and MAE for random
 362 forest, boosted regression trees, and ensemble model.

Traits	Random forest			Boosted regression trees			Ensemble model		
	R ²	N R M SE	MAE	R ²	N R M SE	MAE	R ²	N R M SE	MAE
SLA	0.48	7.02 0.22	5.10	0.48	6.99 0.20	5.08	0.49	6.98 0.21	5.07
LDMC	0.23	0.19 0.21	0.07	0.28	0.09 0.18	0.07	0.24	0.09 0.20	0.07
LNC	0.33	6.64 0.19	4.92	0.34	6.52 0.18	4.85	0.34	6.54 0.19	4.85
LPC	0.51	0.89 0.24	0.53	0.51	0.89 0.22	0.53	0.51	0.89 0.27	0.53
LA	0.37	68.94 0.45	26.76	0.39	67.69 0.51	27.47	0.40	67.28 0.58	26.59
SM	0.24	4547.22	1228.07	0.26	4478.88	1183.61	0.25	4499.67	1201.83
Height	0.49	2.89	2.09	0.49	2.89	2.10	0.49	2.89	2.10
WD	0.64	0.13 0.20	0.10	0.68	0.12 0.13	0.10	0.67	0.13 0.17	0.10

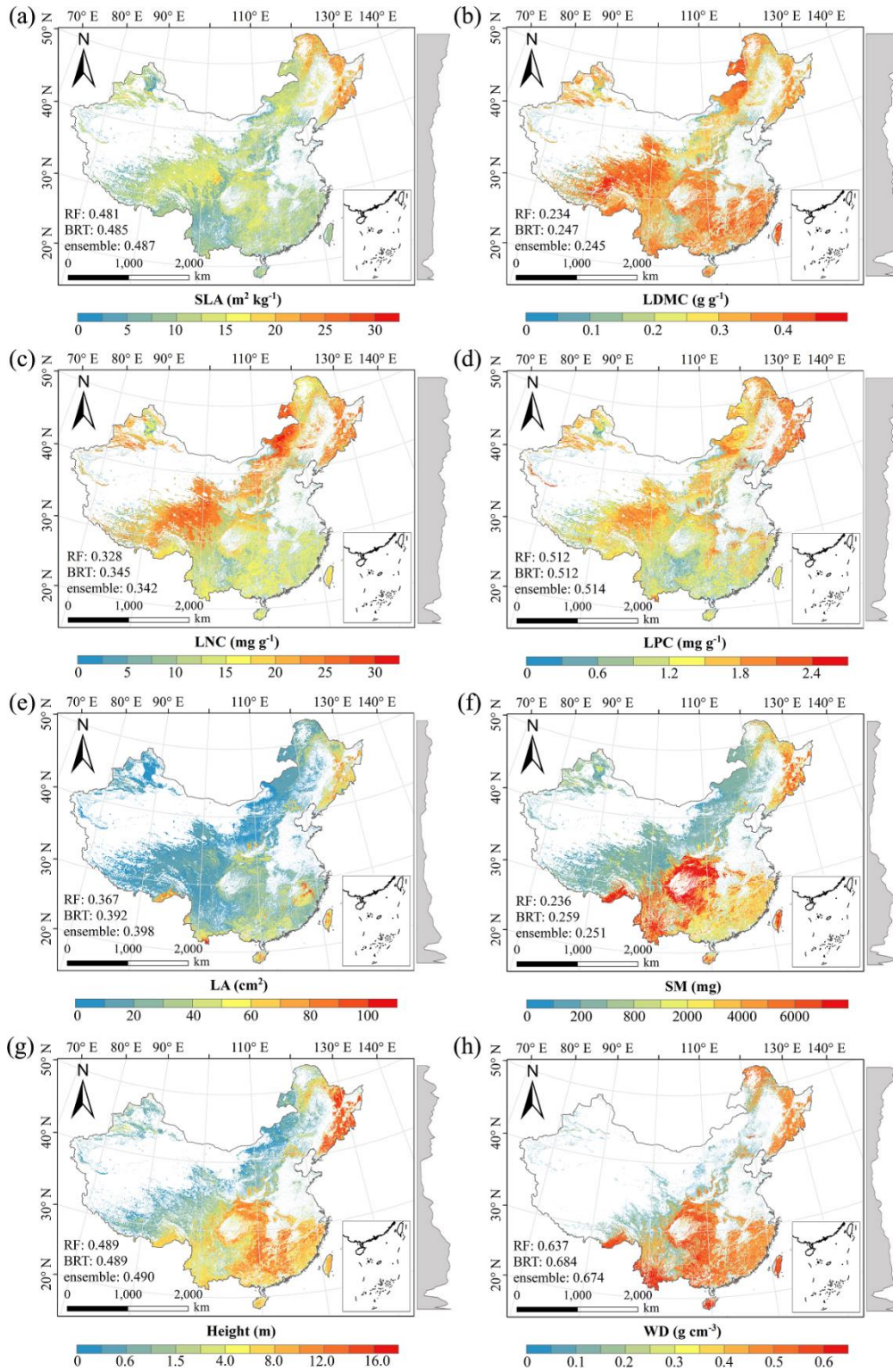
363 SLA, specific leaf area ($\text{m}^2 \text{kg}^{-1}$); LDMC, leaf dry matter content (g g^{-1}); LNC, leaf N
 364 ~~concentration~~ concentration (mg g^{-1}); LPC, leaf P ~~concentration~~ concentration (mg g^{-1}); LA, leaf area (cm^2);
 365 WD, wood density (g cm^{-3}); R², determinate coefficient; ~~N~~R~~M~~SE, normalized root-mean-square error;
 366 ~~MAE, mean absolute error. SM, seed mass.~~

367 3.2 Spatial patterns of predicted plant functional traits

368 There were relatively consistent spatial patterns for SLA, LNC and LPC, with high values in the
 369 northeastern and northwestern regions and the southeastern Qinghai-Tibet Plateau, and low values
 370 in southwestern China (Figs. ~~2a3a~~, ~~2e3c~~ and ~~2d3d~~, Figs. D1 ~~and~~, D2 in Appendix D). SLA and LPC
 371 increased with latitude, while LNC did not vary significantly along the latitudinal gradient. For SLA,
 372 LNC and LPC, the variability was low among ~~the~~ random forest, boosted regression trees and
 373 ensemble model, with an overall CV less than 0.3 (Figs. ~~3a4a~~, ~~3e4c~~, and ~~3d4d~~). LDMC values were

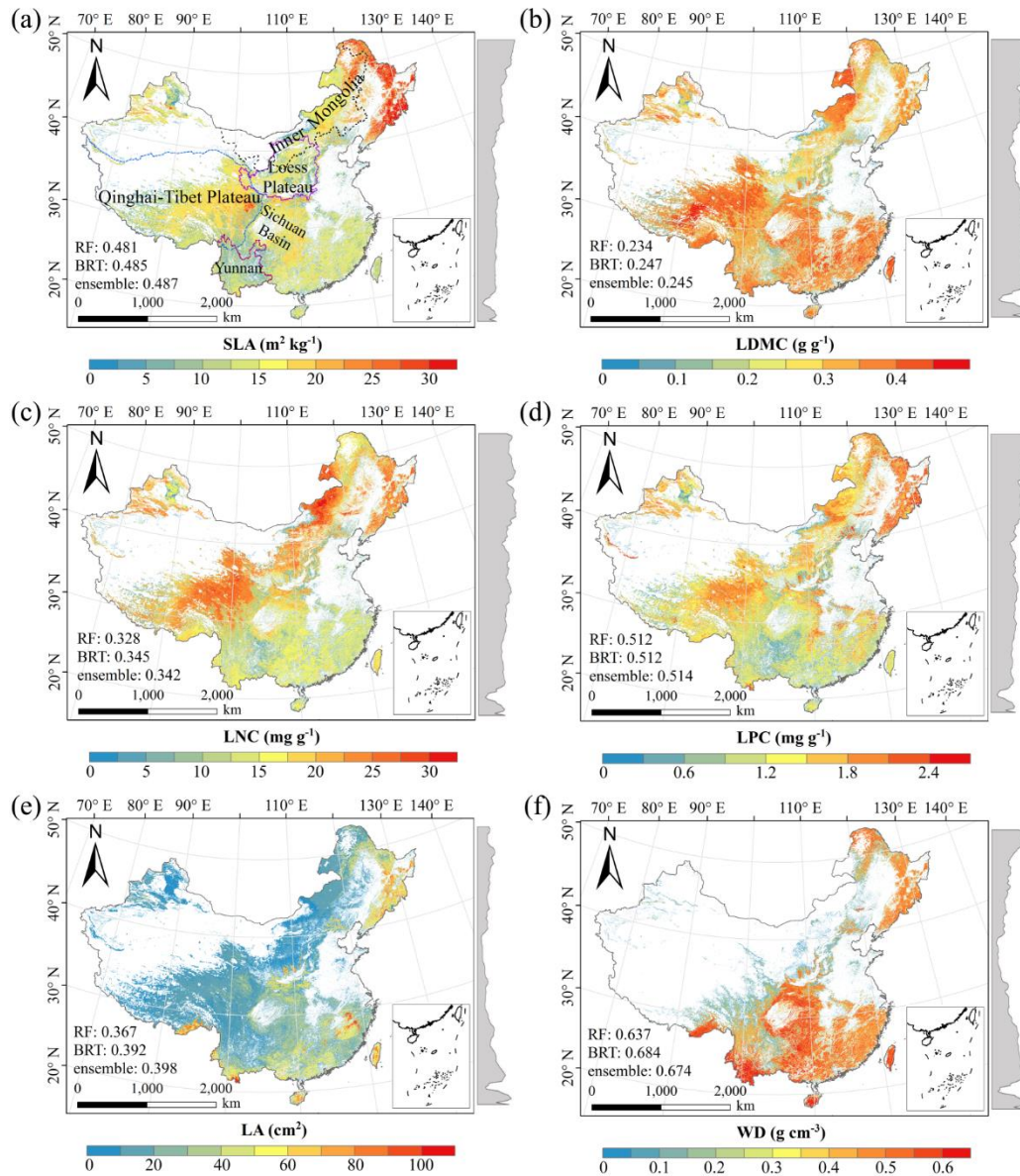
374 relatively high in most regions of China, and the low values were mainly located in eastern Yunnan
375 and the Loess Plateau (Fig. ~~2b~~3b, Figs. D1 and, D2 in Appendix D). LA ~~and SM showed consistent~~
376 ~~spatial patterns, with~~showed high values in the northeastern and southern regions (except for the
377 Sichuan Basin), and the southeastern Qinghai-Tibet Plateau (Figs. ~~23e~~and 2f, Figs. D1, and D2
378 in Appendix D). The strong latitudinal gradients ~~were~~was observed in LA ~~and SM~~, where values
379 decreased with latitude.

380 The CV values of LPC ~~and SM~~ decreased with latitude, but other traits did not show latitudinal
381 patterns (Figs. 34). The CV values of LA were relatively high, especially in the northwestern region,
382 and the Inner Mongolia-Plateau-Loess Plateau region (~~only for LA~~) and Yunnan province (only for
383 ~~SM)~~ (Figs. 34e ~~and 3f~~). ~~Plant height and~~ WD had ~~consistent spatial patterns, with~~ high values in the
384 northeastern and southern regions (Figs. 2g-2f ~~and 2h~~, Figs. D1, and D2 in Appendix D). ~~The CV~~
385 ~~values across models for plant height were higher in northwestern China and Inner Mongolia~~
386 ~~Plateau-Loess Plateau region,~~ while CV values for WD in China were low throughout China (Figs.
387 3g-4f ~~and 3h~~).



388

389



390

391

392

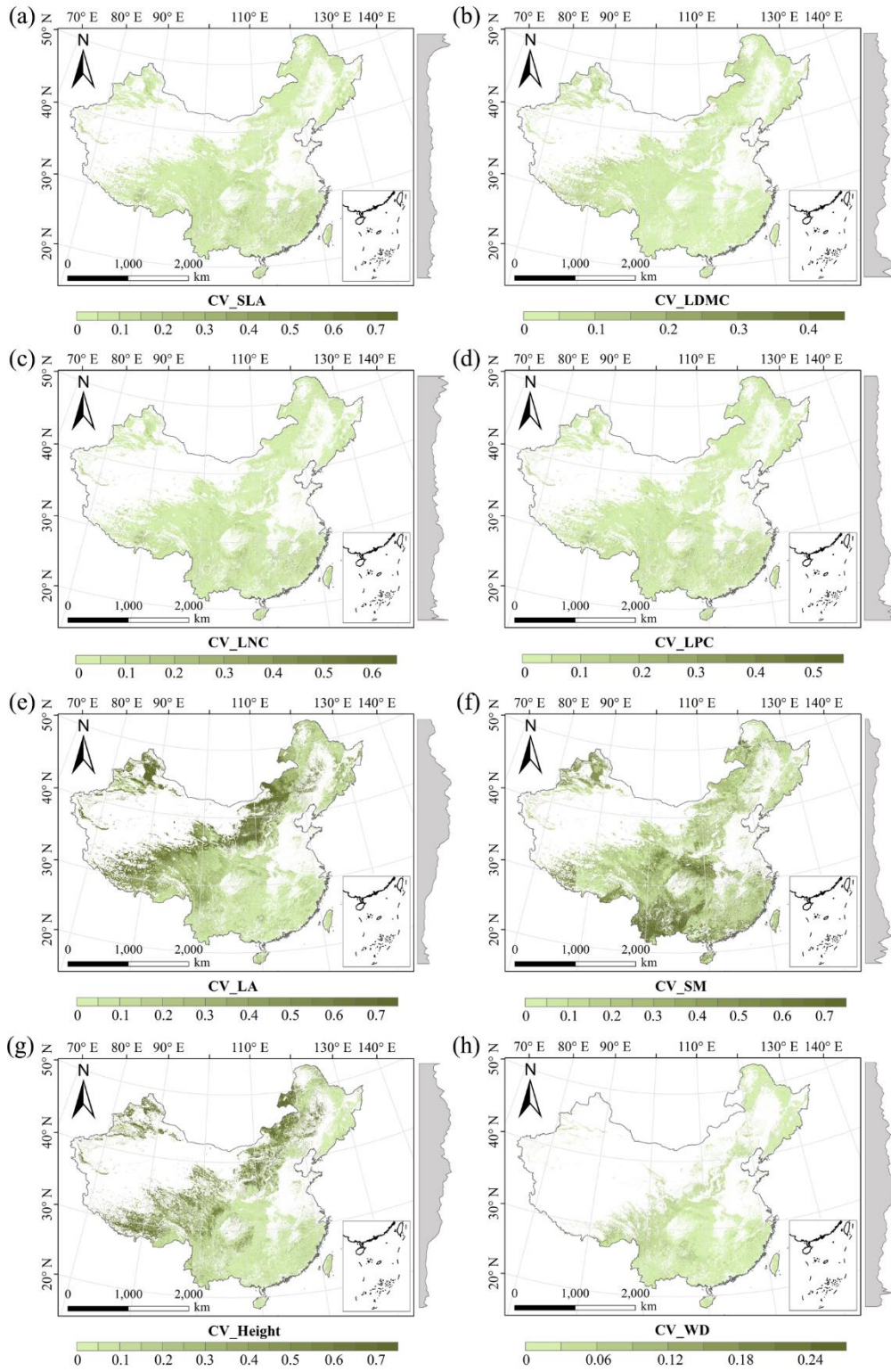
393

394

395

396

Figure 23. Spatial patterns of predicted plant functional traits in China based on the ensemble model. The grey curves to the right of the maps display trait distribution along with latitude. RF, random forest; BRT, boosted regression trees; ensemble, ensemble model; SLA, specific leaf area; LDMC, leaf dry matter content; LNC, leaf N ~~concentration~~~~concentration~~; LPC, leaf P ~~concentration~~~~concentration~~; LA, leaf area; WD, wood density; ~~SM, seed mass.~~



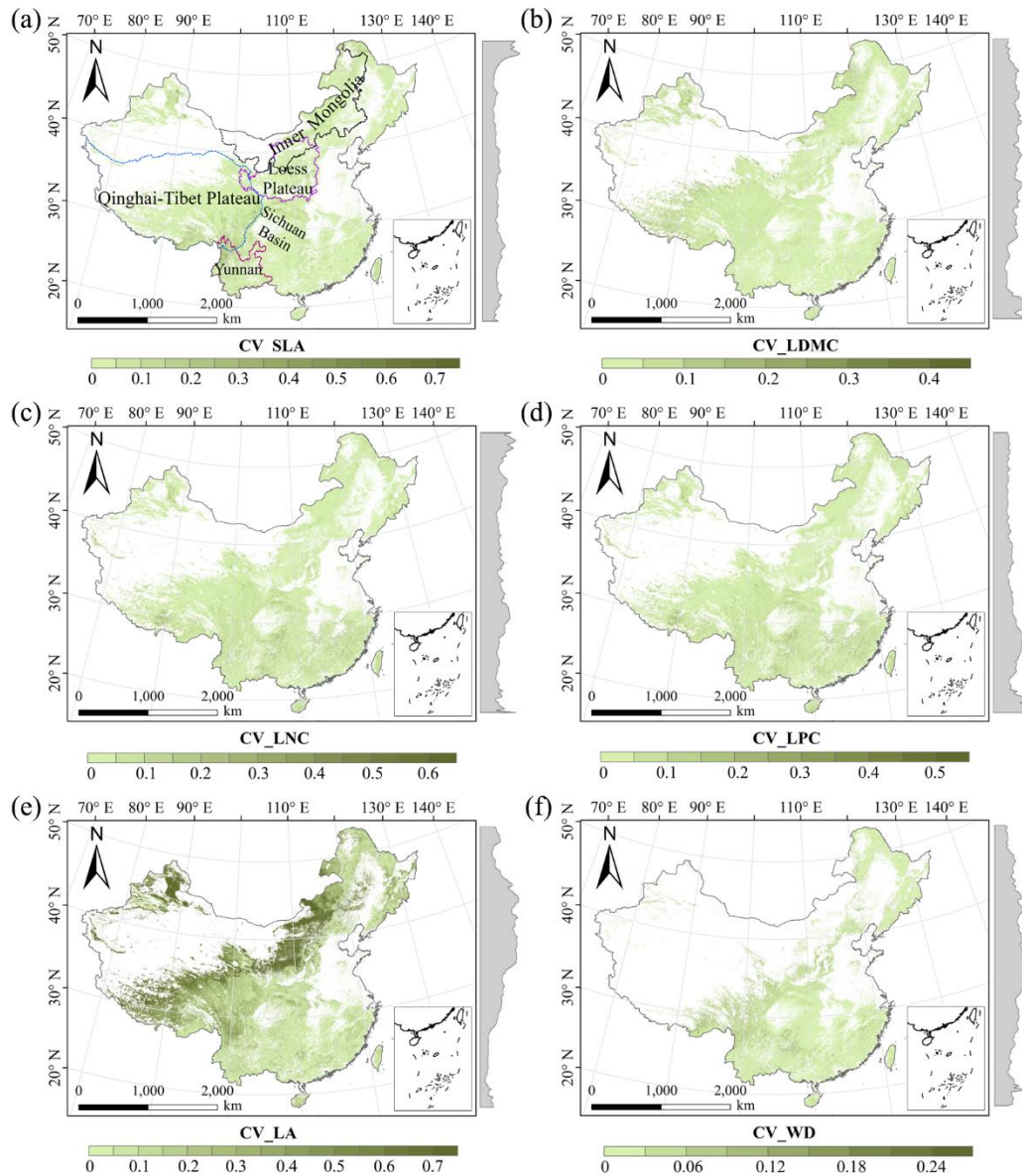


Figure 34. The variability in plant functional trait predictions among random forest, boosted regression trees and ensemble model. The grey curves to the right of the maps display coefficient of variation along with latitude. SLA, specific leaf area; LDMC, leaf dry matter content; LNC, leaf N concentration; LPC, leaf P concentration; LA, leaf area; WD, wood density; SM, seed mass.

3.3 Relative importance of predictive variables

The dominant factors explaining spatial variation differed greatly among the eight plant functional traits (Table 3). Overall, climate variables were more important for predicting plant functional traits than were soil variables. Temperature variables (i.e., MAT, MDR and TS) showed close relationships with SLA, LDMC, LPC and WD, while precipitation variables (i.e., PS, PEQ, MAP and PDQ) were more important for predicting the spatial patterns of LNC, LPC, and LA and plant

410 ~~height~~. RAD was the fourth most dominant factor in predicting the spatial patterns of SLA, ~~SM,~~
 411 ~~and WD and plant height~~. Elevation also played an important role in the LDMC and LPC predictions.
 412 Within soil variables, soil nutrients ~~{(i.e., pH and soil available P (SAP))}~~ showed close
 413 associations with SLA, ~~and LNC and SM~~. In addition to the environmental variables, MTCI
 414 emerged as an important predictor for explaining SLA, LDMC, ~~and LA and plant height~~. Finally,
 415 EVI was the most important predictor for LA ~~and SM~~, and MIR in January and May were the
 416 primary predictors of WD. The relationships between plant functional traits and the most important
 417 variables were shown in Figs. E1 and E2 in Appendix E.

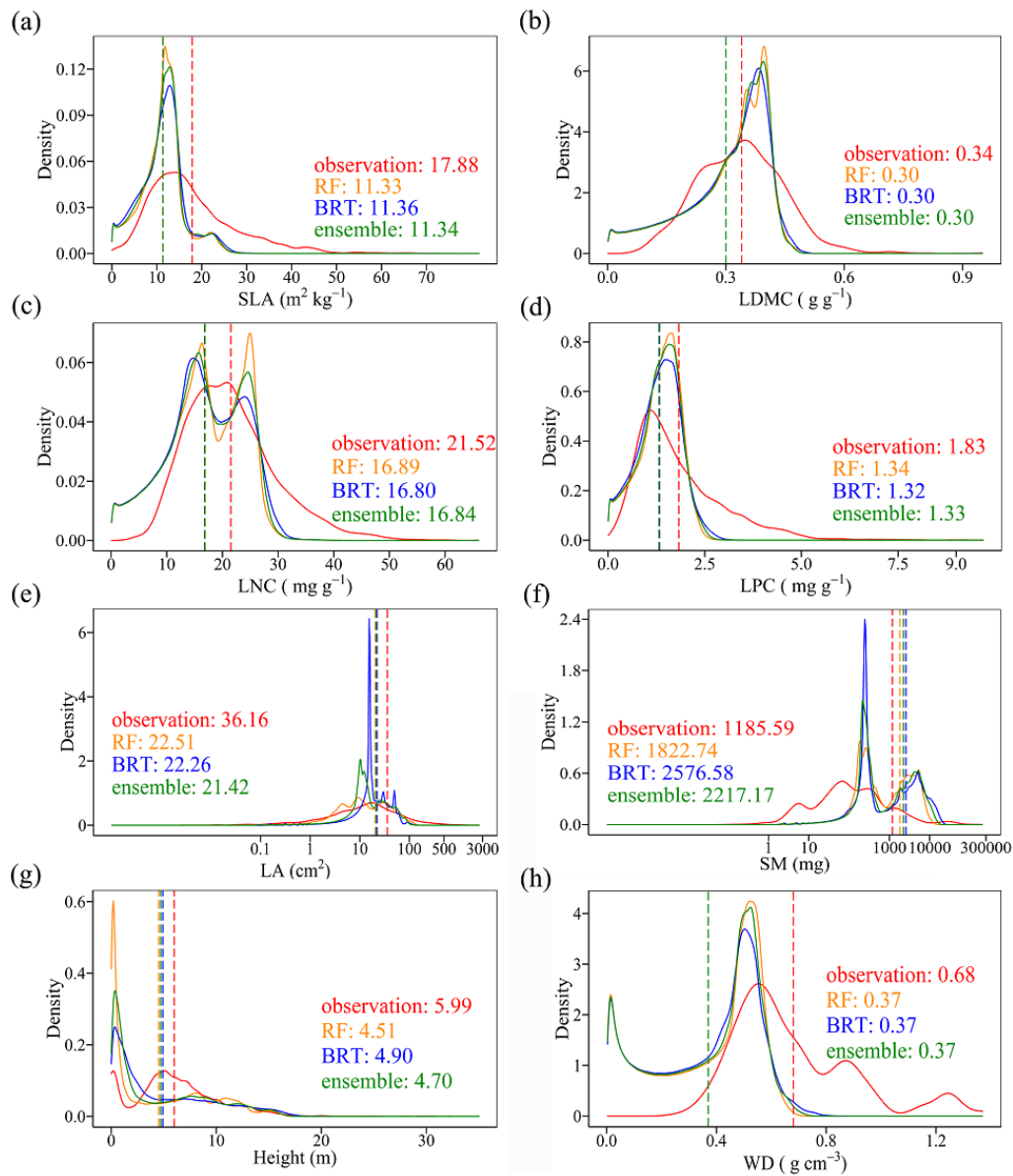
418 **Table 3** List of the eight most important variables for plant functional trait predictions.

Rank	SLA	LDMC	LNC	LPC	LA	SM	Height	WD
1	SAP	MAT	PS	MDR	EVI5	EVI8	PEQ	MIR1
2	TS	Elevation	SAP	PDQ	PEQ	SAP	EVI6	TS
3	blue9	MTCI5	pH	Elevation	MTCI9	MAT	MTCI6	MIR5
4	RAD	blue8	MDR	MIR8	NIR9	RAD	RAD	RAD
5	MTCI4	MTCI4	MAP	Tmax	AI	NIR1	pH	MIR6
6	MTCI6	MTCI6	PEQ	MTCI6	MTCI6	NIR8	MAP	pH
7	Elevation	NIR1	MIR1	MIR7	MAP	SAND	red9	red5
8	MTCI7	CEC	Tmax	MIR9	red5	BD	red5	PS

419 SLA, specific leaf area ($\text{m}^2 \text{kg}^{-1}$); LDMC, leaf dry matter content (g g^{-1}); LNC, leaf N ~~concentration~~ (mg
 420 ~~g⁻¹)eoneertation~~; LPC, leaf P ~~concentration~~ (mg g^{-1})eoneertation; LA, leaf area (cm^2); WD, wood density
 421 (g cm^{-3}); ~~SM, seed mass~~; SAP, soil available P; TS, temperature seasonality; blue, blue reflectance; RAD,
 422 solar radiation; MTCI, MERIS terrestrial chlorophyll index; MAT, mean annual temperature; NIR, near-
 423 infrared reflectance; CEC, cation exchange capacity; PS, precipitation seasonality; MDR, mean diurnal
 424 range; MAP, mean annual precipitation; PEQ, precipitation of wettest quarter of a year; MIR, middle
 425 infrared reflectance; Tmax, max temperature of warmest month of a year; PDQ, precipitation of driest
 426 quarter of a year; EVI, enhanced vegetation index; AI, aridity index; red, red reflectance; ~~SAND, soil~~
 427 ~~sand content~~; ~~BD, bulk density~~.

428 3.4 Model performance

429 The distributions of the predictive trait values based on random forest, boosted regression trees, and
 430 ensemble model were consistent with the original trait observations, especially the peak values (Fig.
 431 ~~45~~). ~~Except for SM, t~~The mean values of trait observations were relatively higher than those of the
 432 predictive values.
 433



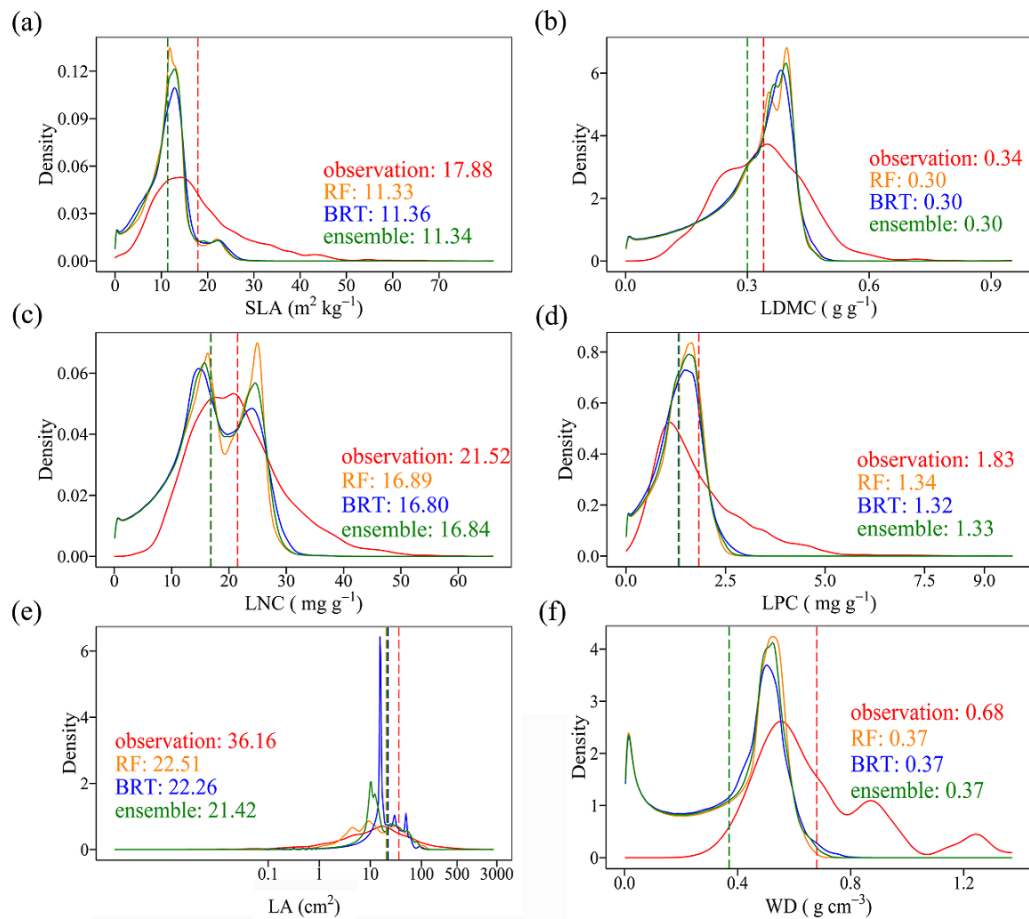
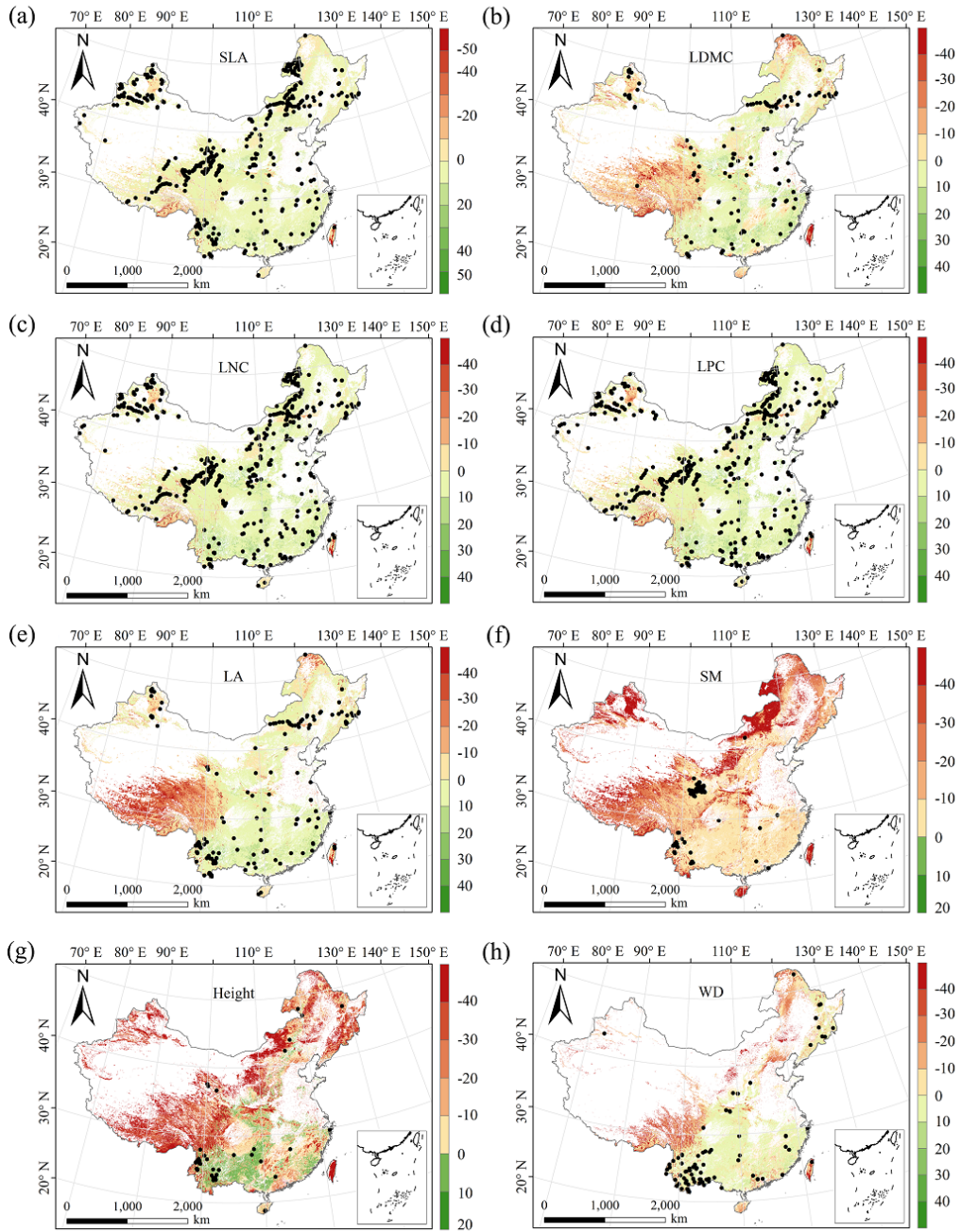


Figure 45. Comparison of trait distribution between observations and predictive values in each of the different models. Each panel depicts the distribution of observations in solid red, of the random forest (RF) model in yellow, of the boosted regression trees (BRT) model in blue, and of the ensemble model in green. The dashed vertical lines indicate mean values. SLA, specific leaf area; LDMC, leaf dry matter content; LNC, leaf N ~~concentration~~; LPC, leaf P ~~concentration~~; LA, leaf area; WD, wood density; ~~SM, seed mass.~~

3.5 Uncertainty assessments

The MESS values of ~~five leaf traits and WD~~ all plant functional traits were positive in most regions, indicating a wide applicability domain of our models (Fig. 56). Nevertheless, trait predictions should be interpreted carefully for northeastern China and the Qinghai-Tibet Plateau due to the sparse samplings in these regions. ~~In addition, spatial predictions for SM and plant height were extrapolated to a larger extent than were the other plant functional traits.~~



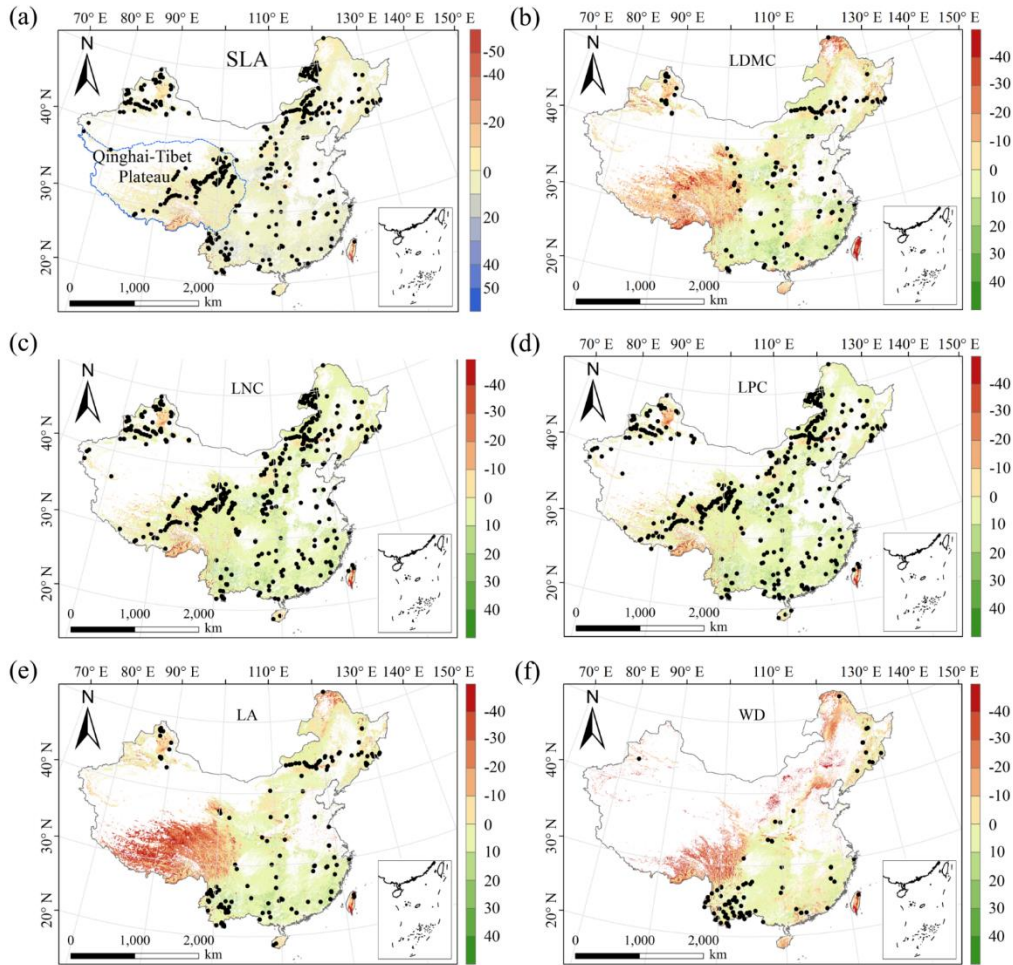


Figure 56. Multivariate environmental similarity surface (MESS) assessments for the eight-six plant functional traits. The black dots represented the locations of trait observations. More intense shades indicate greater similarity (blue) or difference (red) in environmental conditions of the location compared to the predictive factors covered by the training dataset. SLA, specific leaf area; LDMC, leaf dry matter content; LNC, leaf N concentration~~concentration~~; LPC, leaf P concentration~~concentration~~; LA, leaf area; WD, wood density; ~~SM, seed mass.~~

4 Discussion

4.1 Comparison with previous work

Our study predicted the spatial patterns of eight-six key plant functional traits across China using machine learning methods and identified the applicability domain of the models. WD had the highest precision with an R^2 of 0.66, which was higher than the global WD prediction (Boonman et al., 2020). This improvement in precision may be attributed to the large number and dense occurrence of sample sites as well as the inclusion of vegetation indices in our study. In addition, SLA and LPC also showed good accuracy with R^2 values of 0.50, which was higher than that of Boonman et al. (2020) and consistent with that of Moreno-MartínezMartínez et al. (2018). However,

466 LNC and LA showed relatively poor performance, which may be related to the reason that these
467 two traits were more influenced by phylogeny than environmental variables (Yang et al., 2017; An
468 et al., 2021).

469 The frequency distribution of plant functional traits in China differed between our study and
470 previous studies (Fig. 7, Fig. F1, Table F1 in Appendix F). Given that the spatial resolution of trait
471 maps in most previous studies is 0.5° (except for Moreno-Martínez et al. (2018) and Vallicrosa et
472 al. (2022)), we resampled the data products of previous studies and our study to 0.5° spatial
473 resolution. The distribution in our study contained more predictions at lower values of SLA, LNC
474 and LPC and was broader than those for SLA and LNC in previous global studies. However, the
475 distribution of LNC in our study was consistent with that in Vallicrosa et al. (2022) at the 1 km
476 spatial resolution (Fig. F1 in Appendix F). LA in our study contained more predictions at higher
477 values and was also broader than those in previous global studies. WD did not show the lower and
478 higher predictive values, however, the WD values in the studies of Boonman et al. (2020) and
479 Schiller et al. (2021) had more predictions at higher values and no lower values ($< 0.3 \text{ g cm}^{-3}$). Our
480 predicted values of SLA showed the highest spatial correlation with those of Dong et al. (2023), and
481 LNC showed the strongest spatial correlation with those of Butler et al. (2017) (Table 5). LA and
482 WD showed the best spatial correlation with those of Schiller et al. (2021), but LPC showed
483 relatively weak spatial correlation with those of published studies.

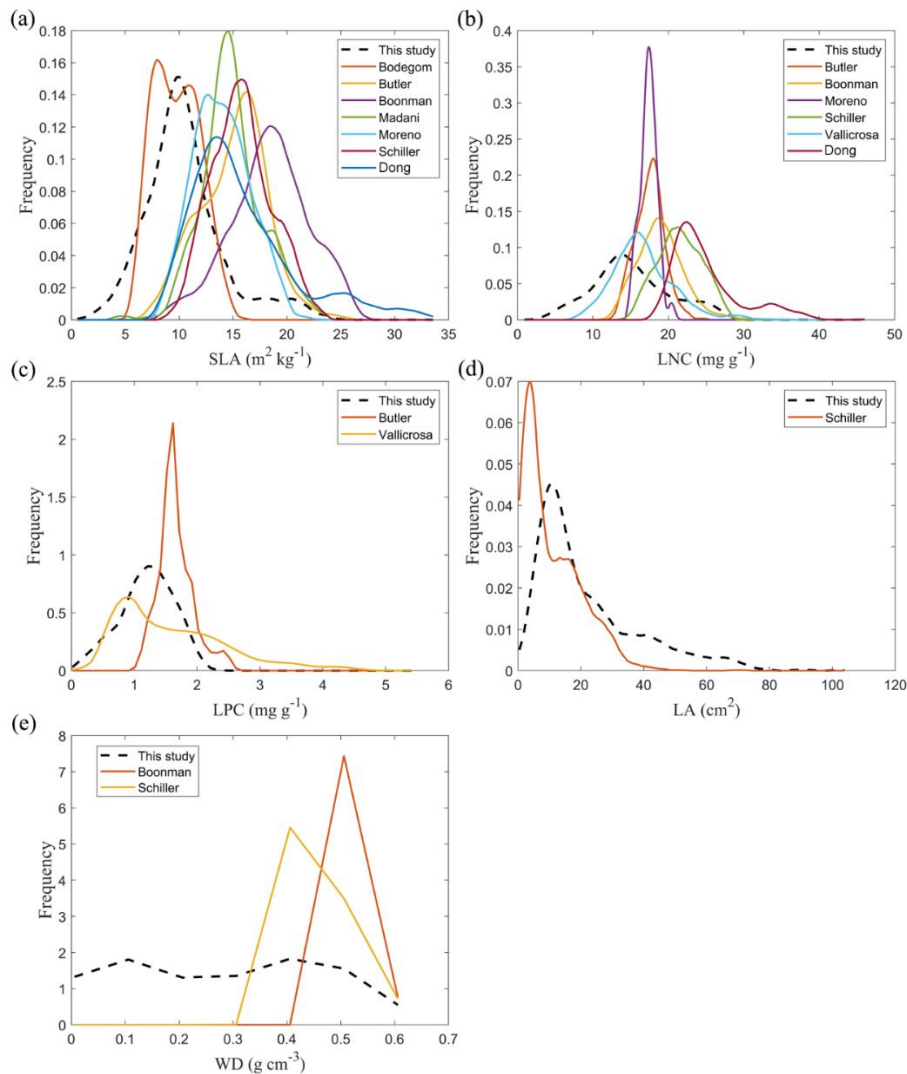
484 Our study also predicted the spatial pattern of SM with an R^2 of 0.24, which was lower than in the
485 global study of Madani et al. (2018) in which environmental variables explained 45.5% of SM
486 variation. The low precision of SM may be explained in two ways. First, with few sampling sites
487 included in our study, the environmental gradients were narrow. Second, previous studies and our
488 unpublished study have suggested that SM variation is primarily controlled by a phylogenetic effect,
489 whereas the environmental effect is weak (Moles et al., 2006). Therefore, phylogenetic relatedness
490 among species should be considered to improve the predictive precision of the spatial pattern of SM
491 in further work.

492 There was no consensus in the spatial patterns of plant functional traits among the global
493 studies. ThusIn addition, we compared our results to the other studies focused on China. Yang et al.
494 (2016) predicted the spatial distribution of leaf mass per area (1/SLA) and LNC based on trait-
495 environment relationships in China and had an R^2 of 0.13-0.16. The lower predictive precision may
496 be because Yang et al. (2016) only used MAT, MAP, and RAD as predictors in estimating the spatial
497 patterns of leaf mass per area and LNC, which likely led to poor performance and low heterogeneity.
498 These results also demonstrated the advantage of our methods in mapping the spatial patterns of
499 plant functional traits at a regional scale.

500 **Table 5** Spatial correlations for SLA, LNC, LPC, LA and WD between this study and other
 501 previous trait maps, labelled by the first author of the corresponding publication (see Table F1 in
 502 Appendix F for citations)

<u>Spatial</u> <u>correlation</u>	<u>Dong</u>	<u>Vallicrosa</u>	<u>Schiller</u>	<u>Boonman</u>	<u>Moreno</u>	<u>Madani</u>	<u>Butler</u>	<u>Bodegom</u>
<u>SLA</u>	<u>0.398</u>		<u>-0.082</u>	<u>0.327</u>	<u>0.242</u>	<u>0.136</u>	<u>-0.042</u>	<u>0.319</u>
<u>LNC</u>	<u>0.156</u>	<u>0.359</u>	<u>0.229</u>	<u>0.252</u>			<u>0.394</u>	
<u>LPC</u>		<u>0.136</u>					<u>0.057</u>	
<u>LA</u>			<u>0.514</u>					
<u>WD</u>			<u>0.647</u>	<u>0.107</u>				

503 The spatial correlation of LDMC between our study and previous study was not included, as the LDMC
 504 maps were not available. SLA, specific leaf area ($\text{m}^2 \text{kg}^{-1}$); LNC, leaf N concentration (mg g^{-1}); LPC,
 505 leaf P concentration (mg g^{-1}); LA, leaf area (cm^2); WD, wood density (g cm^{-3}).



506
 507 **Figure 7.** Frequency distributions of plant functional traits in our study (“This study”, dashed
 508 black lines) and other trait maps, identified by the first author of the corresponding publication (see
 509 Table F1 for citations). SLA, specific leaf area ($\text{m}^2 \text{kg}^{-1}$); LNC, leaf N concentration (mg g^{-1}); LPC,
 510 leaf P concentration (mg g^{-1}); LA, leaf area (cm^2); WD, wood density (g cm^{-3}).

511 4.2 Spatial patterns of plant functional traits in China

512 Our study revealed the spatial patterns of different plant functional traits across China, and the
513 variability among the two machine learning methods was relatively low. We compared the spatial
514 differences of trait maps between our study and previous studies at the global scale. In some regions,
515 there were consistent patterns in plant functional traits between our study and the previous
516 studies(Figs. F2-F6 in Appendix F). For example, our study showed high SLA values in the
517 southeastern Qinghai-Tibet Plateau, which concurred with the global study of Boonman et al. (2020).
518 The spatial difference of SLA between our study and Bodegom et al. (2014) was relatively low, and
519 the predictive values in most regions were slightly lower in our study than those in Bodegom et al.
520 (2014). The spatial pattern of difference in SLA between our study and Moreno et al. (2018), Bulter
521 et al. (2017) and Bodegom et al. (2020) was consistent, and the values were higher in northeastern
522 China and southwestern Qinghai-Tibet Plateau in our study than those studies. Our study showed
523 higher LNC values in the northern Inner Mongolia-the Loess Plateau-the eastern Qinghai-Tibet
524 Plateau and northwestern China than those studies at the global studies (Butler et al., 2017; Moreno-
525 Martínez et al., 2018; Boonman et al., 2020; Vallicrosa et al., 2022; Dong et al., 2023), reflecting
526 the consistent spatial pattern among these studies. However, Yang et al. (2016) predicted high LNC
527 values in northeastern and northwestern China, northern Inner Mongolia and the entire Qinghai-
528 Tibet Plateau, and SLA and LNC had low heterogeneity overall. The discrepancy with Yang et al.
529 (2016) may be attributed to spatial extrapolation based on trait-climate relationships with a low
530 predictive precision. There was no consistent spatial pattern in LPC between our study and previous
531 studies. Consistent with the global pattern (Wright et al., 2017), LA was larger in southern regions
532 than in northern regions and showed a decreasing trend with latitude. In addition, LA and WD values
533 in our study were lower in most regions than those ones at the global scale. These discrepancies
534 between our study and previous studies at the global scale may be related to three reasons. First,
535 there is bias in the available in-situ field measurement data from China in these global studies, with
536 large gaps in western China for SLA and no data in China for WD (Boonman et al., 2020). Second,
537 some trait-environment relationships may be scale dependent (Bruehlheide et al., 2018), and these
538 studies we compared are from the global scale due to the trait maps in China are not available. Third,
539 the methods used for trait mapping were different among studies, including eco-evolutionary
540 optimality models (Dong et al., 2023), Convolutional Neural Networks based on RGB photographs
541 (Schiller et al., 2021), machine learning algorithms (Vallicrosa et al., 2022; Boonman et al., 2020)
542 and multiple regression analysis (Bodegom et al., 2014).
543 Consistent with the global pattern (Wright et al., 2017), LA was larger in southern regions than in
544 northern regions and showed a decreasing trend along a latitudinal gradient. Potapov et al. (2021)
545 mapped global forest canopy height at a spatial resolution of 30 m by integrating GEDI and Landsat
546 data, and their resulting spatial pattern of plant height in China was consistent with our study. This
547 confirms the accuracy and reliability of predicting plant height through spatial extrapolation as in
548 our study. However, in some regions there were contradictory patterns in the plant functional traits

~~between our study and previous ones. Our study showed high LNC values in the northern Inner Mongolia Plateau Loess Plateau eastern Qinghai-Tibet Plateau and high heterogeneity in southern China, whereas Yang et al. (2016) predicted high LNC values in northeastern and northwestern China, northern Inner Mongolia Plateau, and the entire Qinghai-Tibet Plateau, but low heterogeneity overall. In addition, Yang et al. (2016) predicted low SLA variability in China, especially in the Qinghai-Tibet Plateau. These discrepancies may be attributed to spatial extrapolation based on trait-climate relationships with a low predictive precision.~~

Moreover, our study also identified the applicability domain of our models for predicting the spatial patterns of plant functional traits across China. Five leaf traits and WD appeared to have poor applicability in northeastern China and the Qinghai-Tibet Plateau, primarily due to sparse samplings. ~~Although the predictions of plant height and SM were obtained in most regions through spatial extrapolation, the results were consistent with previous studies. This demonstrates the reliability of our methods.~~ Future studies predicting plant functional traits across a large scale through remote sensing observations or other supplementary data will be needed to re-evaluate our results.

4.3 The role of predictive variables

Our study indicates that environmental variables are important for predicting the spatial patterns of plant functional traits, especially climate variables. Temperature variables were primary predictors for SLA, LDMC, LPC and WD. The relationships between leaf traits and temperature have been widely discussed in global and regional studies (Reich and Oleksyn, 2004; Bruelheide et al., 2018). The positive linkage between WD and temperature may be driven by changes in the viscosity of water. Plants can adapt to the low water viscosity at high temperatures by reducing the diameter and density of their vessels and by thickening cell walls (Roderick and Berry, 2002; Thomas et al., 2004). Precipitation variables were important predictors for leaf nutrient traits, ~~and LA, and plant height.~~ For example, precipitation of wettest quarter of a year was the factor that most influenced LA variation, which has been confirmed by a previous study (An et al., 2021). A smaller LA could be an adaptive strategy to decrease water loss via reducing the surface area for transpiration under dry environmental conditions (Du et al., 2019). ~~Water availability emerged as the primary predictor of plant height, which may be explained by the hydraulic limitation hypothesis. Relative to shorter plants, taller plants tend to be at a higher risk of embolisms due to their increased xylem length and conduit width. Thus, tall plants may be forced to close their stomata and reduce the amount of photosynthesis (Renninger et al., 2009; Wang et al., 2019).~~ Although the effects of soil on trait predictions were relatively weak, we found that SAP and pH played key roles in SLA, ~~and LNC and SM~~ predictions. These results were similar with the previous studies that reported that soil pH was an important driver of trait variation at the global scale and in tundra regions (~~Kemppinen et al., 2021;~~ Maire et al., 2015; Kemppinen et al., 2021). Additionally, from the perspective of cost-efficient theory, the strong effects of SAP reflected that high SLA ~~and small seeds~~ may be an adaptation for facilitating soil exploration more efficiently in fertile soils (Freschet et al., 2010).

586 Vegetation indices have recently been proposed as important predictors of spatial patterns of
587 plant functional traits (Loozen et al., 2018). Our results corroborate these findings and further
588 suggest that EVI, MTCI and MIR reflectance are important predictors in models. Here, the
589 underlying mechanisms between vegetation indices and plant functional traits are not further
590 discussed due to their complexity and uncertainty. However, our results indicated that vegetation
591 indices and NIR reflectance are not key predictors of LNC estimation, which contrasts the findings
592 from global and regional studies ([Wang et al., 2016](#); Loozen et al., 2018; Moreno-Martínez et al.,
593 2018; ~~Wang et al., 2016~~). This may be related to the multitude of factors that influence the
594 relationship between LNC and vegetation indices and NIR reflectance, such as forest type and
595 canopy structure (Dahlin et al., 2013).

596 4.4 Uncertainties

597 Although our study mapped the spatial patterns of key functional traits of seed plants in China
598 through large-scale field investigations and compared the predictions with previous studies
599 performed at global and regional scales, there persists some uncertainties in the interpretation of
600 these results. First, the predictive ability of ~~machine learning method models~~ was relatively worse
601 for certain traits, especially ~~for SM and~~ LDMC. Beyond the environmental effects, the variation in
602 plant functional traits is also regulated by phylogenetic structure among plant species (e.g., family,
603 order and phylogenetic clade) (Li et al., 2017). Consequently, incorporating the phylogenetic
604 information will be a promising avenue ~~in future studies~~ for further improving the accuracy of
605 spatial predictions of plant functional traits (Butler et al., 2017). A second potential issue is sampling
606 bias; there were major spatial gaps in field investigation in both the northeastern China and the
607 Qinghai-Tibet Plateau, ~~especially for SM and plant height. There are an increasing number of~~
608 ~~available datasets and studies on SM and plant height, but many did not provide the corresponding~~
609 ~~geographic coordinates, thus rendering the data unusable. In addition, d~~Due to the ~~challenges lack~~
610 of measurements for small shrubs and low vegetation, WD data is mainly confined to eastern forests
611 (~~Perez Harguindeguy et al., 2013~~), and the overall quantity of WD data was much lower than that
612 of leaf ~~and reproductive~~ traits, even in the TRY database, ~~which is the largest trait database in the~~
613 ~~world (Kattge et al., 2020). The environmental information of sampling sites was not always~~
614 ~~obtained from original literature, thus using the public environmental products is a common~~
615 ~~resolution in large-scale plant trait studies (Boonman et al., 2020; Vallicrosa et al., 2022). Such~~
616 ~~mismatch between in-situ trait measurements and predictors should be resolved in further work.~~
617 Finally, additional key challenges in data availability must be resolved to scale up from the species
618 to the community levels, in particular with data surrounding species co-occurrence and their relative
619 cover or abundance in ecological communities (He et al., 2023). Global biodiversity data (e.g., sPlot
620 and Global Biodiversity Information Agency databases) that contains information on species
621 occurrence or the proportion of species in a community has the potential for enabling the calculation
622 of community-weighted trait values and the re-evaluation of our results in future work (Telenius,

2011; Bruelheide et al., 2019). The lack of consistent time period and spatial resolution of predictors due to limitation of data availability is another key challenges in the spatial mapping of plant functional traits. In addition, although Worldclim version 2.1 product has high spatial resolution and includes various aspects of climatic parameters, there exists certain limitation and uncertainty in predicting trait maps. ~~In addition, Therefore,~~ integrating satellite remote sensing monitoring methods with ~~in~~-in-situ trait data collection can also provide an effective way to estimate and assess the species diversity at a large scale (Cavender-Bares et al., 2022).

4.5 Potential applications

Maps of these key functional traits of seed plants highlighted large-scale variability in space, which will significantly advance ecological analyses and future interdisciplinary research. First, using the spatially continuous trait ~~datasets~~maps, one can optimize and develop trait-flexible vegetation models, which allows for the exploration of the community assembly rules based on how plants with different trait combinations perform under a given set of environmental conditions (Berzaghi et al., 2020). When trait-flexible vegetation models are available, incorporating trait maps into models will bridge the gap for vegetation classifications and predictions of vegetation distribution under global change, which is not feasible in conventional vegetation models (Van Bodegom et al., 2012; Yang et al., 2019). Second, the assessments of China's terrestrial ecosystem carbon sink have had large uncertainties so far (Piao et al., 2022), but the spatial continuous trait ~~datasets~~maps will provide an effective way to link ecosystem characteristics to ecosystem carbon sink estimates in China (Madani et al., 2018; Šímová et al., 2019). These analyses will help shed light on the mechanisms underlying plant functional traits and terrestrial ecosystem carbon storage at a large scale.

5 Data availability

The original ~~eight~~ plant functional traits ~~dataset~~data collected in this study that were used for machine learning models (named by Data file used for machine learning models.csv) and final maps of ~~eight~~ plant functional traits in terrestrial ecosystems in a GeoTIFF format across China (named by plant functional trait category) are now available for the private link <https://figshare.com/s/c527c12d310cb8156ed2> (An et al., 2023). Once the article is accepted, we will publicly publish these ~~datasets~~maps at the figshare website.

6 Conclusions

We ~~created~~generated a set of spatial continuous trait ~~datasets~~maps at a 1-km spatial resolution using machine learning methods in combination with field measurements, environmental variables and vegetation indices. Models for leaf traits (except for LDMC), ~~and~~ WD and plant height showed good accuracy and robustness, whereas models of ~~SM and~~ LDMC had relatively poor precision and robustness. Temperature variables were the most important predictors for leaf traits (except for LA)

658 and WD, and precipitation variables were the most important predictors for leaf nutrient traits, ~~and~~
659 ~~LA and plant height~~. We caution that plant functional trait predictions should be interpreted carefully
660 for northeastern China and the Qinghai-Tibet Plateau. The spatial continuous trait ~~datasets maps~~
661 generated in our study are complementary to current terrestrial in-situ observations and offer new
662 avenues for predicting large-scale changes in vegetation and ecosystem function under climate
663 scenarios in China.

664

665 **Appendix A Data collection from literature**

666 An H. and Shangguan Z. P. Photosynthetic characteristics of dominant plant species at different succession stages of
667 vegetation on Loess Plateau. Chinese Journal of Applied Ecology, 2007, 18, 1175-1180.

668 Bai K. D., Jiang D. B., Wan C. X. Photosynthesis-nitrogen relationship in evergreen and deciduous tree species at
669 different altitudes on Mao'er Mountain, Guangxi. Acta Ecologica Sinica, 2013, 33, 4930-4938.

670 Bai W. J., Zheng F. L., Dong L. L., et al. Leaf traits of species in different habits in the water-wind erosion region of
671 the Loess Plateau. Acta Ecologica Sinica, 2010, 30, 2529-2540.

672 Chai Y. F., Shang H. L., Zhang X. F., et al. Ecological variations of woody species along an altitudinal gradient in
673 the Qinling Mountains of Central China: area-based versus mass-based expression of leaf traits. Journal of
674 Forestry Research, 2021, 32, 599-608.

675 Chang Y. N., Zhong Q. L., Cheng D. L., et al. Stoichiometric characteristics of C, N, P and their distribution pattern
676 in plants of *Castanopsis carlesii* natural forest in Youxi. Journal of Plant Resources and Environment, 2013, 22,
677 1-10.

678 Chen F. Y., Luo T. X., Zhang L., et al. Comparison of leaf construction cost in dominant tree species of the evergreen
679 broadleaved forest in Julian Mountain, Jiangxi Province. Acta Ecologica Sinica, 2006, 26, 2485-2493.

680 Chen H. Y., Huang Y. M., He K. J., et al. Temporal intraspecific trait variability drives responses of functional
681 diversity to interannual aridity variation in grasslands. Ecology and Evolution, 2018, 9, 5731-5742.

682 Chen L. X., Xiang W. H., Wu H. L., et al. Tree growth traits and social status affect the wood density of pioneer
683 species in secondary subtropical forest. Ecology and Evolution, 2017, 7, 5366-5377.

684 Chen L., Yang X. G., Song N. P., et al. Leaf water uptake strategy of plants in the arid-semiarid region of Ningxia.
685 Journal of Zhejiang University, 2013, 39, 565-574.

686 Chen Y. H., Han W. X., Tang L. Y., et al. Leaf nitrogen and phosphorus concentrations of woody plants differ in
687 responses to climate, soil and plant growth form. Ecography, 2011, 36, 178-184.

688 ~~Chen Y. S., Zhou S. B., Ou Z. L., et al. Seed mass variation in common plant species in Wanfoshan Natural~~
689 ~~Reservation Region, Anhui, China. Chinese Journal of Plant Ecology, 2012, 36, 739-746.~~

690 ~~Chen Z. H., Peng J. F., Zhang D. M., et al. Seed germination and storage of woody species in the lower subtropical~~
691 ~~forest. Acta Botanica Sinica, 2002, 44, 1469-1476.~~

692 Cheng J. H., Chu P. F., Chen D. M., et al. Functional correlations between specific leaf area and specific root length
693 along a regional environmental gradient in Inner Mongolia grasslands. Functional Ecology, 2016, 30, 985-997.

694 Cheng W., Yu C. H., Xiong K. N., et al. Leaf functional traits of dominant species in karst plateau-canyon areas.
695 Guihaia, 2019, 39, 1039-1049.

696 Dong H. and Shekhar R. B. Negative relationship between interspecies spatial association and trait dissimilarity.
697 Oikos, 2019, 128, 659-667.

698 Dong T. F., Feng Y. L., Lei Y. B., et al. Comparison on leaf functional traits of main dominant woody species in wet
699 and dry habitats. Chinese Journal of Ecology, 2012, 31, 1043-1049.

700 Du H. D. Ecological responses of foliar anatomical structural & physiological characteristics of dominant plants at
701 different site conditions in north Shaanxi Loss Plateau. 2010, Graduation Thesis.

702 Fan Z. X., Zhang S. B., Hao G. Y., et al. Hydraulic conductivity traits predict growth rates and adult stature of 40
703 Asian tropical tree species better than wood density. *Journal of Ecology*, 2012, 100, 732-741.

704 Feng J B., Fan S. X., Hou Y. F., et al. Interspecific and intraspecific variation of leaf function traits of herbaceous
705 plants in a forest-steppe zone, Hebei Province, China. *Journal of Northeast Forestry University*, 2021, 49, 23-
706 28.

707 Feng Q. H. The study on the response of foliar $\delta^{13}C$ of different life form plants to altitude in subalpine area of
708 Western Sichuan, China. 2011, Graduation Thesis.

709 Fu P. L., Zhu S. D., Zhang J. L., et al. The contrasting leaf functional traits between a karst forest and a nearby non-
710 karst forest in south-west China. *Functional Plant Biology*, 2019, 46, 907-915.

711 Gao S. P., Li J. X., Xu M. C., et al. Leaf N and P stoichiometry of common species in successional stages of the
712 evergreen broad-leaved forest in Tiantong National Forest Park, Zhejiang Province, China. *Acta Ecologica
713 Sinica*, 2007, 27, 947-952.

714 Geekiyana N., Goodale, U. M., Cao, K. F., et al. Leaf trait variations associated with habitat affinity of tropical
715 karst tree species. *Ecology and Evolution*, 2017, 8, 286-295.

716 Geng Y., Ma W. H., Wang L., et al. Linking above- and belowground traits to soil and climate variables: an integrated
717 database on China's grassland species. *Ecology*, 2017, 98, 1471.

718 ~~Gong H. D., Tang C. Z. and Wang B. Post-dispersal seed predation and its relations with seed traits: a thirty species-
719 comparative study. *Plant Species Biology*, 2015, 30, 193-201.~~

720 Guo F. C. The photosynthetic characteristics of precious broad-leaved tree species in south subtropics and their
721 relationship with leaf functional traits. 2015, Graduation Thesis.

722 Guo W. J. Exploring the relationship between arbuscular mycorrhizal fungi and plant based on phylogeny and plant
723 traits. 2015, Graduation Thesis.

724 ~~Guo Z. W., Zhao W. X., Luo J. F., et al. The variation characteristics of plant functional traits among 16 woody plants
725 in subtropical broad-leaved forest at Dagang Mountain. *Journal of Fujian Normal University (Natural Science
726 Edition)*, 2019, 35, 82-87.~~

727 Hau C. H. Tree seed predation on degraded hillsides in Hong Kong. *Forest Ecology & Management*. 1997, 99, 215-
728 221.

729 He J. S., Wang Z. H., Wang X. P., et al. A test of the generality of leaf trait relationships on the Tibetan Plateau. *New
730 Phytologist*, 2006, 170, 835-848.

731 He P. C., Wright I. J., Zhu S. D., et al. Leaf mechanical strength and photosynthetic capacity vary independently
732 across 57 subtropical forest species with contrasting light requirements. *New Phytologist*, 2019, 223, 607-618.

733 He Y. T. Studies on physioecological traits of 30 plant species in the Subalpine Meadow of the Qinling Mountains.
734 2007, Graduation Thesis.

735 Hou M M. Adaptive evolution of some species from sedges (*Carex Cyperaceae*) based on phylogeny and leaf
736 functional traits to habitat in the Poyang Lake Area. 2017, Graduation Thesis.

737 Hou Y., Liu M. X., Sun H. R., et al. Response of plant leaf traits to microhabitat change in a subalpine meadow on
738 the eastern edge of Qinghai-Tibetan Plateau, China. *Chinese Journal of Applied Ecology*, 2017, 28, 71-79.

739 Hu Z. Z., Michaletz S. T., Johnson D. J., et al. Traits drive global wood decomposition rates more than climate.
740 *Global Change Biology*, 2018, 24, 5259-5269.

741 Hua L., He P., Goldstein G., et al. Linking vein properties to leaf biomechanics across 58 woody species from a
742 subtropical forest. *Plant Biology*, 2019, 22, 212-220.

743 Huang J. J. and Wang X. H. Leaf nutrient and structural characteristics of 32 evergreen broad-leaved species. *Journal*

744 of East China Normal University (Natural Science), 2003, 1, 92-97.

745 Huang Y. L. The research about the turnover patterns and moisture adaptation mechanism of major species on the
746 South-North-facing slope. 2012, Graduation Thesis.

747 Iida Y., Kohyama T. S., Swenson N. G., et al. Linking functional traits and demographic rates in a subtropical tree
748 community: the importance of size dependency. *Journal of Ecology*, 2014, 102, 641-650.

749 Jia Q. Q. Functional traits of fine roots and their relationship with leaf traits of 50 major species in a subtropical
750 forest in Gutianshan. 2011, Graduation Thesis.

751 Jiang Y., Chen X., Ma J., et al., Interspecific and intraspecific variation in functional traits of subtropical evergreen
752 and deciduous broadleaved mixed forests in karst topography, Guilin, Southwest China. *Tropical Conservation
753 Science*, 2016, 9.

754 Jin Y., Wang C. K., Zhou Z. H., et al. Co-ordinated performance of leaf hydraulics and economics in 10 Chinese
755 temperate tree species. *Functional Plant Biology*, 2016, 43, 1082-1090.

756 Jing G. H. Responses of grassland community structure and functions to management practices on the semi-arid area
757 of Loess Plateau. 2017, Graduation Thesis.

758 Kang M. Spatial distribution pattern and its causes of woody plant functional traits in Tiantong region, Zhejiang
759 Province. 2012, Graduation Thesis.

760 Krober W., Li Y., Hardtle W., et al. Early subtropical forest growth is driven by community mean trait values and
761 functional diversity rather than the abiotic environment. *Ecology and Evolution*, 2015, 5, 3541-3556.

762 Krober W., Bohnke M., Welk E., et al. Leaf trait-environment relationships in a subtropical broadleaved forest in
763 south-east China. *PloS One*, 2012, 7, e35742.

764 Krober W., Zhang, S. R. Ehmgig, M., et al. Linking xylem hydraulic conductivity and vulnerability to the leaf
765 economics spectrum-a cross-species study. *PloS One*, 2014, e109211.

766 Li F. Comparison of functional traits in semi-humid evergreen broad-leaved in Western Hill of Kunming. 2011,
767 Graduation Thesis.

768 ~~Li H. Response of plant community functional traits to karst mountain tourism and its maintenance mechanism —A
769 case study of Shi Bing World Natural Heritage Site in Guizhou. 2019, Graduation Thesis.~~

770 Li K. and Xiang W. H. Comparison of specific leaf area, SPAD value and seed mass among subtropical tree species
771 in hilly area of Central Hunan, China. *Journal of Central South University of Forestry & Technology*, 2011, 31,
772 213-218.

773 Li L., McCormack M. L., Ma C.G., et al. Leaf economics and hydraulic traits are decoupled in five species-rich
774 tropical-subtropical forests. *Ecology Letters*, 2015, 18, 899-906.

775 Li Q. Leaf functional traits and their relationships with environmental factors in Beishan Mountain of Jinhua,
776 Zhejiang Province. 2020, Graduation Thesis.

777 Li S. J., Su P. X., Zhang H. N., et al. Characteristics and relationships of foliar water and leaf functional traits of
778 desert plants. *Plant Physiology Journal*, 2013, 49, 153-160.

779 Li W. H., Xu F. W., Zheng S. X., et al. Patterns and thresholds of grazing-induced changes in community structure
780 and ecosystem functioning: species-level responses and the critical role of species traits. *Journal of Applied
781 Ecology*, 2017, 54, 963-975.

782 Li W. Q., Xu Q., Li J., et al. Quantification of ecotone width of returned forest land from farmland based on specific
783 leaf area. *Journal of West China Forestry Science*, 2017, 46, 117-121.

784 Li X. F., Pei K. Q., Kery M., et al. Decomposing functional trait associations in a Chinese subtropical forest. *PloS
785 One*, 2017, 12, e0175727.

786 Li X. F., Schmid B., Wang F., et al. Net assimilation rate determines the growth rates of 14 species of subtropical
787 forest trees. *PloS One*, 2016, 11, e0150644.

- 788 Li X. L., Li X. H., Jiang D. M., et al. Leaf morphological characters of 22 compositae herbaceous species in Horqin
789 sandy land. Chinese Journal of Ecology, 2005, 24, 1397-1401.
- 790 Li Y. H., Luo T. X., Lu Q., et al. Comparisons of leaf traits among 17 major plant species in Shazhuyu Sand Control
791 Experimental Station of Qinghai Province. Acta Ecologica Sinica, 2005, 25, 994-999.
- 792 Li Y. L., Meng Q. T., Zhao X. Y., et al. Relationships of fresh leaf traits and leaf litter decomposition in Kerqin Sandy
793 Land. Acta Ecologica Sinica, 2008, 28, 2486-2494.
- 794 Li Y., Yao J., Yang S., et al. Trait differences research on leaf function of Liaodong oak forest main species in
795 Dongling mountain. Guangdong Agricultural Sciences, 2012, 23, 159-162, 171.
- 796 Liang X. Y., Ye Q., Liu H., et al. Wood density predicts mortality threshold for diverse trees. New Phytologist, 2021,
797 229, 3053-3057.
- 798 Li, R., Zhu, S., Chen, H. Y. H., et al. Are functional traits a good predictor of global change impacts on tree species
799 abundance dynamics in a subtropical forest? Ecology Letters, 2015, 18, 1181-1189.
- 800 Li Y. Y., Shi H., Shao M. A. Cavitation resistance of dominant trees and shrubs in Loess hilly region and their
801 relationship with xylem structure. Journal of Beijing Forestry University, 2010, 32, 8-13.
- 802 Lin G. G., Guo, D. L., Li, L., et al. Contrasting effects of ectomycorrhizal and arbuscular mycorrhizal tropical tree
803 species on soil nitrogen cycling: the potential mechanisms and corresponding adaptive strategies. Oikos, 2018,
804 127, 518-530.
- 805 Liu C. H. and Li Y. Y. Relationship between leaf traits and PV curve parameters in the typical deciduous woody
806 plants occurring in Southern Huanglong Mountain. Journal of Northwest Forestry University, 2013, 28, 1-5.
- 807 Liu G. F., Freschet G. T., Pan X., et al. Coordinated variation in leaf and root traits across multiple spatial scales in
808 Chinese semi-arid and arid ecosystems. New Phytologist, 2010, 188, 543-553.
- 809 Liu G. F., Wang L., Jiang L., et al. Specific leaf area predicts dryland litter decomposition via two mechanisms.
810 Journal of Ecology, 2017, 106, 218-229.
- 811 Liu J. H., Zeng D. H. and Don K. L. Leaf traits and their interrelationships of main plant species in southeast Horqin
812 sandy land. Chinese Journal of Ecology, 2006, 25, 921-925.
- 813 Liu J. X., Chen J., Jiang M. X., et al. Leaf traits and persistence of relict and endangered tree species in a rare plant
814 community. Functional Plant Biology, 2012, 39, 512-518.
- 815 Liu L. H. The traits and adaptive strategies of main herbaceous plants and lianas on micro-topographical units in
816 Huangcangyu reserves of Anhui Province. 2012, Graduation Thesis.
- 817 Liu M. C., Kong D. L., Lu X. R., et al. Higher photosynthesis, nutrient- and energy-use efficiencies contribute to
818 invasiveness of exotic plants in a nutrient poor habitat in northeast China. Physiologia Plantarum, 2017, 160,
819 373-382.
- 820 Liu R. H., Bai J. L., Bao H., et al. Variation and correlation in functional traits of main woody plants in the
821 *Cyclobalanopsis glauca* community in the karst hills of Guilin, southwest China. Chinese Journal of Plant
822 Ecology, 2020, 44, 828-841.
- 823 Liu W. D., Su J. R., Li S. F., et al. Stoichiometry study of C, N and P in plant and soil at different successional stages
824 of monsoon evergreen broad-leaved forest in Pu'er, Yunnan Province. Acta Ecologica Sinica, 2010, 30, 6581-
825 6590.
- 826 Liu X. C., Jia H. B., Wang Q. Y. Genetic variation and correlation in wood properties of *Betula platyphlla* in natural
827 Stands. Journal of Northeast Forestry University, 2018, 36, 8-10.
- 828 Liu Y. Y. Spatial distribution and habitat associations of trees in a typical mixed broad-leaved Korean pine (*Pinus*
829 *koraiensis*) forest. 2014, Graduation Thesis.
- 830 ~~Liu Z. M., Li R. M., Li X. H., et al. A comparative study of seed weight of 69 plant species in Horqin sandyland,~~
831 ~~China. Acta Phytocologica Sinica, 2004, 28, 225-230.~~

- 832 Luo Y. H., Cadotte M. W., Burgess K. S., et al. Greater than the sum of the parts: how the species composition in
833 different forest strata influence ecosystem function. *Ecology Letters*, 2019, 22, 1449-1461.
- 834 Lv J. Z., Miao Y. M., Zhang H. F., et al. Comparisons of leaf traits among different functional types of plant from
835 Huoshan Mountain in the Shanxi Province. *Plant Science Journal*, 2010, 28, 460-465.
- 836 Ma J., Wu L. F., Wei X., et al. Habitat adaptation of two dominant tree species in a subtropical monsoon forest: leaf
837 functional traits and hydraulic properties. *Guihaia*, 2015, 35, 261-268.
- 838 Mo J. M., Zhang D. Q., Huang Z. L., et al. Distribution pattern of nutrient elements in plants of Dinghushan Lower
839 Subtropical Evergreen Broad-Leaved Forest. *Journal of Tropical and Subtropical Botany*, 2000, 8, 198-206.
- 840 Niu C. Y., Meinzer F. C. and Hao G. Y. Divergence in strategies for coping with winter embolism among co-occurring
841 temperate tree species: the role of positive xylem pressure, wood type and tree stature. *Functional Ecology*,
842 2017, 31, 1550-1560.
- 843 Niu D. C., Li Q., Jiang S. G., et al. Seasonal variations of leaf C:N:P stoichiometry of six shrubs in desert of China's
844 Alxa Plateau. *Chinese Journal of Plant Ecology*, 2013, 37, 317-325.
- 845 Niu K. C., He J. S. and Lechowicz M. J. Grazing-induced shifts in community functional composition and soil
846 nutrient availability in Tibetan alpine meadows. *Journal of Applied Ecology*, 2016, 53, 1554-1564.
- 847 Niu K. C., Zhang S. and Lechowicz M. Harsh environmental regimes increase the functional significance of
848 intraspecific variation in plant communities. *Functional Ecology*, 2020, 34, 1666-1677.
- 849 Niu S. L. Photosynthesis research on the predominant legume species in Hunshandak Sandland. 2004, Graduation
850 Thesis.
- 851 Qi L. X. Response of leaf traits of *Pinus mongoliensis* and *Pinus massoniana* to elevation gradient in Daiyun
852 Mountain. 2015, Graduation Thesis.
- 853 ~~Qian H., Niklas K. J., Yang D. M., et al. The effect of twig architecture and seed number on seed size variation in
854 subtropical woody species. *New Phytologist*, 2009, 183, 1212-1221.~~
- 855 Ren Q. J., Li Q. J., Bu H. Y., et al. Comparison of physiological and leaf morphological traits for photosynthesis of
856 the 51 plant species in the Maqu alpine swamp meadow. *Chinese Journal of Plant Ecology*, 2015, 39, 593-603.
- 857 Ren Y. T. The study of leaf functional traits of typical plants across the Alashan Desert. 2017, Graduation Thesis.
- 858 Ren Y., Wei C. G. and Guo X. Y. Comparison on leaf function traits of six kinds of plant in Ordos. *Journal of Inner
859 Mongolia Forestry Science & Technology*, 2019, 45, 43-46, 55.
- 860 Rios R. S., Salgado-Luarte C. and Gianoli E. Species divergence and phylogenetic variation of ecophysiological
861 traits in lianas and trees. *PloS One*, 2007, 9, e99871.
- 862 Shang K. K. Differentiation and maintenance of relict deciduous broad-leaved forest patterns along micro-
863 topographic gradient in subtropical area, East China. 2011, Graduation Thesis.
- 864 Song Y T. Study on functional plant ecology in Songnen Grassland Northeast China. 2012, Graduation Thesis.
- 865 Song Y T., Zhou D. W., Li Q., et al. Leaf nitrogen and phosphorus stoichiometry in 80 herbaceous plant species of
866 Songnen grassland in Northeast China. *Chinese Journal of Plant Ecology*, 2012, 36, 222-230.
- 867 Tan X. Y. Research on leaf functional diversity of forest communities in rainy area of south-west China. 2014,
868 Graduation Thesis.
- 869 Tang Q. Q. Variation in functional traits of plants in the Subtropical Evergreen and Deciduous Broad-leaved Mixed
870 Forest. 2016, Graduation Thesis.
- 871 Tang Y. Inter-specific variations and relationship in leaf traits of major temperate species in northern China. 2011,
872 Graduation Thesis.
- 873 Tao J. P., Zuo J., He Z., et al. Traits including leaf dry matter content and leaf pH dominate over forest soil pH as
874 drivers of litter decomposition among 60 species. *Functional Ecology*, 2019, 33, 1798-1810.
- 875 Tian M., Yu G. R., He N. P., et al. Leaf morphological and anatomical traits from tropical to temperate coniferous

876 forests: Mechanisms and influencing factors. *Scientific Reports*, 2016, 6, 19703.

877 Wang B. Analysis of leaf functional traits of 13 species trees in northwestern Fujian Province. 2019, Graduation
878 Thesis.

879 Wang B. B. A study on ecological stoichiometry of six kinds of dominant shrubs in Huangcangyu Nature Reserve.
880 2015, Graduation Thesis.

881 Wang G. H. Leaf trait co-variation, response and effect in a chronosequence. *Journal of Vegetation Science*, 2007,
882 18, 563-570.

883 Wang G. H., Liu J. L. and Meng T. T. Leaf trait variation captures climate differences but differs with species
884 irrespective of functional group. *Journal of Plant Ecology*, 2015, 8, 61-69.

885 ~~Wang H. F. and Xu M. Individual size variation reduces spatial variation in abundance of tree community assemblage,
886 not of tree populations. *Ecology and Evolution*, 2017, 7, 10815-10828.~~

887 ~~Wang J. H., Chen W., Baskin C. C., et al. Variation in seed germination of 86 subalpine forest species from the
888 eastern Tibetan Plateau: phylogeny and life-history correlates. *Ecological Research*, 2012, 27, 453-465.~~

889 Wang J. Y., Wang S. Q., Li R. L., et al. C:N:P stoichiometric characteristics of four forest types' dominant tree species
890 in China. *Chinese Journal of Plant Ecology*, 2011, 35, 587-595.

891 Wang K. B. Vegetation ecological features and net primary productivity simulation in Yanggou watershed in the
892 Loess hill-gully areas of China. 2011, Graduation Thesis.

893 Wang S. S. The traits and adaptive strategies of main herbaceous plants and lianas on micro-topographical units in
894 Longjishan reserves of Anhui Province. 2016, Graduation Thesis.

895 ~~Wang X. J., Alvarez M., Donohue K., et al. Elevation filters seed traits and germination strategies in the eastern
896 Tibetan Plateau. *Ecography*, 2021, 44, 242-254.~~

897 Wei L. P. Variations in functional traits of main tree species along tree-crown in broadleaved Korean Pine Forest in
898 Jiaohe, Jilin Province. 2014, Graduation Thesis.

899 Wei L. P., Hou J. H. and Jiang S. S. Changes of leaf functional traits of two main species along tree height in broad-
900 leaved Korean pine forest. *Guangdong Agricultural Sciences*, 2014, 12, 55-58, 71.

901

902 Wei L. Y. and Shangguan Z. P. Relation between specific leaf areas and leaf nutrient contents of plants growing on
903 slopelands with different farming-abandoned periods in the Loess Plateau. *Acta Ecologica Sinica*, 2008, 28,
904 2526-2535.

905 Wei L. Y., Zhou J. W., Xiao H. G., et al. Variations in leaf functional traits among plant species grouped by growth
906 and leaf types in Zhenjiang, China. *Journal of Forestry Research*, 2011, 28, 241-248.

907 Wu D. H., Pietsch K. A., Staab M., et al. Wood species identity alters dominant factors driving fine wood
908 decomposition along a subtropical plantation forests tree diversity gradient in subtropical plantation forests.
909 *Biotropica*, 2021, 53, 643-657.

910 Wu T. G., Chen B. F., Xiao Y. H., et al. Leaf stoichiometry of trees in three forest types in Pearl River Delta, South
911 China. *Chinese Journal of Plant Ecology*, 2009, 34, 58-63.

912 Xie Y. J. The characteristics of 20 dominant plant functional traits in evergreen broad-leaf forest in Daming Mountain
913 Nature Reserve, Guangxi. 2013, Graduation Thesis.

914 Xu M. F., Ke X. H., Zhang Y., et al. Wood densities of six hardwood tree species in Eastern Guangdong and
915 influencing factors. *Journal of South China Agricultural University*, 2016, 37, 100-106.

916 Xu M. S., Zhao Y. T., Yang X. D., et al. Geostatistical analysis of spatial variations in leaf traits of woody plants in
917 Tiantong, Zhejiang Province. *Chinese Journal of Plant Ecology*, 2016, 40, 48-59.

918 Xu Y. Z. Biomass estimate and storage mechanisms in northern subtropical forest ecosystems, central China. 2016,
919 Graduation Thesis.

920 Xun Y. H., Di X. Y. and Jin G. Z. Vertical variation and economic strategy of leaf trait of major tree species in a
921 typical mixed broadleaved-Korean pine forest. *Chinese Journal of Plant Ecology*, 2020, 44, 730-741.

922 ~~Yan E. R., Milla R., Aarssen L. W., et al. Functional relationships of leafing intensity to plant height, growth form
923 and leaf habit. *Acta Oecologica-International Journal of Ecology*, 2012, 41, 20-29.~~

924 Yan E. R., Wang X. H., Guo M., et al. C:N:P stoichiometry across evergreen broad-leaved forests, evergreen
925 coniferous forests and deciduous broad-leaved forests in the Tiantong region, Zhejiang Province, eastern China.
926 *Chinese Journal of Plant Ecology*, 2010, 34, 48-57.

927 Yang S. The adaptive strategies of main herbaceous plants traits to different micro-topographical units in Dashushan
928 Mountain, Hefei. 2017, Graduation Thesis.

929 Yang Y., Xu X., Xu M., et al. Adaptation strategies of three dominant plants in the trough-valley karst region of
930 northern Guizhou Province, Southwestern China, evidence from associated plant functional traits and
931 ecostochiometry. *Earth and Environment*, 2020, 48, 413-423.

932 Yang Z., Fan S. X., Zhou B. C., et al. Leaf function and soil nutrient differences of dominant tree species on different
933 slope aspects at the south foothills of Taihang Mountains. *Journal of Henan Agricultural University*, 2020, 54,
934 408-414.

935 ~~Yi F. Y., Wang Z. R., Baskin C. C., et al. Seed germination responses to seasonal temperature and drought stress are
936 species specific but not related to seed size in a desert steppe: Implications for effect of climate change on
937 community structure. *Ecology and Evolution*, 2019, 9, 2149-2159.~~

938 Yin Q. L., Wang L., Lei, M. L., et al. The relationships between leaf economics and hydraulic traits of woody plants
939 depend on water availability. *Science of the Total Environment*, 2018, 621, 245-252.

940 Yu Y. H., Zhong X. P. and Chen W. Analysis of relationship among leaf functional traits and economics spectrum of
941 dominant species in northwestern Guizhou Province. *Journal of Forest and Environment*, 2018, 38, 196-201.

942 Yuan S. Preliminary research on plant functional traits and the capability of carbon sequestration of major tree species
943 in Changbai Mountain Area. 2011, Graduation Thesis.

944 Zhang H., Chen H. Y. H., Lian J. Y., et al. Using functional trait diversity patterns to disentangle the scale-dependent
945 ecological processes in a subtropical forest. *Functional Ecology*, 2018, 32, 1379-1389.

946 Zhang J. G., Fu S. L., Wen Z. D., et al. Relationship of key leaf traits of 16 woody plant species in Low Subtropical
947 China. *Journal of Tropical and Subtropical Botany*, 2009, 17, 395-400.

948 Zhang J. L., Poorter L., Cao K. F. Productive leaf functional traits of Chinese savanna species. *Plant Ecology*, 2012,
949 213, 1449-1460.

950 Zhang J. Y. Comparative study on the different plant functional groups leaf traits at the Maoershan Region. 2008,
951 Graduation Thesis.

952 Zhang Q. W., Zhu S. D., Jansen S., et al. Topography strongly affects drought stress and xylem embolism resistance
953 in woody plants from a karst forest in Southwest China. *Functional Ecology*, 2020, 35, 566-577.

954 Zhang S. B. and Cao K. F. Stem hydraulics mediates leaf water status, carbon gain, nutrient use efficiencies and
955 plant growth rates across dipterocarp species. *Functional Ecology*, 2009, 23, 658-667.

956 Zhang S. B., Cao K. F., Fan Z. X., et al. Potential hydraulic efficiency in angiosperm trees increases with growth-
957 site temperature but has no trade-off with mechanical strength. *Global Ecology and Biogeography*, 2013, 22,
958 971-981.

959 ~~Zhang S. T., Du G. Z. and Chen J. K. Seed size in relation to phylogeny, growth form and longevity in a subalpine
960 meadow on the east of the Tibetan Plateau. *Folia Geobotanica*, 2004, 39, 129-142.~~

961 Zhang Y., Ren Y. X., Yao J., et al. Leaf nitrogen and phosphorous stoichiometry of trees in *Pinus tabulaeformis* Carr
962 stands, North China. *Journal of Anhui Agricultural University*, 2012, 39, 247-251.

963 Zhao Y. T., Ali, A. and Yan, E. R. The plant economics spectrum is structured by leaf habits and growth forms across

- 964 subtropical species. *Tree Physiology*, 2016, 37, 173-185.
- 965 Zheng X. J., Li S. and Li Y. Leaf water uptake strategy of desert plants in the Junggar Basin, China. *Chinese Journal*
966 of *Plant Ecology*, 2011, 35, 893-905.
- 967 Zheng Y. M. Carbon, nitrogen and phosphorus stoichiometry of plant and soil in the sandy hills of Poyang Lake.
968 2014, Graduation Thesis.
- 969 Zheng Z. X. Comparison of plant leaf, height and seed functional traits in dry-hot valleys. 2010, Graduation Thesis.
- 970 Zhou J. Y., He J. J., Guo Z. Y., et al. A study on specific leaf area and leaf dry matter content of five dominant species
971 in Xiangshan Mountain, Huaibei City, Anhui Province. *Journal of Huaibei Normal University (Natural*
972 *Sciences)*, 2013, 34, 51-54.
- 973 Zhou X., Zuo X. A., Zhao X. Y., et al. Plant functional traits and interrelationship of 34 plant species in south central
974 Horqin Sandy Land, China. *Journal of Desert Research*, 2015, 35, 1489-1495.
- 975 Zhu B. R., Xu B. and Zhang D. Y. Extent and sources of variation in plant functional traits in grassland. *Journal of*
976 *Beijing Normal University (Natural Science)*, 2011, 47, 485-489.
- 977 Zhu S. D., Song J. J., Li R. H., et al. Plant hydraulics and photosynthesis of 34 woody species from different
978 successional stages of subtropical forests. *Plant Cell and Environment*, 2013, 36, 879-891.
- 979 Zhu X B, Liu Y. M. and Sun S. C. Leaf expansion of the dominant woody species of three deciduous oak forests in
980 Nanjing, East China. *Chinese Journal of Plant Ecology*, 2005, 29, 125-136.

981 **Appendix B**

982 **Table B1** Summary of statistics in plant functional traits, environmental variables and geographical
 983 distribution in China.

Trait	Unit	Range	Mean	CV (%)	No. of species	Entries	Sites
SLA	m ² kg ⁻¹	0.06–81.68	17.88	54.96	2463	9195	1032
LDMC	g g ⁻¹	0.06–0.95	0.34	100.00	1582	3957	193
LNC	mg g ⁻¹	3.41–66.02	21.52	37.44	2335	7407	567
LPC	mg g ⁻¹	0.09–9.70	1.83	62.19	2074	6266	515
LA	cm ²	0.0033–2553.33	36.16	259.64	1838	5976	691
Height	m	0.01–35.00	5.99	67.58	1171	16324	636
WD	g cm ⁻³	0.25–1.37	0.68	33.16	768	1788	639
SM	mg	0.10–201300.00	1185.59	562.32	1163	3080	134
Altitude	m	-144–5454					1541 1430
MAT	°C	-12.07–24.32					1541 1430
MAP	mm	15–2982					1541 1430
Soil total N	g kg ⁻¹	0.11–10.25					1541 1430
Bulk density	g cm ⁻³	0.83–1.45					1541 1430

984 SLA, specific leaf area; LDMC, leaf dry matter content; LNC, leaf N ~~concentration~~~~concentration~~; LPC, leaf P
 985 ~~concentration~~~~concentration~~; LA, leaf area; WD, wood density; ~~SM, seed mass~~; MAT, mean annual temperature; MAP,
 986 mean annual precipitation.

987 **Table B2** List of all the predictors including environment and remote sensing variables used in this study.

Type of variables	Variable name	Abbreviations	Units	Time periods	Spatial resolution	Source
Climate	Mean annual temperature	MAT	°C	1970-2000	1 km	WorldClim version 2.4.1
	Mean diurnal range	MDR	°C	1970-2000	1 km	WorldClim version 2.4.1
	Temperature seasonality	TS	°C	1970-2000	1 km	WorldClim version 2.4.1
	Max temperature of warmest month	Tmin	°C	1970-2000	1 km	WorldClim version 2.4.1
	Min temperature of coldest month	Tmax	°C	1970-2000	1 km	WorldClim version 2.4.1
	Temperature annual range	TAR	°C	1970-2000	1 km	WorldClim version 2.4.1
	Isothermality	IS	%	1970-2000	1 km	WorldClim version 2.4.1
	Mean temperature of wettest quarter	MTEQ	°C	1970-2000	1 km	WorldClim version 2.4.1
	Mean temperature of driest quarter	MTDQ	°C	1970-2000	1 km	WorldClim version 2.1
	Mean temperature of warmest quarter	MTWQ	°C	1970-2000	1 km	WorldClim version 2.1
	Mean temperature of coldest quarter	MTCQ	°C	1970-2000	1 km	WorldClim version 2.1
	Mean annual precipitation	MAP	mm	1970-2000	1 km	WorldClim version 2.1
	Precipitation of wettest month	PEM	mm	1970-2000	1 km	WorldClim version 2.1
	Precipitation of driest month	PDM	mm	1970-2000	1 km	WorldClim version 2.1
	Precipitation seasonality	PS	%	1970-2000	1 km	WorldClim version 2.1
	Precipitation of wettest quarter	PEQ	mm	1970-2000	1 km	WorldClim version 2.1
	Precipitation of driest quarter	PDQ	mm	1970-2000	1 km	WorldClim version 2.1
	Precipitation of warmest quarter	PWQ	mm	1970-2000	1 km	WorldClim version 2.1
	Precipitation of coldest quarter	PCQ	mm	1970-2000	1 km	WorldClim version 2.1
	Aridity index	AI	/	1970-2000	1 km	Global CGIAR-CSI
Solar radiation	RAD	kJ m ⁻² day ⁻¹	1970-2000	1 km	WorldClim version 2.1	
Topography	Elevation	/	m		1 km	SRTM 90m V4.1
Soil	Soil sand content	SAND	%	/	1 km	Shangguan et al. (2013)
	Soil silt content	SILT	%	/	1 km	Shangguan et al. (2013)
	Soil clay content	CLAY	%	/	1 km	Shangguan et al. (2013)
	Bulk density	BD	g cm ⁻³	/	1 km	Shangguan et al. (2013)
	Soil pH	pH	/	/	1 km	Shangguan et al. (2013)

Continued

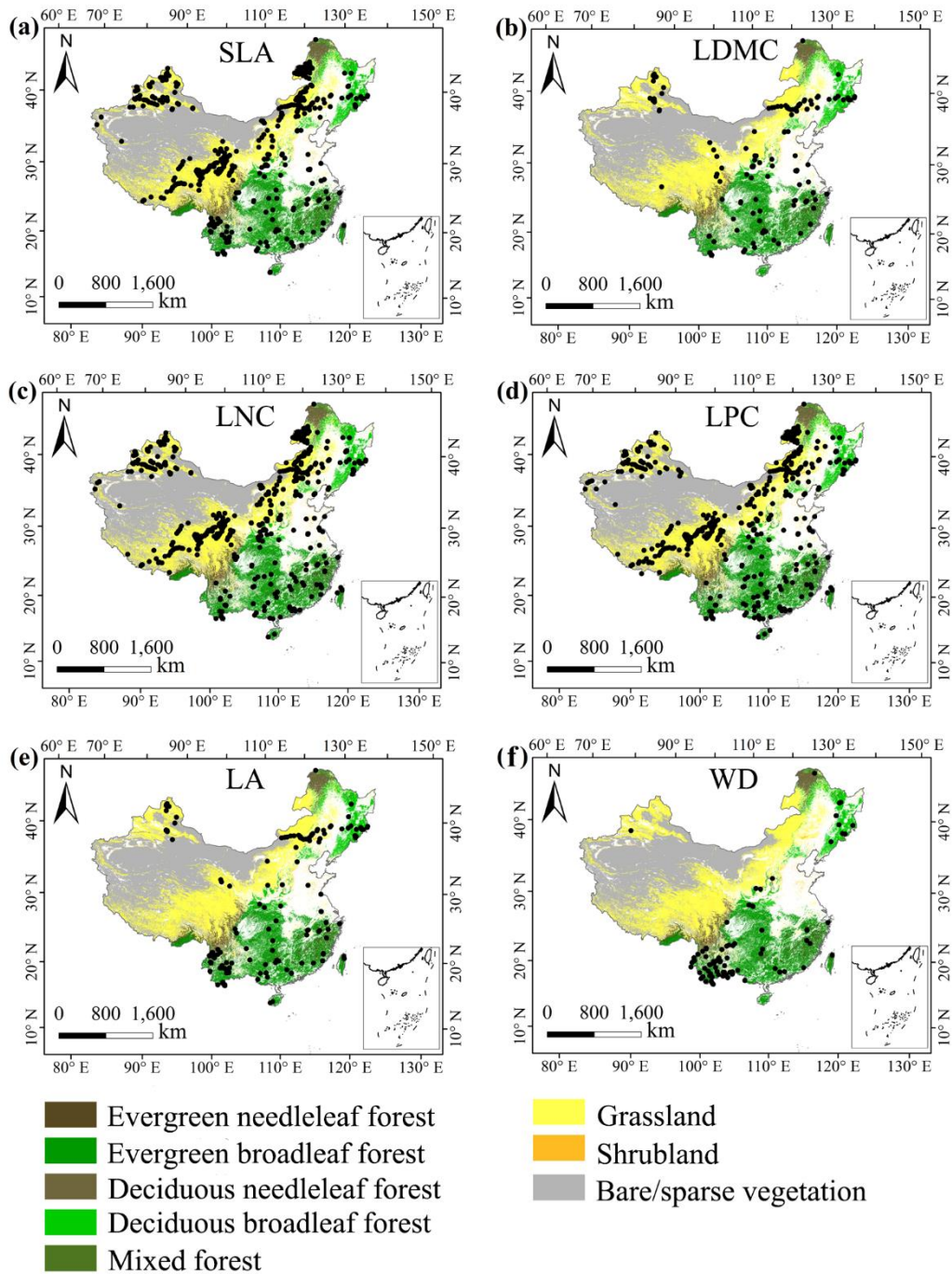
Type of variables	Variable name	Abbreviations	Units	Time periods	Spatial resolution	Source
	Soil organic matter	SOC	g kg ⁻¹	/	1 km	Shangguan et al. (2013)
	Soil total N	STN	g kg ⁻¹	/	1 km	Shangguan et al. (2013)
	Soil total P	STP	g kg ⁻¹	/	1 km	Shangguan et al. (2013)
	Soil alkali-hydrolysable N	SAN	mg kg ⁻¹	/	1 km	Shangguan et al. (2013)
	Soil available P	SAP	mg kg ⁻¹	/	1 km	Shangguan et al. (2013)
	Soil available K	SAK	mg kg ⁻¹	/	1 km	Shangguan et al. (2013)
	Cation exchange capacity	CEC	me kg ⁻¹	/	1 km	Shangguan et al. (2013)
EVI	MODIS EVI long-term monthly averages		/	2001-2018	1 km	MOD13A3 V006
NIR	MODIS NIR long-term monthly averages		/	2001-2018	1 km	MOD13A3 V006
MIR	MODIS MIR long-term monthly averages		/	2001-2018	1 km	MOD13A3 V006
Red	MODIS red long-term monthly averages		/	2001-2018	1 km	MOD13A3 V006
Blue	MODIS blue long-term monthly averages		/	2001-2018	1 km	MOD13A3 V006
MTCI	MTCI long-term monthly averages		/	2003-2011	4.63 km	MTCI level 3 product
Land cover	Land cover map		/	2015	100 m	Copernicus Global Land Service Collection 3

988 The remote sensing variables are calculated as long-term monthly averages from 2001 to 2018. Thus 12 variables of
989 each remote sensing category are obtained.

990 **Table B3** The number of samples of eight plant functional trait used for model training (80%) and
991 validation (20%).

<u>Traits</u>	<u>No. of samples</u>	<u>No. of samples used for</u> <u>model training</u>	<u>No. of samples used for</u> <u>model validation</u>
<u>SLA</u>	<u>9195</u>	<u>7356</u>	<u>1839</u>
<u>LDMC</u>	<u>3957</u>	<u>3166</u>	<u>791</u>
<u>LNC</u>	<u>7407</u>	<u>5926</u>	<u>1481</u>
<u>LPC</u>	<u>6266</u>	<u>5013</u>	<u>1253</u>
<u>LA</u>	<u>5976</u>	<u>4781</u>	<u>1195</u>
<u>WD</u>	<u>1787</u>	<u>1430</u>	<u>357</u>

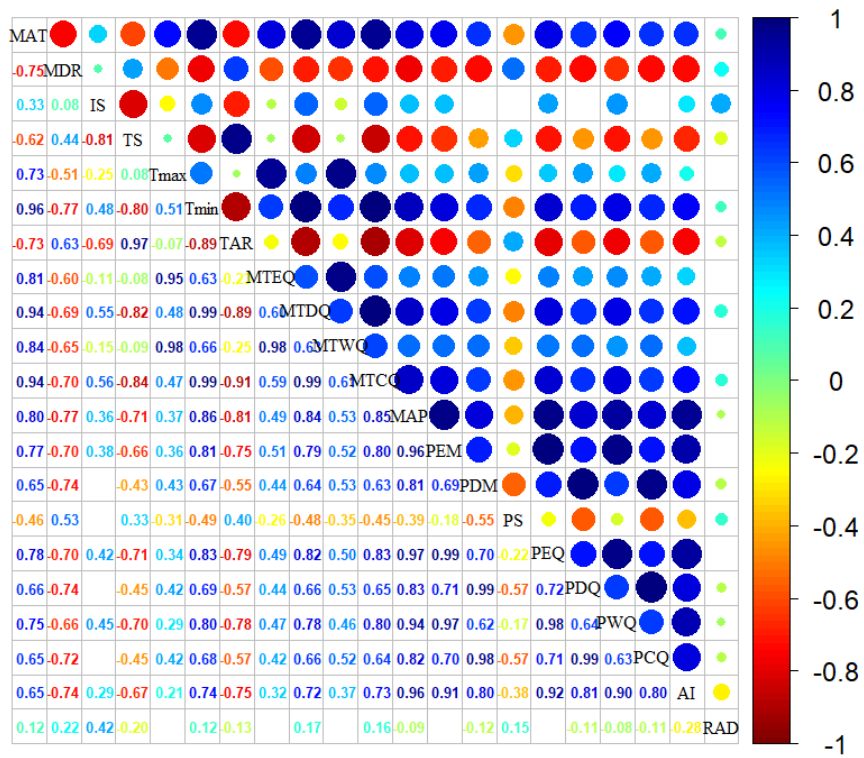
992 SLA, specific leaf area (m² kg⁻¹); LDMC, leaf dry matter content (g g⁻¹); LNC, leaf N concentration (mg
993 g⁻¹); LPC, leaf P concentration (mg g⁻¹); LA, leaf area (cm²); WD, wood density (g cm⁻³).



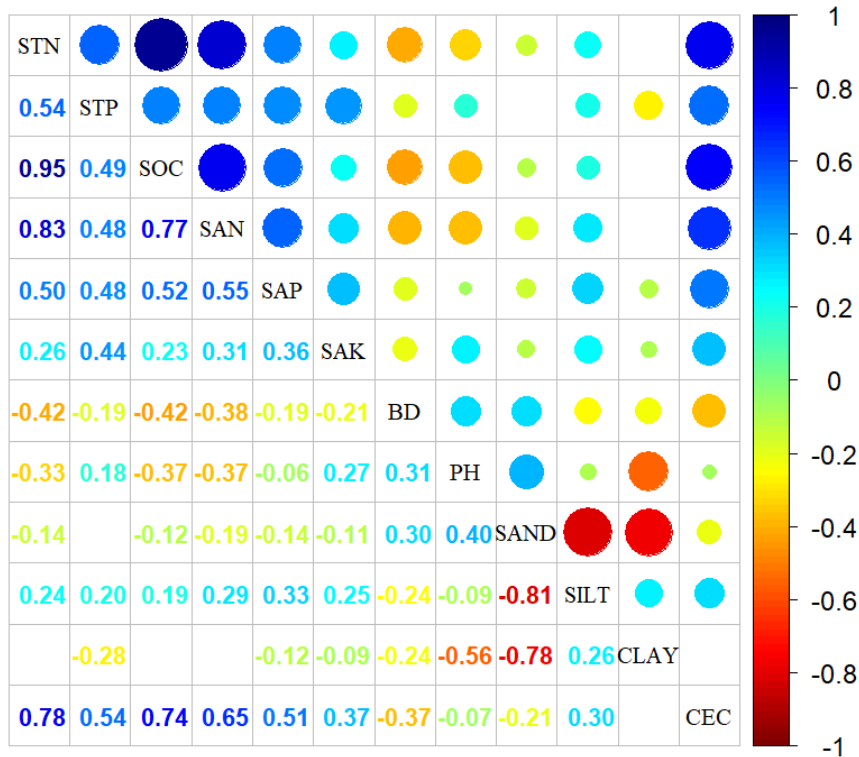
994

995 **Figure B1.** The distribution of sampling site of each plant functional traits across China. The black

996 dots represented the locations of trait observations.

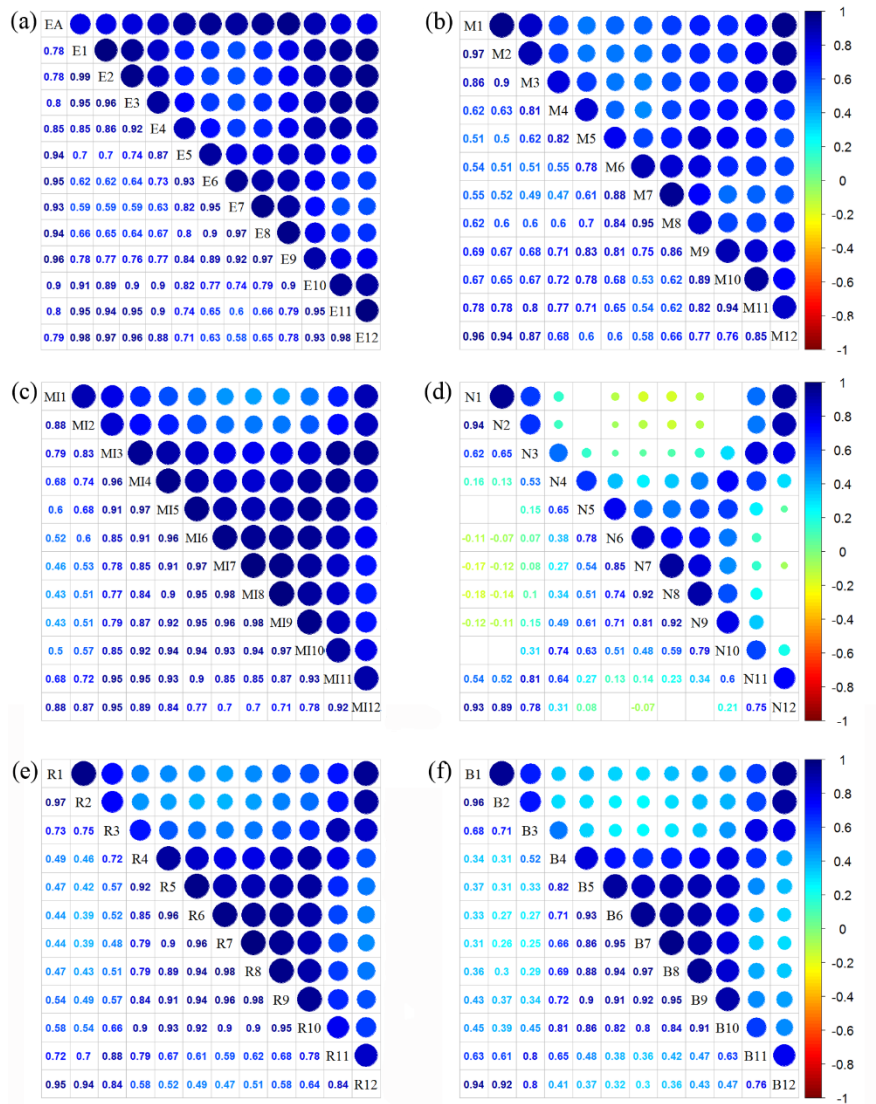


997
998 **Figure B1B2.** Correlations among climate variables. The blank indicates that the correlations are
999 not significant ($P > 0.05$). The size of the circles is proportional to the correlation coefficient. The
1000 abbreviation of climate variables is seen in Table B2.



1001
 1002
 1003
 1004

Figure B2B3. Correlations among soil variables. The blank indicates that the correlations are not significant ($P > 0.05$). The size of the circles is proportional to the correlation coefficient. The abbreviation of soil variables is seen in Table B2.



1005

1006

1007

1008

1009

Figure B3B4. Correlations among monthly remote sensing variables. The blank indicates that the correlations are not significant ($P > 0.05$). The size of the circles is proportional to the correlation coefficient. (a) enhanced vegetation index (EVI); (b) MERIS terrestrial chlorophyll index (MTCI); (c) MIR reflectance; (d) NIR reflectance; (e) red reflectance; (f) blue reflectance.

1010 **Appendix C**

1011 **Table C1** Optimal parameter combination and model performance of random forest (~~RF~~) for plant
 1012 functional traits

Traits	n.tree	mtry	R ²	<u>NRMSE</u>	MAE
SLA	1000	24	0.476	7.0490.22	5.134
LDMC	1000	11	0.234	0.0950.20	0.072
LNC	1000	57	0.392	0.1290.00	0.098
LPC	1000	20	0.587	0.1760.05	0.129
LA	1000	18	0.278	72.9960.48	26.622
Height	1000	38	0.871	0.234	0.178
WD	1000	9	0.531	0.092	0.072
SM	1000	22	0.197	6043.95	1290.866

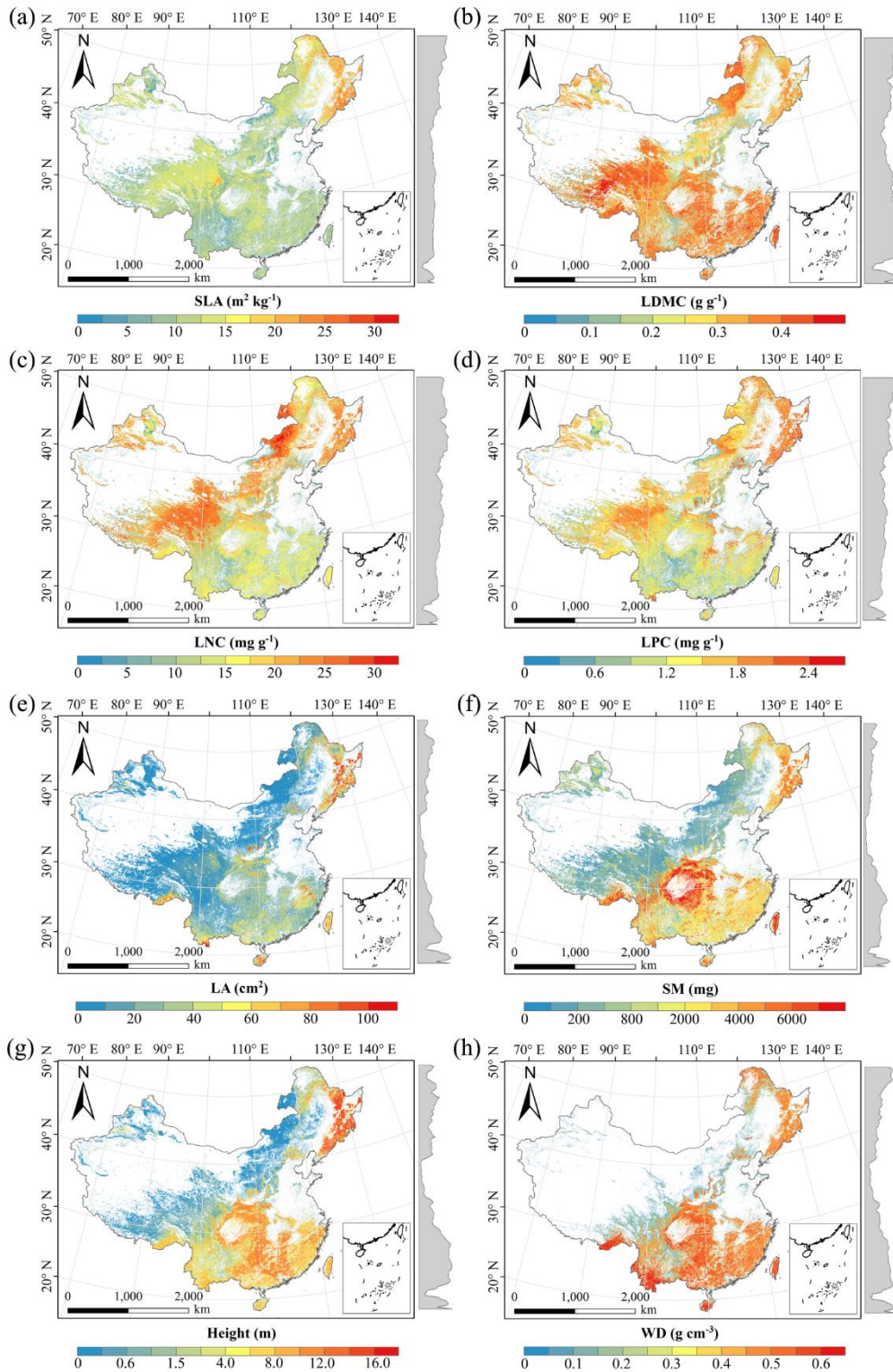
1013 SLA, specific leaf area; LDMC, leaf dry matter content; LNC, leaf N ~~concentration~~~~concentration~~; LPC,
 1014 leaf P ~~concentration~~~~concentration~~; LA, leaf area; WD, wood density; ~~SM, seed mass.~~

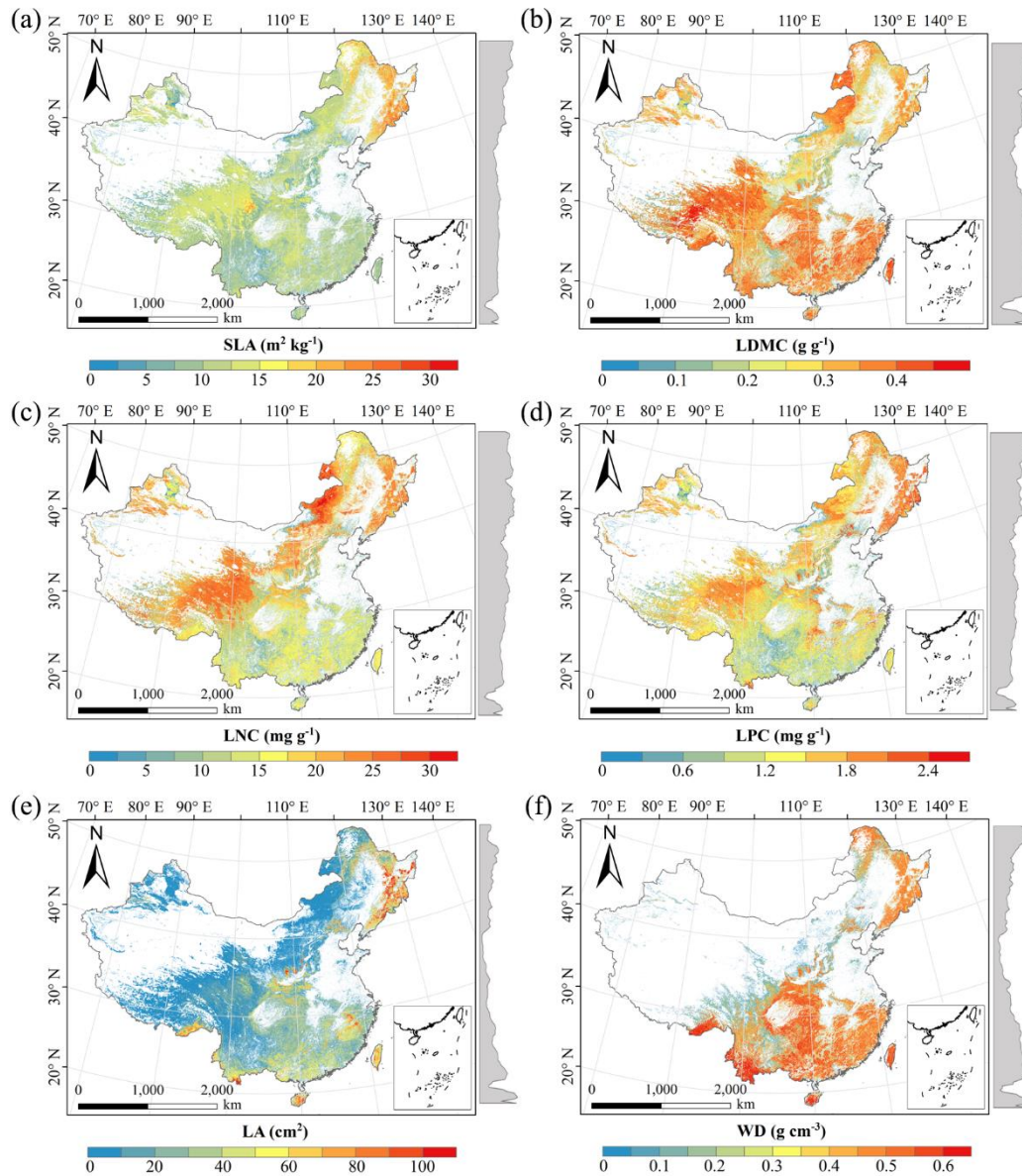
1015

1016 **Table C2** Optimal parameter combination and model performance of boosted regression trees (~~BRT~~) for
 1017 plant functional traits

Traits	n.tree	interaction. depth	shrinkage	learning rate	bag fractions	R ²	<u>NRMSE</u>	MAE
SLA	3000	6	0.01	10	0.75	0.486	6.9860.20	5.082
LDMC	3000	2	0.01	10	0.75	0.247	0.0940.19	0.071
LNC	3000	6	0.01	10	0.70	0.414	0.1260.00	0.096
LPC	3000	7	0.01	10	0.75	0.591	0.1750.05	0.129
LA	3000	3	0.001	10	0.75	0.282	72.3080.5	27.556
Height	3000	3	0.05	10	0.6	0.871	0.234	0.178
WD	3000	4	0.01	10	0.70	0.627	0.0820.01	0.066
SM	3000	7	0.001	10	0.50	0.192	6070.703	1268.386

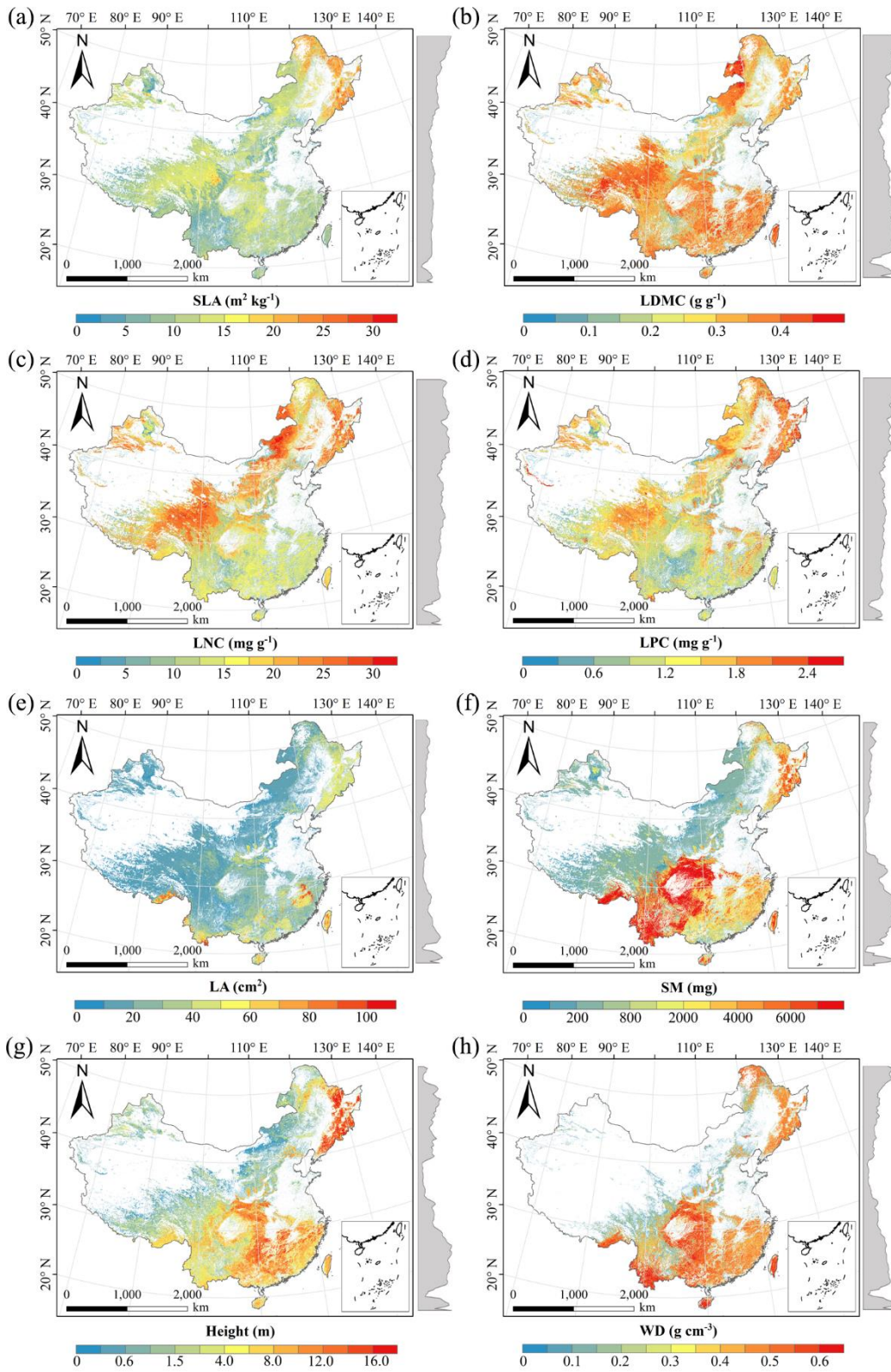
1018 SLA, specific leaf area; LDMC, leaf dry matter content; LNC, leaf N ~~concentration~~~~concentration~~; LPC,
 1019 leaf P ~~concentration~~~~concentration~~; LA, leaf area; WD, wood density; ~~SM, seed mass.~~

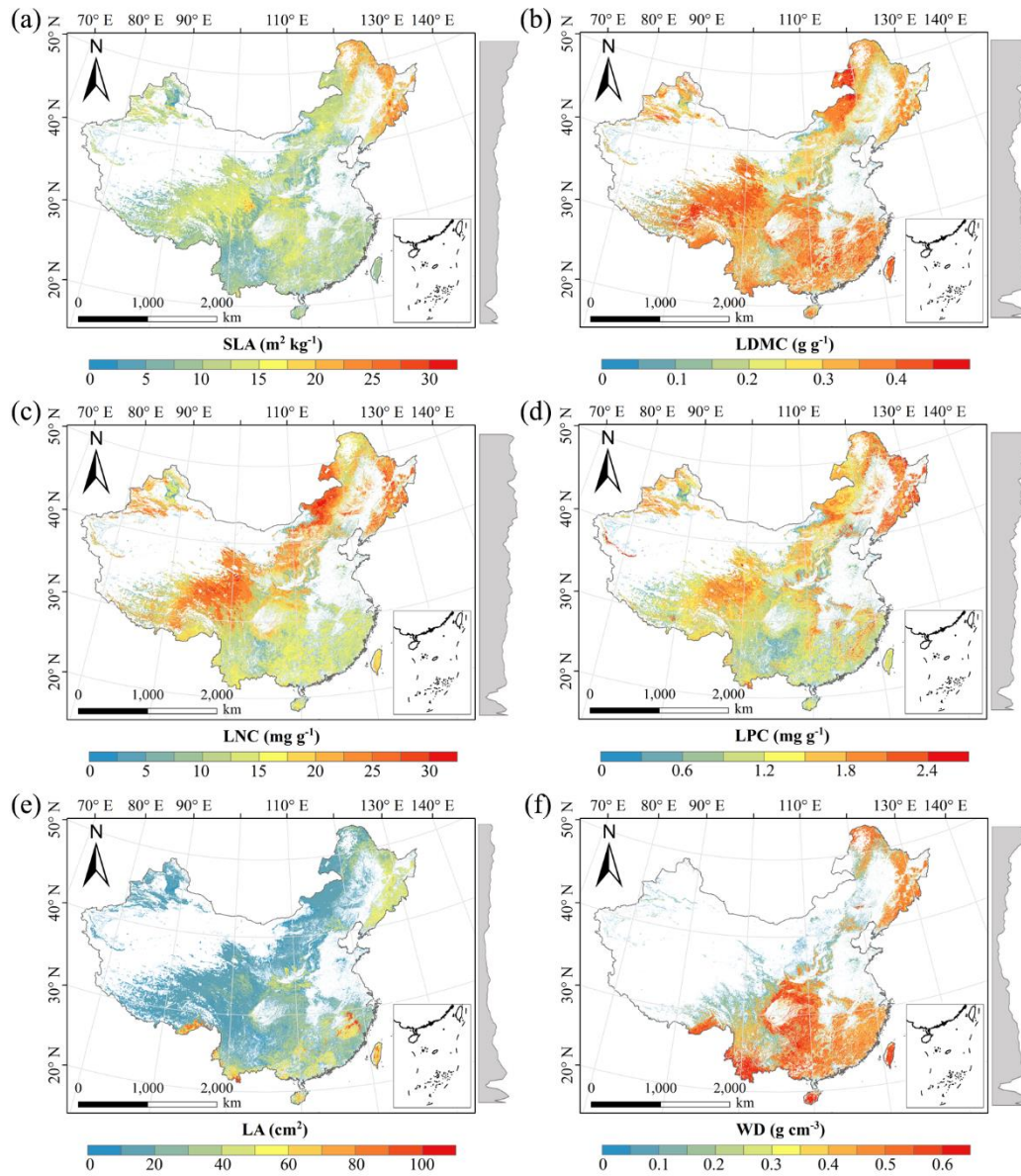




1022

1023 **Figure D1.** Spatial distribution of plant functional traits based on random forest-(RF). The grey
 1024 curves on the right of maps were trait distribution along with latitude. SLA, specific leaf area;
 1025 LDMC, leaf dry matter content; LNC, leaf N ~~concentration~~
 1026 ~~concentration~~; LA, leaf area; WD, wood density; ~~SM, seed mass.~~





1028

1029

Figure D2. Spatial distribution of plant functional traits based on boosted regression trees (~~BRT~~).

1030

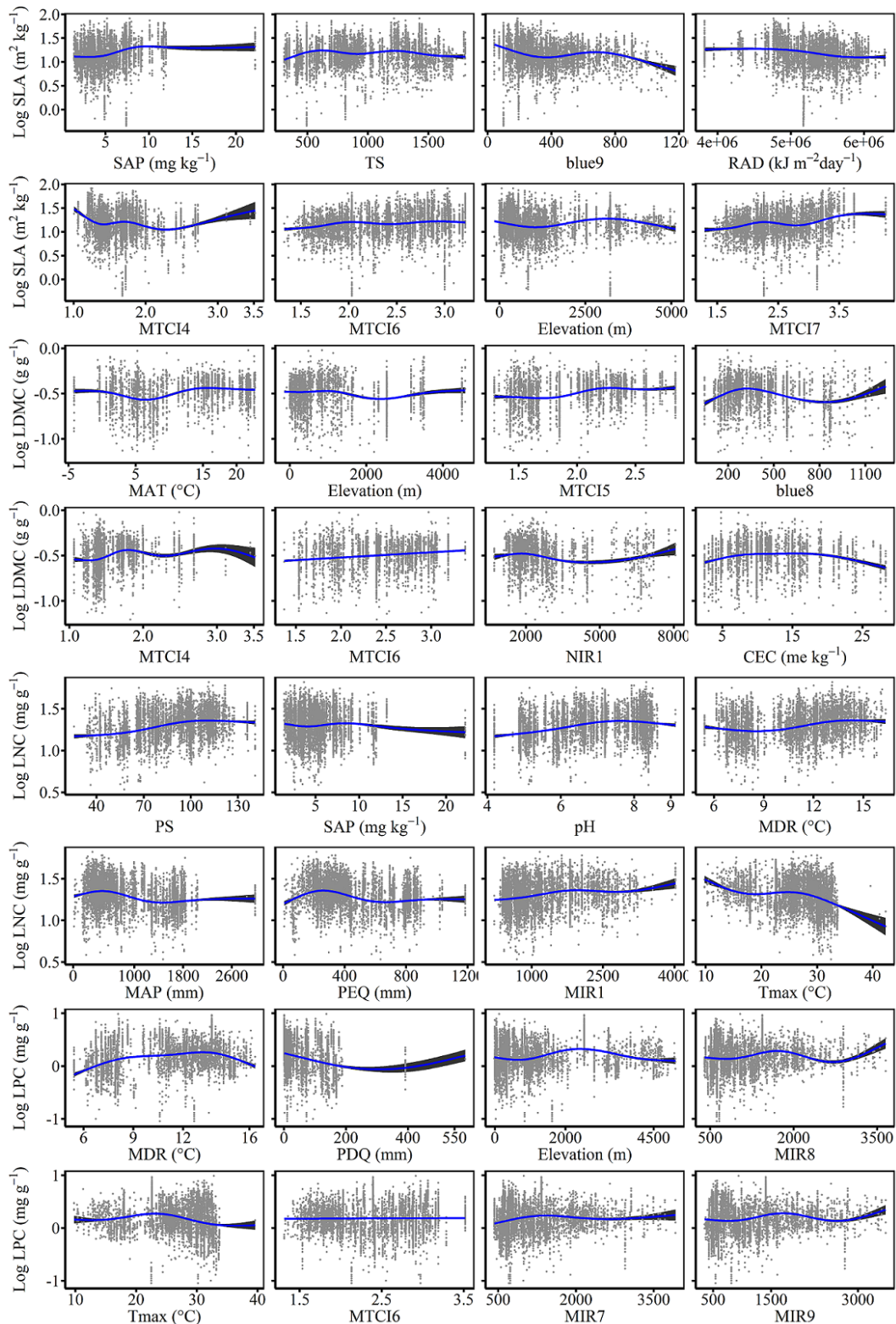
The grey curves on the right of maps were trait distribution along with latitude. SLA, specific leaf

1031

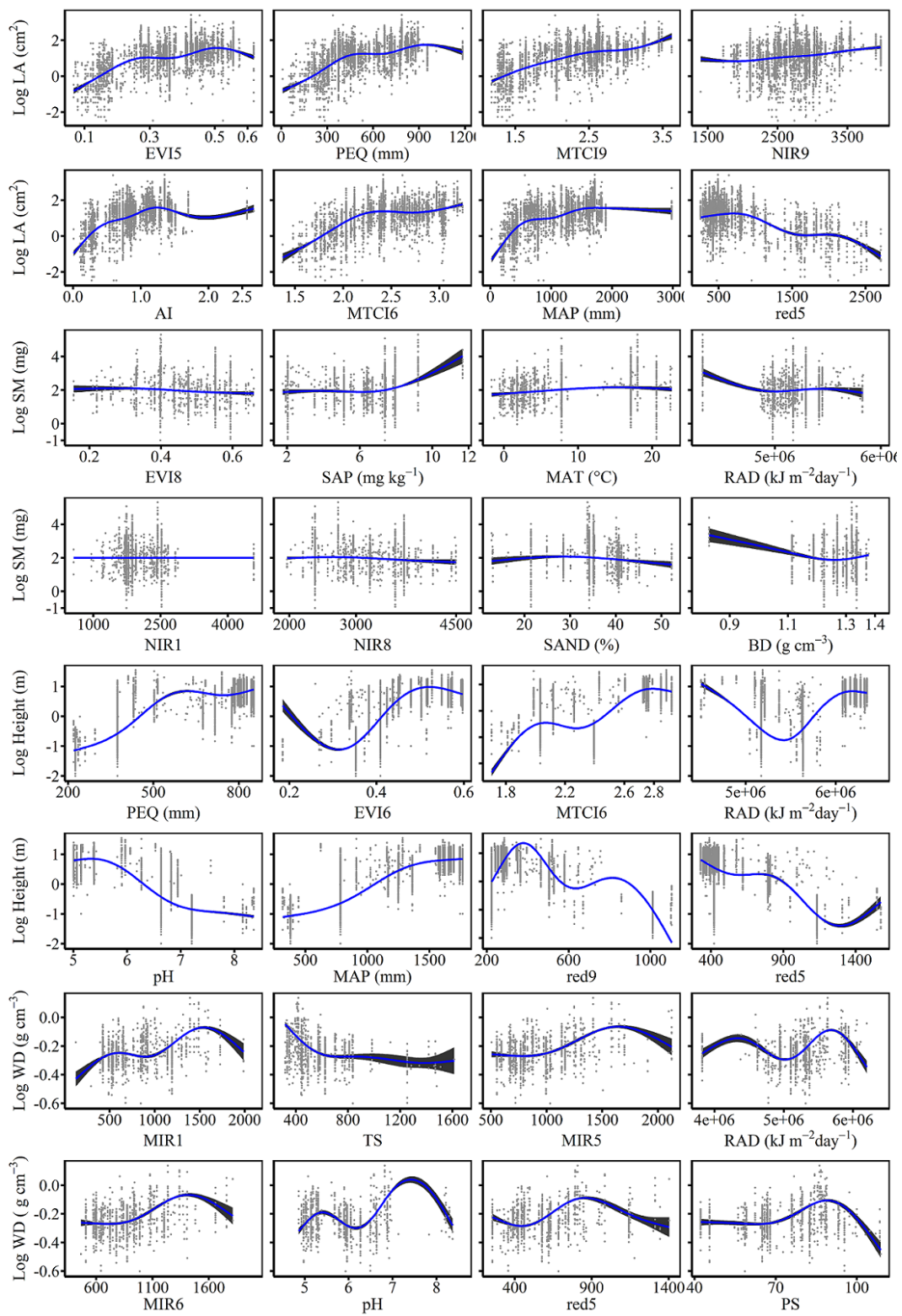
area; LDMC, leaf dry matter content; LNC, leaf N ~~concentration~~~~oncertation~~;

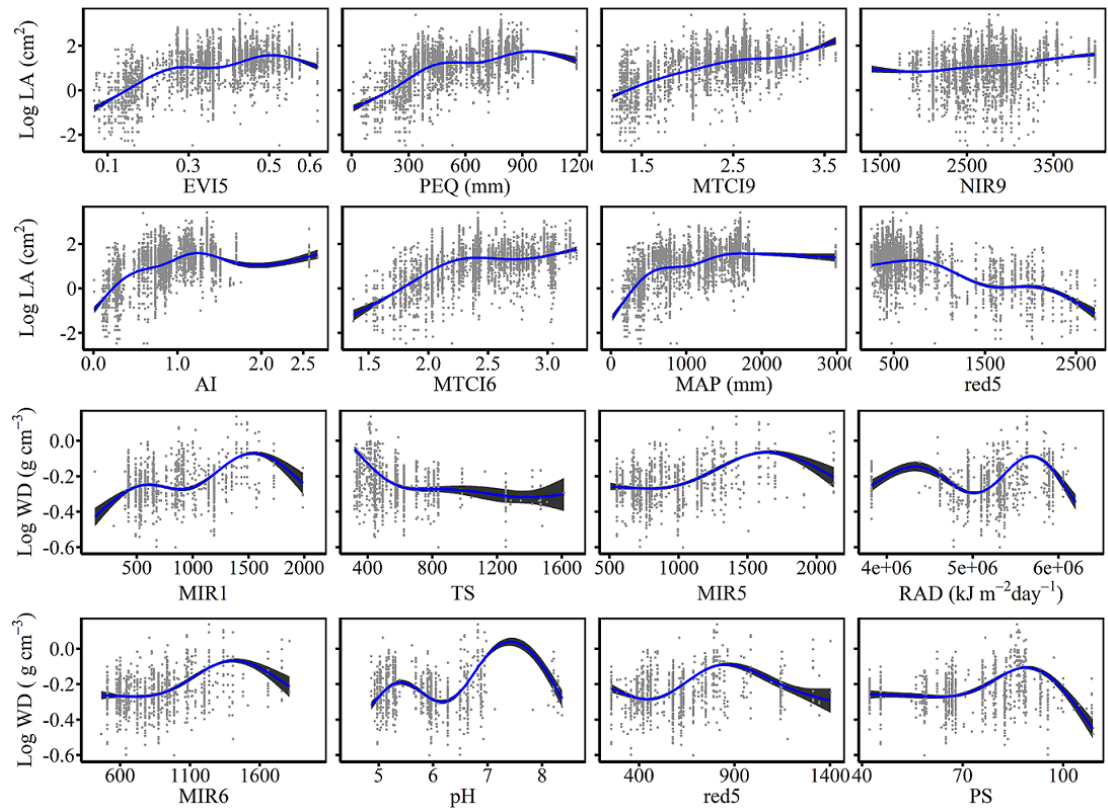
1032

LPC, leaf P ~~concentration~~~~oncertation~~; LA, leaf area; WD, wood density; ~~SM~~, seed mass.



1034
 1035 **Figure E1.** The relationships between SLA (specific leaf area), LDMC (leaf dry matter content),
 1036 LNC (leaf N concentration), LPC (leaf P concentration) and their eight most important predictors.





1038

1039

1040

Figure E2. The relationships between LA (leaf area), SM, Height, WD (wood density) and their eight most important predictors.

Appendix F Comparisons between our study with trait maps from previous studies

Given that the trait maps predicted for China were not available from the literature and authors, we compared our study with those studies performed at the global scale (see Table F1). Thus, we extracted the data in China from global trait maps. Before the quantitative comparisons with previous studies, we performed two steps to make the data products as comparable as possible and improve the consistency between different studies. First, due to different spatial resolution of global trait maps (mainly 0.5°) and our study, we resampled the data products of previous studies and our maps to 0.5° spatial resolution. In addition, Vallicrosa et al. (2022) generated the global maps of LNC and LPC with a 1 km spatial resolution, we also compared the frequency distribution of Vallicrosa et al. (2022) with that of our study at a 1 km spatial resolution. Second, our study focused on natural vegetation, so the global trait maps were used to filter out non-natural vegetation (e.g., croplands). For example, Madani et al. (2018) predicted the spatial distributions of SLA that included croplands. We quantitatively compared our maps with previous studies from two perspectives. The comparisons among trait maps were made using frequency plots and spatial correlations (Figure 7 and Table 5). And the maps of spatial differences between our study and previous studies were displayed as Figs F1-F5 in Appendix F.

Table F1. Summary table of related trait maps of previous studies used in this study.

<u>References</u>	<u>Related traits</u>	<u>Methods</u>	<u>Predictors</u>	<u>Consideration of PFT</u>	<u>Resolution</u>
<u>Dong et al. (2023)</u>	<u>SLA</u> <u>LNC</u>	<u>Optimality models</u>	<u>Climate</u>	<u>Yes</u>	<u>0.5°</u>
<u>Vallicrosa et al. (2022)</u>	<u>LNC</u> <u>LPC</u>	<u>Neural networks</u>	<u>Climate</u> <u>Soil</u> <u>N and P deposition</u>	<u>Yes</u>	<u>0.0083°</u>
<u>Schiller et al. (2021)</u>	<u>SLA</u> <u>LNC</u> <u>LA</u> <u>WD</u>	<u>Convolutional Neural Networks</u>	<u>Climate</u> <u>In-situ RGB images</u>	<u>No</u>	<u>0.5°</u>
<u>Boonman et al. (2020)</u>	<u>SLA</u> <u>LNC</u> <u>WD</u>	<u>Generalized linear model, Generalized additive model, Random forest, Boosted regression trees, Ensemble model</u>	<u>Climate</u> <u>Soil</u>	<u>No</u>	<u>0.5°</u>
<u>Moreno et al. (2018)</u>	<u>SLA</u> <u>LNC</u> <u>LPC</u> <u>LDMC</u>	<u>Regularized linear regression, Random forest, Neural networks, Kernel networks</u>	<u>Climate</u> <u>Elevation</u> <u>Reflectance</u>	<u>Yes</u>	<u>0.0045°</u>
<u>Madani et al.</u>	<u>SLA</u>	<u>Generalized additive</u>	<u>Climate</u>	<u>No</u>	<u>0.5°</u>

(2018)		model			
Butler et al.	SLA	Bayesian model	Climate	Yes	0.5°
(2017)	LNC		Soil		
	LPC				
Bodegom et al.	SLA	Multiple regression	Climate	No	0.5°
(2014)	WD	analysis	Soil		

The resolutions 0.5°, 0.0083° and 0.0045° correspond to square grid cell sizes of about 50 km, 1 km and 500 m at the equator. PFT, plant functional type; SLA, specific leaf area; LDMC, leaf dry matter content; LNC, leaf N concentration; LPC, leaf P concentration; LA, leaf area; WD, wood density.

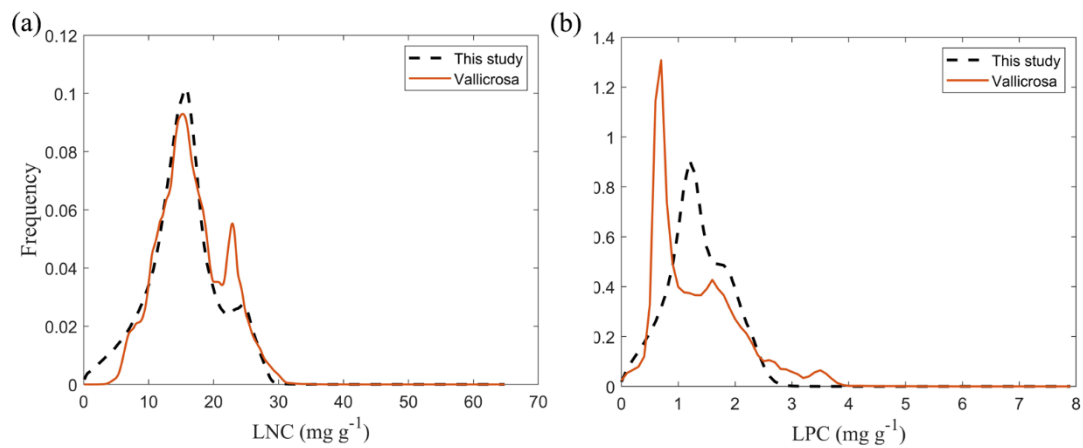
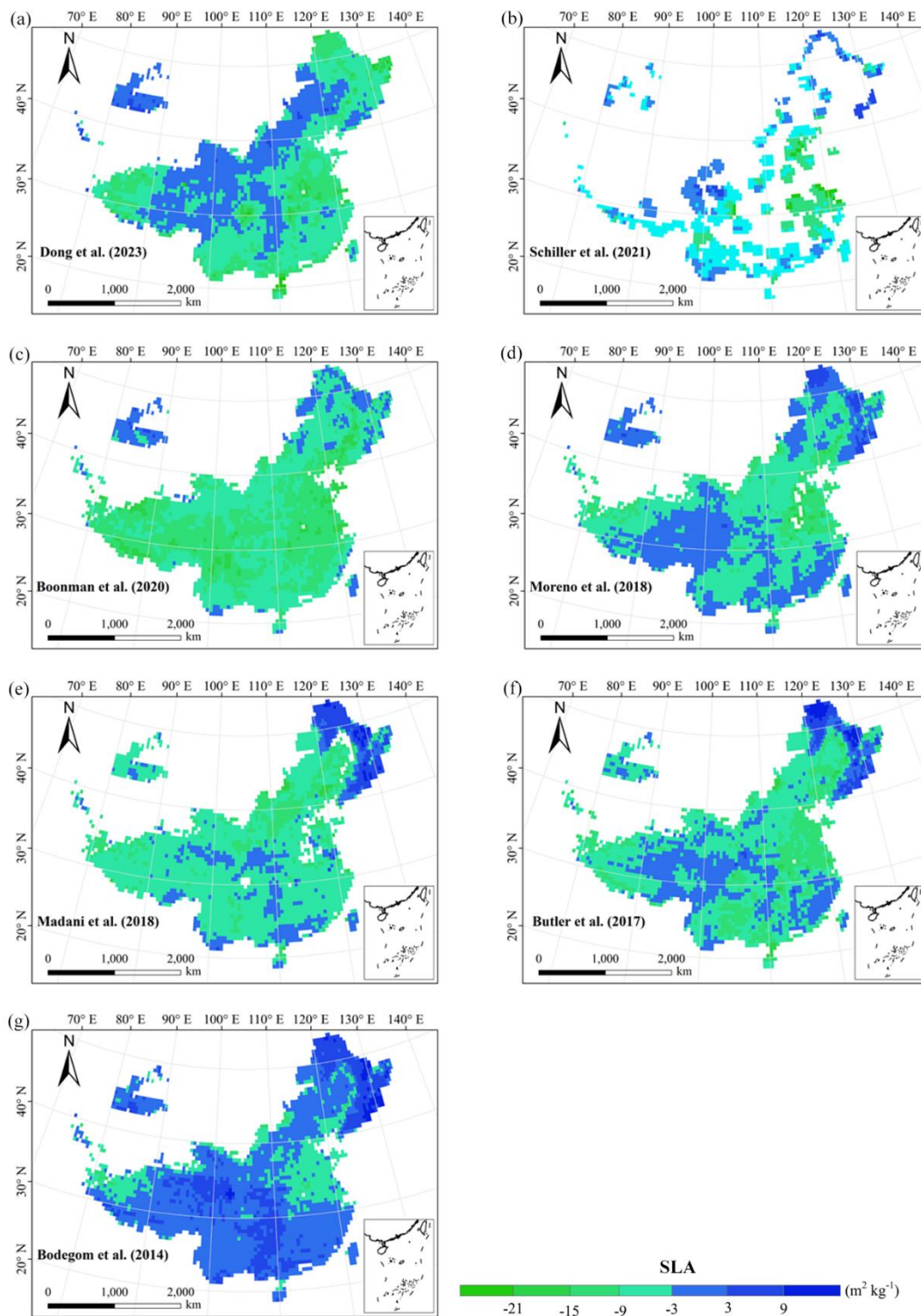


Figure F1. Frequency distributions of plant functional traits in our study (“This study”, dashed black lines) and Vallicrosa et al. (2022) at 1 km spatial resolution. LNC, leaf N concentration (mg g⁻¹); LPC, leaf P concentration (mg g⁻¹).

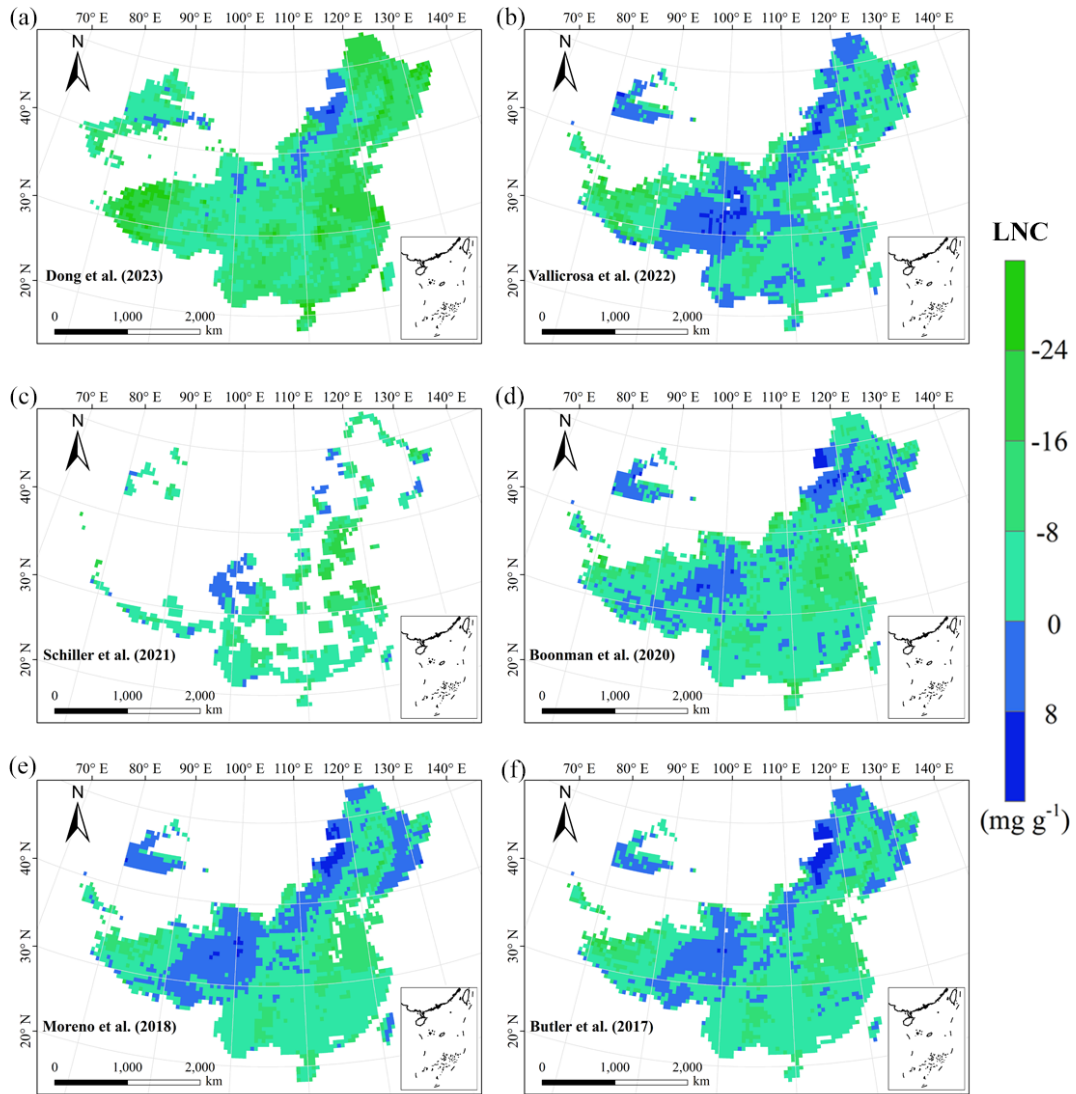


1066

1067

1068

Figure F2. Spatial differences in SLA (specific leaf area, $\text{m}^2 \text{kg}^{-1}$) between our study and trait maps from previous studies (see Table F1 for citations).

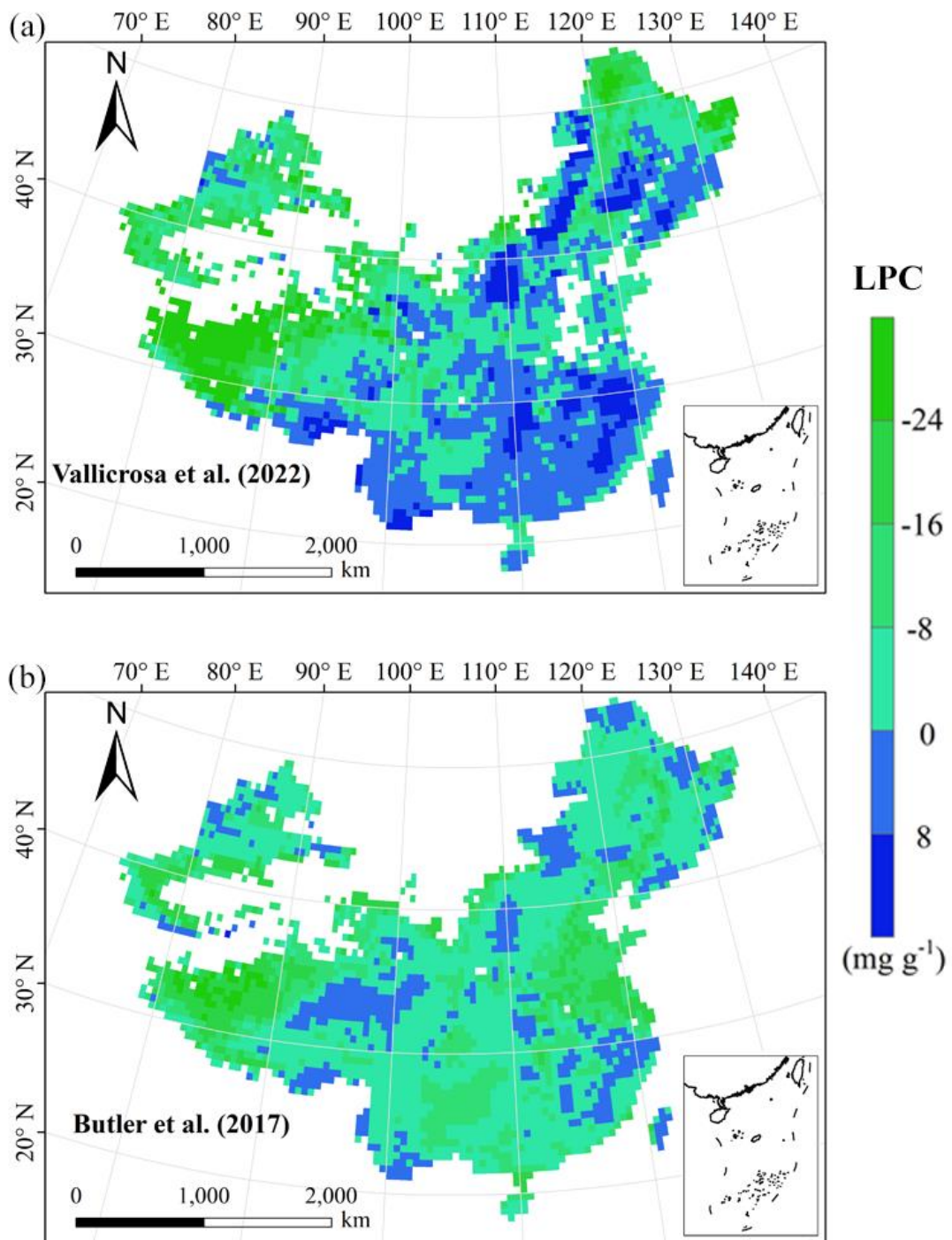


1069

1070

1071

Figure F3. Spatial differences in LNC (leaf N concentration, mg g^{-1}) between our study and trait maps from previous studies (see Table F1 for citations).

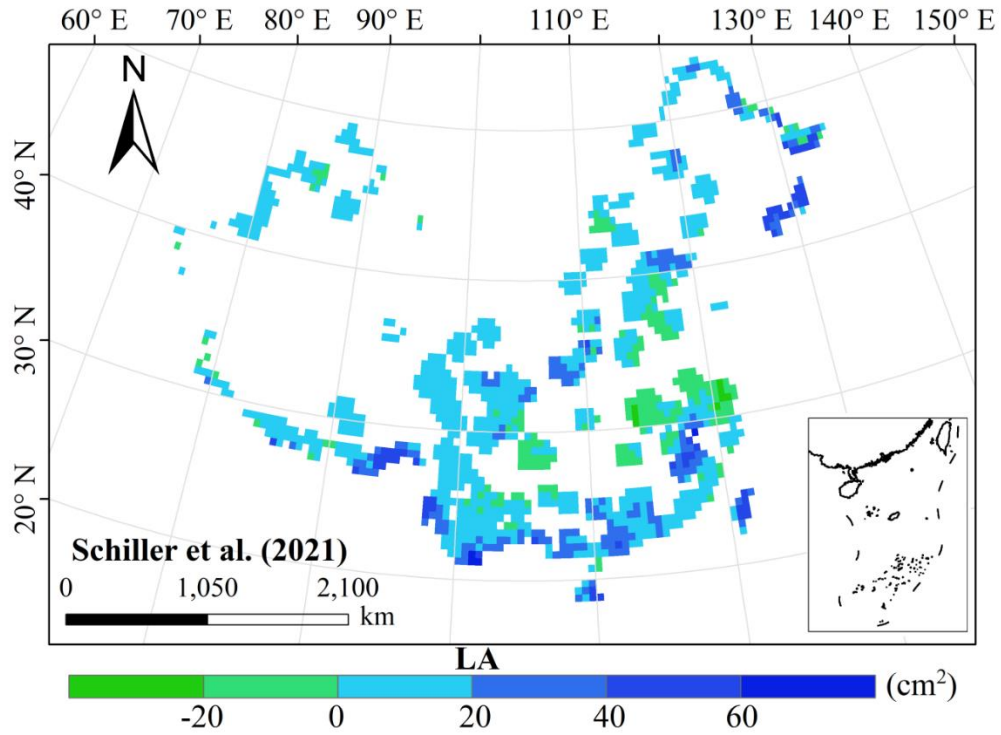


1072

1073

1074

Figure F4. Spatial differences in LPC (leaf P concentration, mg g⁻¹) between our study and trait maps from previous studies (see Table F1 for citations).

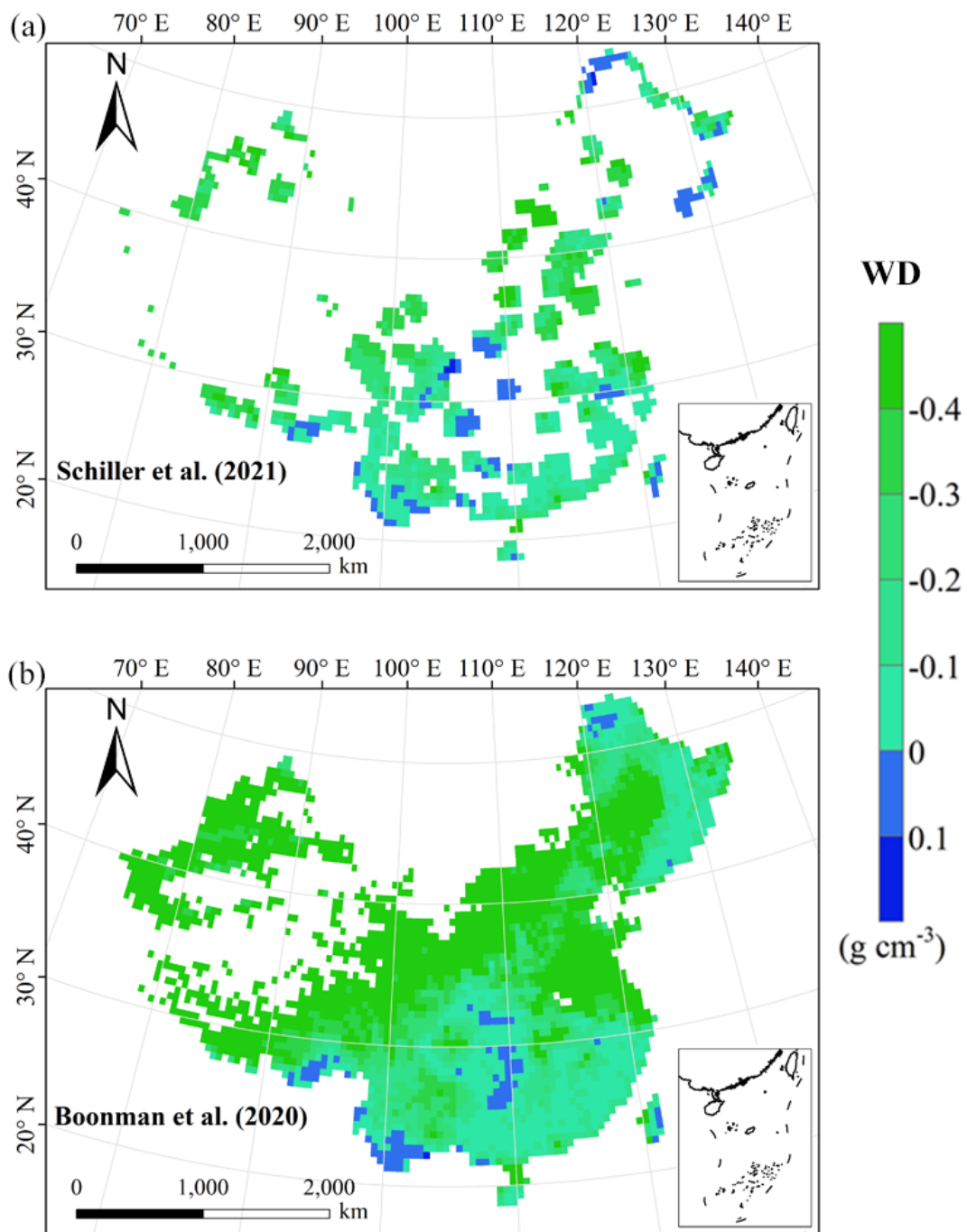


1075

1076

1077

Figure F5. Spatial differences in LA (leaf area, cm²) between our study and trait maps from previous studies (see Table F1 for citations).



1078

1079

1080

Figure F6. Spatial differences in WD (wood density, g cm^{-3}) between our study and trait maps from previous studies (see Table F1 for citations).

1081 **Author contributions.** NA and NL designed the research. NA did the analysis, processed the data
1082 and wrote the draft of the paper. All co-authors commented on the manuscript and agreed upon the
1083 final version of the paper.

1084
1085 **Competing interests.** The contact author has declared that none of the authors has any competing
1086 interests.

1087
1088 **Disclaimer.** Publisher's note: Copernicus Publications remains neutral with regard to jurisdictional
1089 claims in published maps and institutional affiliations.

1090
1091 **Acknowledgement.** We acknowledge financial supports from the National Natural Science
1092 Foundation of China (41991234) and the Joint CAS-MPG Research Project (HZXM20225001MI).

1093
1094 **Financial support.** This work has been supported by the National Natural Science Foundation of
1095 China (grant no. 41991234) and the Joint CAS-MPG Research Project (grant no.
1096 HZXM20225001MI).

1097

1098 **References**

1099 Ali, A. M., Darvishzadeh, R., Skidmore, A. K., [van Duren, I.](#), Heiden, U., and Heurich, M.:
1100 Estimating leaf functional traits by inversion of PROSPECT: assessing leaf dry matter content
1101 and specific leaf area in mixed mountainous forest. *Int. J. Appl. Earth Obs. Geoinf.*, 45, 66–76,
1102 <https://doi.org/10.1016/j.jag.2015.11.004>, 2016.

1103 [An, N. N., Lu, N., Fu, B. J., Wang, M. Y., and He, N. P.: Distinct responses of leaf traits to](#)
1104 [environment and phylogeny between herbaceous and woody angiosperm species in China.](#)
1105 [Front. Plant Sci. 12, 799401, https://doi.org/10.3389/fpls.2021.799401, 2021.](#)

1106 Bakker, M. A., Carreño-Rocabado, G., and Poorter, L.: Leaf economics traits predict litter
1107 decomposition of tropical plants and differ among land use types. *Funct. Ecol.*, 25, 473–483,
1108 <https://doi.org/10.1111/j.1365-2435.2010.01802.x>, 2011.

1109 Berzaghi, F., Wright, I. J., Kramer, K., Oddou-Muratorio, S., Bohn, F. J., Reyer, C. P. O., Sabate, S.,
1110 Sanders, T. G. M., and Hartig, F.: Towards a new generation of trait-flexible vegetation models.
1111 *Trends Ecol. Evol.*, 35, 191–205, <https://doi.org/10.1016/j.tree.2019.11.006>, 2020.

1112 Blumenthal, D. M., Mueller, K. E., Kray, J. A., Ocheltree, T. W., Augustine, D. J., Wilcox, K. R.,
1113 and Cornelissen, H.: Traits link drought resistance with herbivore defence and plant economics
1114 in semi-arid grasslands: The central roles of phenology and leaf dry matter content. *J. Ecol.*,
1115 108, 2336–2351, <https://doi.org/10.1111/1365-2745.13454>, 2020.

1116 Bohner, A. Soil chemical properties as indicators of plant species richness in grassland communities.
1117 Integrating efficient grassland farming and biodiversity, Proceedings of the 13th International
1118 Occasional Symposium of the European Grassland Federation, Tartu, Estonia, 29–31 August,

1119 48-51, 2005.

1120 Boonman, C. C. F., Benitez-Lopez, A., Schipper, A. M., Thuiller, W., Anand, M., Cerabolini, B. E.
1121 L., Cornelissen, J. H. C., Gonzalez-Melo, A., Hattingh, W. N., Higuchi, P., Laughlin, D. C.,
1122 Onipchenko, V. G., Penuelas, J., Poorter, L., Soudzilovskaia, N. A., Huijbregts, M. A. J., and
1123 Santini, L.: Assessing the reliability of predicted plant trait distributions at the global scale.
1124 *Glob. Ecol. Biogeogr.*, 29, 1034–1051, <https://doi.org/10.1111/geb.13086>, 2020.

1125 Breiman, L.: Random forests. *Mach. Learn.*, 45, 5–32, <https://doi.org/10.1023/a:1010933404324>,
1126 2001.

1127 Bruelheide, H., Dengler, J., Purschke, O., Lenoir, J., Jimenez-Alfaro, B., Hennekens, S. M., Botta-
1128 Dukat, Z., Chytry, M., Field, R., Jansen, F., Kattge, J., Pillar, V. D., Schrodte, F., Mahecha, M.
1129 D., Peet, R. K., Sandel, B., van Bodegom, P., Altman, J., Alvarez-Davila, E., Arfin Khan, M.
1130 A. S., et al.: Global trait-environment relationships of plant communities. *Nat. Ecol. Evol.*, 2,
1131 1906–1917, <https://doi.org/10.1038/s41559-018-0699-8>, 2018.

1132 Bruelheide, H., Dengler, J., Jiménez-Alfaro, B., Purschke, O., Hennekens, S. M., Chytrý, M., Pillar,
1133 V. D., Jansen, F., Kattge, J., Sandel, B., Aubin, I., Biurrun, I., Field, R., Haider, S., Jandt, U.,
1134 Lenoir, J., Peet, R. K., Peyre, G., Sabatini, F. M., Schmidt, M., et al.: sPlot – A new tool for
1135 global vegetation analyses. *J. Veg. Sci.*, 30, 161–186, <https://doi.org/10.1111/jvs.12710>, 2019.

1136 Buchhorn, M., Bertels, L., Smets, B., De Roo, B., Lesiv, M., Tsendbazar, N. E., Masiliunas, D., and
1137 Linlin, L.: Copernicus Global Land Service: Land Cover 100m: Version 3 Globe 2015-2019:
1138 Algorithm Theoretical Basis Document. <https://doi.org/10.5281/zenodo.3938968>, 2020.

1139 Butler, E. E., Datta, A., Flores-Moreno, H., Chen, M., Wythers, K. R., Fazayeli, F., Banerjee, A.,
1140 Atkin, O. K., Kattge, J., Amiaud, B., Blonder, B., Boenisch, G., Bond-Lamberty, B., Brown,
1141 K. A., Byun, C., Campetella, G., Cerabolini, B. E. L., Cornelissen, J. H. C., Craine, J. M.,
1142 Craven, D., de Vries, F. T., Diaz, S., Domingues, T. F., Forey, E., Gonzalez-Melo, A., Gross,
1143 N., Han, W., Hattingh, W. N., Hickler, T., Jansen, S., Kramer, K., Kraft, N. J. B., Kurokawa,
1144 H., Laughlin, D. C., Meir, P., Minden, V., Niinemets, U., Onoda, Y., Penuelas, J., Read, Q.,
1145 Sack, L., Schamp, B., Soudzilovskaia, N. A., Spasojevic, M. J., Sosinski, E., Thornton, P. E.,
1146 Valladares, F., van Bodegom, P. M., Williams, M., Wirth, C., and Reich, P. B.: Mapping local
1147 and global variability in plant trait distributions. *P. Nat. Acad. Sci. USA*, 114, 10937–10946,
1148 <https://doi.org/10.1073/pnas.1708984114>, 2017.

1149 Cavender-Bares, J., Schneider, F. D., Santos, M. J., Armstrong, A., Carnaval, A., Dahlin, K. M.,
1150 Fatoyinbo, L., Hurtt, G. C., Schimel, D., Townsend, P. A., Ustin, S. L., Wang, Z. H., and Wilson,
1151 A. M.: Integrating remote sensing with ecology and evolution to advance biodiversity
1152 conservation. *Nat. Ecol. Evol.*, 6, 506–519, <https://doi.org/10.1038/s41559-022-01702-5>, 2022.

1153 Clevers, J. G. P. W., and Gitelson, A. A.: Remote estimation of crop and grass chlorophyll and
1154 nitrogen content using red-edge bands on Sentinel-2 and -3. *Int. J. Appl. Earth Obs. Geoinf.*,
1155 23, 344–351, <https://doi.org/10.1016/j.jag.2012.10.008>, 2013.

1156 ~~Conti, G., Diaz, S., and Lavorel, S.: Plant functional diversity and carbon storage—an empirical test~~

1157 ~~in semi-arid forest ecosystems. *Journal of Ecology*, 101, 18–28, [https://doi.org/10.1111/1365-](https://doi.org/10.1111/1365-2745.12012)~~
1158 ~~[2745.12012](https://doi.org/10.1111/1365-2745.12012), 2013.~~

1159 Dahlin, K. M., Asner, G. P., and Field, C. B.: Environmental and community controls on plant
1160 canopy chemistry in a Mediterranean-type ecosystem. *P. Nat. Acad. Sci. USA*, 110, 6895–6900,
1161 <https://doi.org/10.1073/pnas.1215513110>, 2013.

1162 Darvishzadeh, R., Skidmore, A., Schlerf, M., and Atzberger, C.: Inversion of a radiative transfer
1163 model for estimating vegetation LAI and chlorophyll in a heterogeneous grassland. *Remote*
1164 *Sens. Environ.*, 112, 2592–2604, <https://doi.org/10.1016/j.rse.2007.12.003>, 2008.

1165 Diaz, S., Kattge, J., Cornelissen, J. H., Wright, I. J., Lavorel, S., Dray, S., Reu, B., Kleyer, M., Wirth,
1166 C., Prentice, I. C., Garnier, E., Bonisch, G., Westoby, M., Poorter, H., Reich, P. B., Moles, A.
1167 T., Dickie, J., Gillison, A. N., Zanne, A. E., Chave, J., Wright, S. J., Sheremet'ev, S. N., Jactel,
1168 H., Baraloto, C., Cerabolini, B., Pierce, S., Shipley, B., Kirkup, D., Casanoves, F., Joswig, J.
1169 S., Gunther, A., Falczuk, V., Ruger, N., Mahecha, M. D., and Gorne, L. D.: The global spectrum
1170 of plant form and function. *Nature*, 529, 167–171, <https://doi.org/10.1038/nature16489>, 2016.

1171 Diaz, S., Hodgson, J. G., Thompson, K., Cabido, M., Cornelissen, J. H. C., Jalili, A., Montserrat-
1172 Marti, G., Grime, J. P., Zarrinkamar, F., Asri, Y., Band, S. R., Basconcelo, S., Castro-Diez, P.,
1173 Funes, G., Hamzehee, B., Khoshnevi, M., Perez-Harguindeguy, N., Perez-Rontome, M. C.,
1174 Shirvany, F. A., Vendramini, F., Yazdani, S., Abbas-Azimi, R., Bogaard, A., Boustani, S.,
1175 Charles, M., Dehghan, M., de Torres-Espuny, L., Falczuk, V., Guerrero-Campo, J., Hynd, A.,
1176 Jones, G., Kowsary, E., Kazemi-Saeed, F., Maestro-Martinez, M., Romo-Diez, A., Shaw, S.,
1177 Siavash, B., Villar-Salvador, P., and Zak, M. R.: The plant traits that drive ecosystems: evidence
1178 from three continents. *J. Veg. Sci.*, 15, 295–304, [https://doi.org/10.1111/j.1654-](https://doi.org/10.1111/j.1654-1103.2004.tb02266.x)
1179 [1103.2004.tb02266.x](https://doi.org/10.1111/j.1654-1103.2004.tb02266.x), 2004.

1180 [Dong, N., Dechant, B., Wang, H., Wright, I. J., and Prentice, I. C.: Global leaf-trait mapping based](https://doi.org/10.1111/geb.13680)
1181 [on optimality theory. *Glob. Ecol. Biogeogr.*, <https://doi.org/10.1111/geb.13680>, 2023.](https://doi.org/10.1111/geb.13680)

1182 [Du, L., Liu, H., Guan, W., Li, J., and Li, J.: Drought affects the coordination of belowground and](https://doi.org/10.1002/ece3.5536)
1183 [aboveground resource-related traits in *Solidago canadensis* in China. *Ecol. Evol.*, 9, 9948–](https://doi.org/10.1002/ece3.5536)
1184 [9960, <https://doi.org/10.1002/ece3.5536>, 2019.](https://doi.org/10.1002/ece3.5536)

1185 Elith, J., Leathwick, J. R., and Hastie, T.: A working guide to boosted regression trees. *J. Anim.*
1186 *Ecol.*, 77, 802–813, <https://doi.org/10.1111/j.1365-2656.2008.01390.x>, 2008.

1187 Elith, J., Kearney, M., and Phillips, S.: The art of modelling range-shifting species. *Methods Ecol.*
1188 *Evol.*, 1, 330–342, <https://doi.org/10.1111/j.2041-210X.2010.00036.x>, 2010.

1189 Elith, J., Graham, C. H., Anderson, R. P., Dudik, M., Ferrier, S., Guisan, A., Hijmans, R. J.,
1190 Huettmann, F., Leathwick, J. R., Lehmann, A., Li, J., Lohmann, L. G., Loiselle, B. A., Manion,
1191 G., Moritz, C., Nakamura, M., Nakazawa, Y., Overton, J. M., Peterson, A. T., Phillips, S. J.,
1192 Richardson, K., Scachetti-Pereira, R., Schapire, R. E., Soberon, J., Williams, S., Wisz, M. S.,
1193 and Zimmermann, N. E.: Novel methods improve prediction of species' distributions from
1194 occurrence data. *Ecography*, 29, 129–151, <https://doi.org/10.1111/j.2006.0906-7590.04596.x>,

1195 2006.

1196 Finzi, A. C., Austin, A. T., Cleland, E. E., Frey, S. D., Houlton, B. Z., and Wallenstein, M. D.:

1197 Responses and feedbacks of coupled biogeochemical cycles to climate change: examples from

1198 terrestrial ecosystems. *Front. Ecol. Environ.*, 9, 61–67, <https://doi.org/10.1890/100001>, 2011.

1199 Foley, J. A., Prentice, I. C., Ramankutty, N., Levis, S., Pollard, D., Sitch, S., and Haxeltine, A.: An

1200 integrated biosphere model of land surface processes, terrestrial carbon balance, and vegetation

1201 dynamics. *Global Biogeochem. Cy.*, 10, 603–628, <https://doi.org/10.1029/96gb02692>, 1996.

1202 Freschet, G. T., Cornelissen, J. H. C., van Logtestijn, R. S. P., and Aerts, R.: Evidence of the ‘plant

1203 economics spectrum’ in a subarctic flora. *J. Ecol.*, 98, 362–373, [https://doi.org/10.1111/j.1365-](https://doi.org/10.1111/j.1365-2745.2009.01615.x)

1204 [2745.2009.01615.x](https://doi.org/10.1111/j.1365-2745.2009.01615.x), 2010.

1205 Grime, J. P.: Benefits of plant diversity to ecosystems: immediate, filter and founder effects. *J. Ecol.*,

1206 86, 902–910, <https://doi.org/10.1046/j.1365-2745.1998.00306.x>, 1998.

1207 He, N., Yan, P., Liu, C., Xu, L., Li, M., Van Meerbeek, K., Zhou, G., Zhou, G., Liu, S., Zhou, X.,

1208 Li, S., Niu, S., Han, X., Buckley, T. N., Sack, L., and Yu, G.: Predicting ecosystem productivity

1209 based on plant community traits. *Trends Plant Sci.*, 28, 43–53,

1210 <https://doi.org/10.1016/j.tplants.2022.08.015>, 2023.

1211 Hodgson, J. G., Montserrat-Marti, G., Charles, M., Jones, G., Wilson, P., Shipley, B., Sharafi, M.,

1212 Cerabolini, B. E. L., Cornelissen, J. H. C., Band, S. R., Bogard, A., Castro-Diez, P., Guerrero-

1213 Campo, J., Palmer, C., Perez-Rontome, M. C., Carter, G., Hynd, A., Romo-Diez, A., Espuny,

1214 L. D., and Pla, F. R.: Is leaf dry matter content a better predictor of soil fertility than specific

1215 leaf area? *Ann. Bot.*, 108, 1337–1345, <https://doi.org/10.1093/aob/mcr225>, 2011.

1216 Hoeber, S., Leuschner, C., Köhler, L., Arias-Aguilar, D., and Schuldt, B.: The importance of

1217 hydraulic conductivity and wood density to growth performance in eight tree species from a

1218 tropical semi-dry climate. *Forest Ecol. Manag.*, 330, 126–136,

1219 <https://doi.org/10.1016/j.foreco.2014.06.039>, 2014.

1220 Jónsdóttir, I. S., Halbritter, A. H., Christiansen, C. T., Althuisen, I. H. J., Haugum, S. V., Henn, J. J.,

1221 Björnsdóttir, K., Maitner, B. S., Malhi, Y., Michaletz, S. T., Roos, R. E., Klanderud, K., Lee,

1222 H., Enquist, B. J., and Vandvik, V.: Intraspecific trait variability is a key feature underlying

1223 high Arctic plant community resistance to climate warming. *Ecol. Monogr.*, 93,

1224 <https://doi.org/10.1002/ecm.1555>, 2022.

1225 Jung, V., Violle, C., Mondy, C., Hoffmann, L., and Muller, S.: Intraspecific variability and trait-

1226 based community assembly. *J. Ecol.*, 98, 1134–1140, [https://doi.org/10.1111/j.1365-](https://doi.org/10.1111/j.1365-2745.2010.01687.x)

1227 [2745.2010.01687.x](https://doi.org/10.1111/j.1365-2745.2010.01687.x), 2010.

1228 Kattge, J., Diaz, S., Lavorel, S., Prentice, C., Leadley, P., Bonisch, G., Garnier, E., Westoby, M.,

1229 Reich, P. B., Wright, I. J., Cornelissen, J. H. C., Violle, C., Harrison, S. P., van Bodegom, P. M.,

1230 Reichstein, M., Enquist, B. J., Soudzilovskaia, N. A., Ackerly, D. D., Anand, M., Atkin, O., et

1231 al.: TRY - a global database of plant traits. *Glob. Change Biol.*, 17, 2905–2935,

1232 <https://doi.org/10.1111/j.1365-2486.2011.02451.x>, 2011.

1233 Kattge, J., Bonisch, G., Diaz, S., Lavorel, S., Prentice, I. C., Leadley, P., Tautenhahn, S., Werner, G.
1234 D. A., Aakala, T., Abedi, M., Acosta, A. T. R., Adamidis, G. C., Adamson, K., Aiba, M., Albert,
1235 C. H., Alcantara, J. M., Alcazar, C. C., Aleixo, I., Ali, H., Amiaud, B., et al.: TRY plant trait
1236 database - enhanced coverage and open access. *Global Change Biol.*, 26, 119–188,
1237 <https://doi.org/10.1111/gcb.14904>, 2020.

1238 King, D. A., Davies, S. J., Tan, S., and Noor, N. S. M.: The role of wood density and stem support
1239 costs in the growth and mortality of tropical trees. *J. Ecol.*, 94, 670–680,
1240 <https://doi.org/10.1111/j.1365-2745.2006.01112.x>, 2006.

1241 Kirilenko, A. P., Belotelov, N. V., and Bogatyrev, B. G.: Global model of vegetation migration:
1242 incorporation of climatic variability. *Ecol. Model.*, 132, 125–133,
1243 [https://doi.org/10.1016/S0304-3800\(00\)00310-0](https://doi.org/10.1016/S0304-3800(00)00310-0), 2000.

1244 LeBauer, D. S., and Treseder, K. K.: Nitrogen limitation of net primary productivity in terrestrial
1245 ecosystems is globally distributed. *Ecology*, 89, 371–379, <https://doi.org/10.1890/06-2057.1>,
1246 2008.

1247 ~~Leishman, M. R., Wright, I. J., Moles, A. T., and Westoby, M.: The evolutionary ecology of seed size~~
1248 ~~in: *Seeds: the ecology of regeneration in plant communities*, 2nd edn, edited by: Fenner, M.~~
1249 ~~CAB International, Wallingford, UK, 31–57, <https://doi.org/10.1079/9780851994321.0031>,~~
1250 ~~2000.~~

1251 Li, C. X., Wulf, H., Schmid, B., He, J. S., and Schaepman, M. E.: Estimating plant traits of alpine
1252 grasslands on the Qinghai-Tibetan Plateau using remote sensing. *IEEE J. Sel. Top. Appl. Earth*
1253 *Obs. Remote Sens.*, 11, 2263–2275, <https://doi.org/10.1109/jstars.2018.2824901>, 2018.

1254 Li, D. J., Ives, A. R., and Waller, D. M.: Can functional traits account for phylogenetic signal in
1255 community composition? *New Phytol.*, 214, 607–618, <https://doi.org/10.1111/nph.14397>,
1256 2017.

1257 Li, Y. Q., Reich, P. B., Schmid, B., Shrestha, N., Feng, X., Lyu, T., Maitner, B. S., Xu, X., Li, Y. C.,
1258 Zou, D. T., Tan, Z. H., Su, X. Y., Tang, Z. Y., Guo, Q. H., Feng, X. J., Enquist, B. J., and Wang,
1259 Z. H.: Leaf size of woody dicots predicts ecosystem primary productivity. *Ecol. Lett.*, 23, 1003–
1260 1013, <https://doi.org/10.1111/ele.13503>, 2020.

1261 Liang, X. Y., Ye, Q., Liu, H., and Brodribb, T. J.: Wood density predicts mortality threshold for
1262 diverse trees. *New Phytol.*, 229, <https://doi.org/10.1111/nph.17117>, 2021.

1263 Liaw, A., and Wiener, M.: Classification and Regression by randomForest. *R News*, 2, 18–22, 2002.

1264 Liu, H. Y., and Yin, Y.: Response of forest distribution to past climate change: an insight into future
1265 predictions. *Chinese Science Bulletin*, 58, 4426–4436, [https://doi.org/10.1007/s11434-013-](https://doi.org/10.1007/s11434-013-6032-7)
1266 [6032-7](https://doi.org/10.1007/s11434-013-6032-7), 2013.

1267 Loozen, Y., Rebel, K. T., Karssenber, D., Wassen, M. J., Sardans, J., Peñuelas, J., and De Jong, S.
1268 M.: Remote sensing of canopy nitrogen at regional scale in Mediterranean forests using the
1269 spaceborne MERIS Terrestrial Chlorophyll Index. *Biogeosciences*, 15, 2723–2742,
1270 <https://doi.org/10.5194/bg-15-2723-2018>, 2018.

1271 Loozen, Y., Rebel, K. T., de Jong, S. M., Lu, M., Ollinger, S. V., Wassen, M. J., and Karssenber,
1272 D.: Mapping canopy nitrogen in European forests using remote sensing and environmental
1273 variables with the random forests method. *Remote Sens. Environ.*, 247, 111933,
1274 <https://doi.org/10.1016/j.rse.2020.111933>, 2020.

1275 Madani, N., Kimball, J. S., Ballantyne, A. P., Affleck, D. L. R., van Bodegom, P. M., Reich, P. B.,
1276 Kattge, J., Sala, A., Nazeri, M., Jones, M. O., Zhao, M., and Running, S. W.: Future global
1277 productivity will be affected by plant trait response to climate. *Sci. Rep.*, 8, 1–10,
1278 <https://doi.org/10.1038/s41598-018-21172-9>, 2018.

1279 Martínez-Vilalta, J., Mencuccini, M., Vayreda, J., and Retana, J.: Interspecific variation in functional
1280 traits, not climatic differences among species ranges, determines demographic rates across 44
1281 temperate and Mediterranean tree species. *J. Ecol.*, 98, 1462–1475,
1282 <https://doi.org/10.1111/j.1365-2745.2010.01718.x>, 2010.

1283 Matheny, A. M., Mirfenderesgi, G., and Bohrer, G.: Trait-based representation of hydrological
1284 functional properties of plants in weather and ecosystem models. *Plant Divers*, 39, 1–12,
1285 <https://doi.org/10.1016/j.pld.2016.10.001>, 2017.

1286 Moles, A. T., Warton, D. I., Warman, L., Swenson, N. G., Laffan, S. W., Zanne, A. E., Pitman, A.,
1287 Hemmings, F. A., and Leishman, M. R.: Global patterns in plant height. *J. Ecol.*, 97, 923–932,
1288 <https://doi.org/10.1111/j.1365-2745.2009.01526.x>, 2009.

1289 Moreno-Martínez, Á., Camps-Valls, G., Kattge, J., Robinson, N., Reichstein, M., van Bodegom, P.,
1290 Kramer, K., Cornelissen, J. H. C., Reich, P., Bahn, M., Niinemets, Ü., Peñuelas, J., Craine, J.
1291 M., Cerabolini, B. E. L., Minden, V., Laughlin, D. C., Sack, L., Allred, B., Baraloto, C., Byun,
1292 C., Soudzilovskaia, N. A., and Running, S. W.: A methodology to derive global maps of leaf
1293 traits using remote sensing and climate data. *Remote Sens. Environ.*, 218, 69–88,
1294 <https://doi.org/10.1016/j.rse.2018.09.006>, 2018.

1295 Myers-Smith, I. H., Thomas, H. J. D., and Bjorkman, A. D.: Plant traits inform predictions of tundra
1296 responses to global change. *New Phytol.*, 221, 1742–1748, <https://doi.org/10.1111/nph.15592>,
1297 2019.

1298 [NEODC, 2015. NEODC - NERC Earth Observation Data Centre. Natural Environment Research](http://neodc.nerc.ac.uk/)
1299 [Council. http://neodc.nerc.ac.uk/.](http://neodc.nerc.ac.uk/)

1300 Peng, C. H.: From static biogeographical model to dynamic global vegetation model: a global
1301 perspective on modelling vegetation dynamics. *Ecol. Model.*, 135, 33–54,
1302 [https://doi.org/10.1016/S0304-3800\(00\)00348-3](https://doi.org/10.1016/S0304-3800(00)00348-3), 2000.

1303 Perez-Harguindeguy, N., Diaz, S., Garnier, E., Lavorel, S., Poorter, H., Jaureguiberry, P., Bret-Harte,
1304 M. S., Cornwell, W. K., Craine, J. M., Gurvich, D. E., Urcelay, C., Veneklaas, E. J., Reich, P.
1305 B., Poorter, L., Wright, I. J., Ray, P., Enrico, L., Pausas, J. G., de Vos, A. C., Buchmann, N.,
1306 Funes, G., Quetier, F., Hodgson, J. G., Thompson, K., Morgan, H. D., ter Steege, H., van der
1307 Heijden, M. G. A., Sack, L., Blonder, B., Poschlod, P., Vaieretti, M. V., Conti, G., Staver, A. C.,
1308 Aquino, S., and Cornelissen, J. H. C.: New handbook for standardised measurement of plant

1309 functional traits worldwide. *Aust. Bot.*, 61, 167–234, <https://doi.org/10.1071/bt12225>, 2013.

1310 Piao, S. L., He, Y., Wang, X. H., and Chen, F. H.: Estimation of China’s terrestrial ecosystem carbon
1311 sink: Methods, progress and prospects. *Science China Earth Sciences*, 65, 641–651,
1312 <https://doi.org/10.1007/s11430-021-9892-6>, 2022.

1313 Potapov, P., Li, X. Y., Hernandez-Serna, A., Tyukavina, A., Hansen, M. C., Kommareddy, A.,
1314 Pickens, A., Turubanova, S., Tang, H., Silva, C. E., Armston, J., Dubayah, R., Blair, J. B.,
1315 Hofton, M.: Mapping global forest canopy height through integration of GEDI and Landsat
1316 data, *Remote Sens. Environ.*, 253, 112165, <https://doi.org/10.1016/j.rse.2020.112165>, 2021.

1317 Qiao, J. J., Zuo, X. A., Yue, P., Wang, S. K., Hu, Y., Guo, X. X., Li, X. Y., Lv, P., Guo, A. X., and
1318 Sun, S. S.: High nitrogen addition induces functional trait divergence of plant community in a
1319 temperate desert steppe. *Plant and Soil*, <https://doi.org/10.1007/s11104-023-05910-1>, 2023.

1320 Reich, P. B., and Oleksyn, J.: Global patterns of plant leaf N and P in relation to temperature and
1321 latitude. *Proc. Natl. Acad. Sci. U. S. A.*, 101, 11001–11006,
1322 https://doi.org/10.1073/pnas.0403588101_2004.

1323 Reich, P. B., and Cornelissen, H.: The world-wide ‘fast-slow’ plant economics spectrum: a traits
1324 manifesto. *Journal of Ecology*, 102, 275–301, <https://doi.org/10.1111/1365-2745.12211>, 2014.

1325 Reich, P. B., Uhl, C., Walters, M. B., and Ellsworth, D. S.: Leaf lifespan as a determinant of leaf
1326 structure and function among 23 Amazonian tree species. *Oecologia*, 86, 16–24,
1327 <https://doi.org/10.1007/BF00317383>, 1991.

1328 ~~Renninger, H. J., Phillips, N., and Hodel, D. R.: Comparative hydraulic and anatomic properties in
1329 palm trees (*Washingtonia robusta*) of varying heights: implications for hydraulic limitation to
1330 increased height growth. *Trees*, 23, 911–921, <https://doi.org/10.1007/s00468-009-0333-0>,
1331 2009.~~

1332 Ridgeway, G.: Gbm: generalized boosted regression models. R package version 1.5-6, Available at:
1333 <http://cran.r-project.org/web/packages/gbm/index.html>, accessed 11/02/20092006.

1334 Roderick, M. L., and Berry, S. L.: Linking wood density with tree growth and environment: a
1335 theoretical analysis based on the motion of water. *New Phytol.*, 149, 473–485,
1336 <https://doi.org/10.1046/j.1469-8137.2001.00054.x>, 2002.

1337 ~~Roll, U., Geffen, E., and Yom-Tov, Y.: Linking vertebrate species richness to tree canopy height on
1338 a global scale. *Glob. Ecol. Biogeogr.*, 24, 814–825, <https://doi.org/10.1111/geb.12325>, 2015.~~

1339 Romero, A., Aguado, I., and Yebra, M.: Estimation of dry matter content in leaves using normalized
1340 indexes and PROSPECT model inversion. *Int. J. Remote Sens.*, 33, 396–414,
1341 <https://doi.org/10.1080/01431161.2010.532819>, 2012.

1342 Sakschewski, B., von Bloh, W., Boit, A., Rammig, A., Kattge, J., Poorter, L., Penuelas, J., and
1343 Thonicke, K.: Leaf and stem economics spectra drive diversity of functional plant traits in a
1344 dynamic global vegetation model. *Global Change Biol.*, 21, 2711–2725,
1345 <https://doi.org/10.1111/gcb.12870>, 2015.

1346 Scheiter, S., Langan, L., and Higgins, S. I.: Next-generation dynamic global vegetation models:

1347 learning from community ecology. *New Phytol.*, 198, 957–969,
1348 <https://doi.org/10.1111/nph.12210>, 2013.

1349 [Schiller, C., Schmidtlein, S., Boonman, C., Moreno-Martinez, A., and Kattenborn, T.: Deep learning](#)
1350 [and citizen science enable automated plant trait predictions from photographs. *Sci. Rep.*, 11,](#)
1351 <https://doi.org/10.1038/s41598-021-95616-0>, 2022.

1352 Shangguan, W., Dai, Y. J., Liu, B. Y., Zhu, A. X., Duan, Q. Y., Wu, L. Z., Ji, D. Y., Ye, A. Z., Yuan,
1353 H., Zhang, Q., Chen, D. D., Chen, M., Chu, J. T., Dou, Y. J., Guo, J. X., Li, H. Q., Li, J. J.,
1354 Liang, L., Liang, X., Liu, H. P., Liu, S. Y., Miao, C. Y., and Zhang, Y. Z.: A China data set of
1355 soil properties for land surface modeling. *J. Adv. Model. Earth Syst.*, 5, 212–224,
1356 <https://doi.org/10.1002/jame.20026>, 2013.

1357 Siefert, A., Violle, C., Chalmandrier, L., Albert, C. H., Taudiere, A., Fajardo, A., Aarssen, L. W.,
1358 Baraloto, C., Carlucci, M. B., Cianciaruso, M. V., de, L. D. V., de Bello, F., Duarte, L. D.,
1359 Fonseca, C. R., Freschet, G. T., Gaucherand, S., Gross, N., Hikosaka, K., Jackson, B., Jung, V.,
1360 Kamiyama, C., Katabuchi, M., Kembel, S. W., Kichenin, E., Kraft, N. J., Lagerstrom, A.,
1361 Bagousse-Pinguet, Y. L., Li, Y., Mason, N., Messier, J., Nakashizuka, T., Overton, J. M., Peltzer,
1362 D. A., Perez-Ramos, I. M., Pillar, V. D., Prentice, H. C., Richardson, S., Sasaki, T., Schamp, B.
1363 S., Schob, C., Shipley, B., Sundqvist, M., Sykes, M. T., Vandewalle, M., and Wardle, D. A.: A
1364 global meta-analysis of the relative extent of intraspecific trait variation in plant communities.
1365 *Ecol. Lett.*, 18, 1406–1419, <https://doi.org/10.1111/ele.12508>, 2015.

1366 Šímová, I., Sandel, B., Enquist, B. J., Michaletz, S. T., Kattge, J., Violle, C., McGill, B. J., Blonder,
1367 B., Engemann, K., Peet, R. K., Wiser, S. K., Morueta-Holme, N., Boyle, B., Kraft, N. J. B.,
1368 Svenning, J. C., and Hector, A.: The relationship of woody plant size and leaf nutrient content
1369 to large-scale productivity for forests across the Americas. *J. Ecol.*, 107, 2278–2290,
1370 <https://doi.org/10.1111/1365-2745.13163>, 2019.

1371 Sitch, S., Huntingford, C., Gedney, N., Levy, P. E., Lomas, M., Piao, S. L., Betts, R., Ciais, P., Cox,
1372 P., Friedlingstein, P., Jones, C. D., Prentice, I. C., and Woodward, F. I.: Evaluation of the
1373 terrestrial carbon cycle, future plant geography and climate-carbon cycle feedbacks using five
1374 Dynamic Global Vegetation Models (DGVMs). *Global Change Biol.*, 14, 2015–2039,
1375 <https://doi.org/10.1111/j.1365-2486.2008.01626.x>, 2008.

1376 Smart, S. M., Glanville, H. C., Blanes, M. d. C., Mercado, L. M., Emmett, B. A., Jones, D. L., Cosby,
1377 B. J., Marrs, R. H., Butler, A., Marshall, M. R., Reinsch, S., Herrero-Jáuregui, C., Hodgson, J.
1378 G., and Field, K.: Leaf dry matter content is better at predicting above-ground net primary
1379 production than specific leaf area. *Funct. Ecol.*, 31, 1336–1344, <https://doi.org/10.1111/1365-2435.12832>, 2017.

1381 Telenius, A.: Biodiversity information goes public: GBIF at your service. *Nord. J. Bot.*, 29, 378–
1382 381, <https://doi.org/10.1111/j.1756-1051.2011.01167.x>, 2011.

1383 Thomas, D. S., Montagu, K. D., and Conroy, J. P.: Changes in wood density of *Eucalyptus*
1384 *camaldulensis* due to temperature—the physiological link between water viscosity and wood

1385 anatomy. *Forest Ecol. Manag.*, 193, 157–165, <https://doi.org/10.1016/j.foreco.2004.01.028>,
1386 2004.

1387 Thomas, S. C.: Photosynthetic capacity peaks at intermediate size in temperate deciduous trees. *Tree*
1388 *Physiol.*, 30, 555–573, <https://doi.org/10.1093/treephys/tpq005>, 2010.

1389 [Thuiller, W., Lafourcade, B., Engler, R., and Araújo, M. B.: BIOMOD – A platform for ensemble](#)
1390 [forecasting of species distributions. *Ecography*, 32, 369–373, \[0587.2008.05742.x, 2009.\]\(https://doi.org/10.1111/j.1600-
1391 <a href=\)](#)

1392 Trabucco, A., and Zomer, R. J.: Global Aridity Index and Potential Evapo-Transpiration (ET0)
1393 Climate Database v2. CGIAR Consortium for Spatial Information (CGIAR-CSI),
1394 <https://cgiarcsi.community>, 2018.

1395 [Vallicrosa, H., Sardans, J., Maspons, J., Zuccarini, P., Fernández-Martínez, M., Bauters, M., Goll,](#)
1396 [D. S., Ciais, P., Obersteiner, M., Janssens, I. A., and Peñuelas, J.: Global maps and factors](#)
1397 [driving forest foliar elemental composition: the importance of evolutionary history. *New*](#)
1398 [Phytol., 233, 169–181, <https://doi.org/10.1111/nph.17771>, 2022.](#)

1399 Van Bodegom, P. M., Douma, J. C., Witte, J. P. M., Ordoñez, J. C., Bartholomeus, R. P., and Aerts,
1400 R.: Going beyond limitations of plant functional types when predicting global ecosystem-
1401 atmosphere fluxes: exploring the merits of traits-based approaches. *Glob. Ecol. Biogeogr.*, 21,
1402 625–636, <https://doi.org/10.1111/j.1466-8238.2011.00717.x>, 2012.

1403 [van Bodegom, P. M., Douma, J. C., and Verheijen, L. M. A fully traits-based approach to modeling](#)
1404 [global vegetation distribution. *P. Nat. Acad. Sci. USA*, 111, 13733–13738,](#)
1405 [https://doi.org/10.1073/pnas.1304551110, 2014.](#)

1406 Verheijen, L. M., Aerts, R., Bonisch, G., Kattge, J., and Van Bodegom, P. M.: Variation in trait trade-
1407 offs allows differentiation among predefined plant functional types: implications for predictive
1408 ecology. *New Phytol.*, 209, 563–575, <https://doi.org/10.1111/nph.13623>, 2016.

1409 Wang, H., Harrison, S. P., Prentice, I. C., Yang, Y. Z., Bai, F., Togashi, H. F., Wang, M., Zhou, S. X.,
1410 and Ni, J.: The China Plant Trait Database: toward a comprehensive regional compilation of
1411 functional traits for land plants. *Ecology*, 99, 500, <https://doi.org/10.1002/ecy.2091>, 2018.

1412 [Wang, Z. H., Li, Y. Q., Su, X. Y., Tao, S. L., Feng, X., Wang, Q. G., Xu, X. T., Liu, Y. P., Michaletz,](#)
1413 [S. T., Shrestha, N., Larjavaara, M., and Enquist, B. J.: Patterns and ecological determinants of](#)
1414 [woody plant height in eastern Eurasia and its relation to primary productivity. *Journal of Plant*](#)
1415 [Ecology, 12, 791–803, <https://doi.org/10.1093/jpe/rtz025>, 2019.](#)

1416 Webb, C. T., Hoeting, J. A., Ames, G. M., Pyne, M. I., and LeRoy Poff, N.: A structured and dynamic
1417 framework to advance traits-based theory and prediction in ecology. *Ecol. Lett.*, 13, 267–283,
1418 <https://doi.org/10.1111/j.1461-0248.2010.01444.x>, 2010.

1419 [Westoby, M.: A leaf height seed \(LHS\) plant ecology strategy scheme. *Plant Soil*, 199, 213–227,](#)
1420 [1998.](#)

1421 Wright, I. J., Dong, N., Maire, V., Prentice, I. C., Westoby, M., Diaz, S., Gallagher, R. V., Jacobs, B.
1422 F., Kooyman, R., Law, E. A., Leishman, M. R., Niinemets, U., Reich, P. B., Sack, L., Villar, R.,

1423 Wang, H., and Wilf, P.: Global climatic drivers of leaf size. *Science*, 357, 917–921,
1424 <https://doi.org/10.1126/science.aal4760>, 2017.

1425 Wright, I. J., Reich, P. B., Westoby, M., Ackerly, D. D., Baruch, Z., Bongers, F., Cavender-Bares, J.,
1426 Chapin, T., Cornelissen, J. H. C., Diemer, M., Flexas, J., Garnier, E., Groom, P. K., Gulias, J.,
1427 Hikosaka, K., Lamont, B. B., Lee, T., Lee, W., Lusk, C., Midgley, J. J., Navas, M. L., Niinemets,
1428 U., Oleksyn, J., Osada, N., Poorter, H., Poot, P., Prior, L., Pyankov, V. I., Roumet, C., Thomas,
1429 S. C., Tjoelker, M. G., Veneklaas, E. J., and Villar, R.: The worldwide leaf economics spectrum.
1430 *Nature*, 428, 821–827, <https://doi.org/10.1038/nature02403>, 2004.

1431 Wullschleger, S. D., Epstein, H. E., Box, E. O., Euskirchen, E. S., Goswami, S., Iversen, C. M.,
1432 Kattge, J., Norby, R. J., van Bodegom, P. M., and Xu, X.: Plant functional types in earth system
1433 models: past experiences and future directions for application of dynamic vegetation models
1434 in high-latitude ecosystems. *Ann. Bot.*, 114, 1–16, <https://doi.org/10.1093/aob/mcu077>, 2014.

1435 Yan, P., He, N. P., Yu, K. L., Xu, L., and Van Meerbeek, K.: Integrating multiple plant functional
1436 traits to predict ecosystem productivity. *Commun Biol*, 6, 239, [https://doi.org/10.1038/s42003-](https://doi.org/10.1038/s42003-023-04626-3)
1437 [023-04626-3](https://doi.org/10.1038/s42003-023-04626-3), 2023.

1438 Yang, Y. Z., Zhu, Q. A., Peng, C. H., Wang, H., Xue, W., Lin, G. H., Wen, Z. M., Chang, J., Wang,
1439 M., Liu, G. B., and Li, S. Q.: A novel approach for modelling vegetation distributions and
1440 analysing vegetation sensitivity through trait-climate relationships in China. *Sci. Rep.*, 6, 24110,
1441 <https://doi.org/10.1038/srep24110>, 2016.

1442 ~~Yang, Y. Z., Wang, H., Harrison, S. P., Prentice, I. C., Wright, I. J., Peng, C. H., and Lin, G. H.:~~
1443 ~~[Quantifying leaf-trait covariation and its controls across climates and biomes. *New Phytol.*,](#)~~
1444 ~~[221, 155-168, <https://doi.org/10.1111/nph.15422>, 2018.](#)~~

1445 Yang, Y. Z., Zhao, J., Zhao, P. X., Wang, H., Wang, B. H., Su, S. F., Li, M. X., Wang, L. M., Zhu,
1446 Q. A., Pang, Z. Y., and Peng, C. H.: Trait-Based Climate Change Predictions of Vegetation
1447 Sensitivity and Distribution in China. *Front. Plant Sci.*, 10, 908,
1448 <https://doi.org/10.3389/fpls.2019.00908>, 2019.

1449 Yurova, A. Y., and Volodin, E. M.: Coupled simulation of climate and vegetation dynamics. *Izv.,*
1450 *Atmos. . Ocean. Phys.*, 47, 531-539, <https://doi.org/10.1134/s0001433811050124>, 2011.

1451 Zaehle, S., and Friend, A. D.: Carbon and nitrogen cycle dynamics in the O-CN land surface model:
1452 1. Model description, site-scale evaluation, and sensitivity to parameter estimates. *Global*
1453 *Biogeochem. Cy.*, 24, n/a-n/a, <https://doi.org/10.1029/2009gb003521>, 2010.

1454 ~~Zepeda, V., and Martorell, C.: Seed mass equalises the strength of positive and negative plant-plant~~
1455 ~~interactions in a semi-arid grassland. *Oecologia*, 190, 287–296,~~
1456 ~~<https://doi.org/10.1007/s00442-018-04326-4>, 2019.~~